NASA Tech Briefs

Transferring Technology to
American Industry and Government

May 1988
Volume 12 Number 5

The ACTS Initiative:
NASA/Industry Plan To Meet Tomorrow's Challenges In Space Communications

Still Crazy After

1946
When the David Sarnoff Research Center was working on color TV in the early 1940's, people may have thought, "That's crazy!" Yet, in '46 we publicly demonstrated a practical, all-electronic compatible color TV system. It was accepted as the industry standard in 1953, and is still used today.

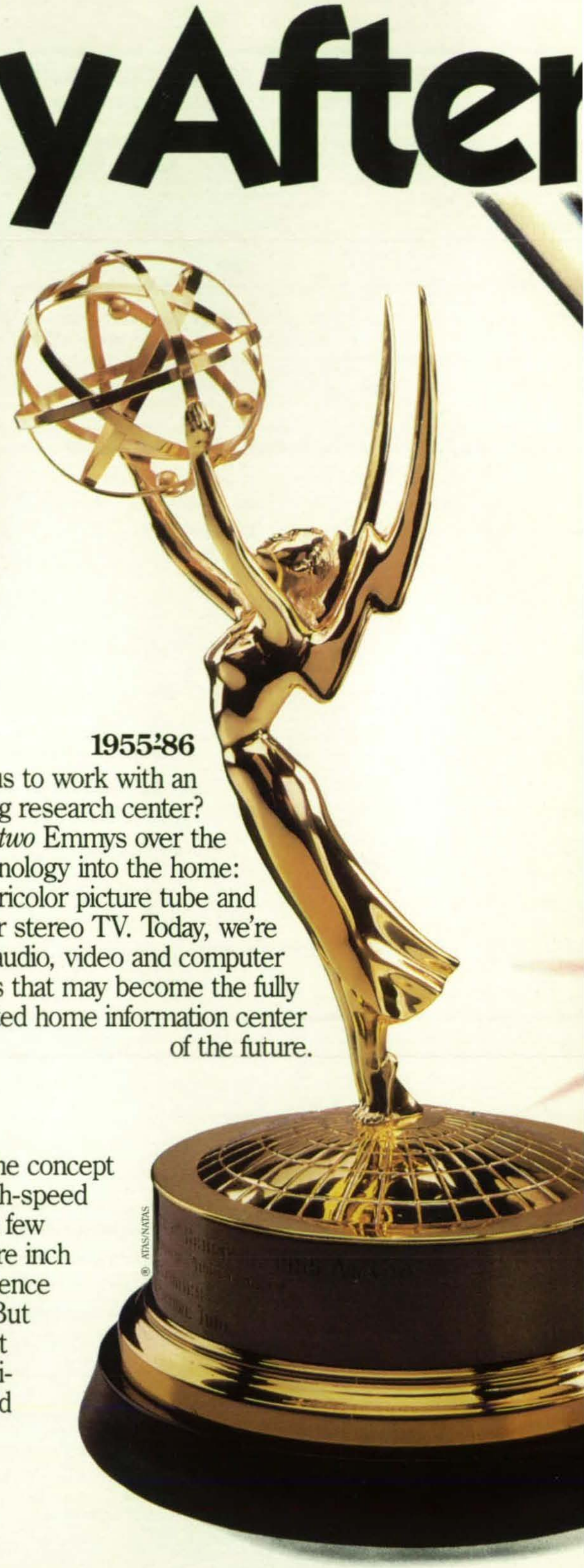

1955-'86
Is it outrageous to work with an Emmy-award winning research center? The fact is, we've won *two* Emmys over the years for bringing new technology into the home: one in 1955 for the tricolor picture tube and another in 1986 for stereo TV. Today, we're advancing audio, video and computer technologies that may become the fully integrated home information center of the future.

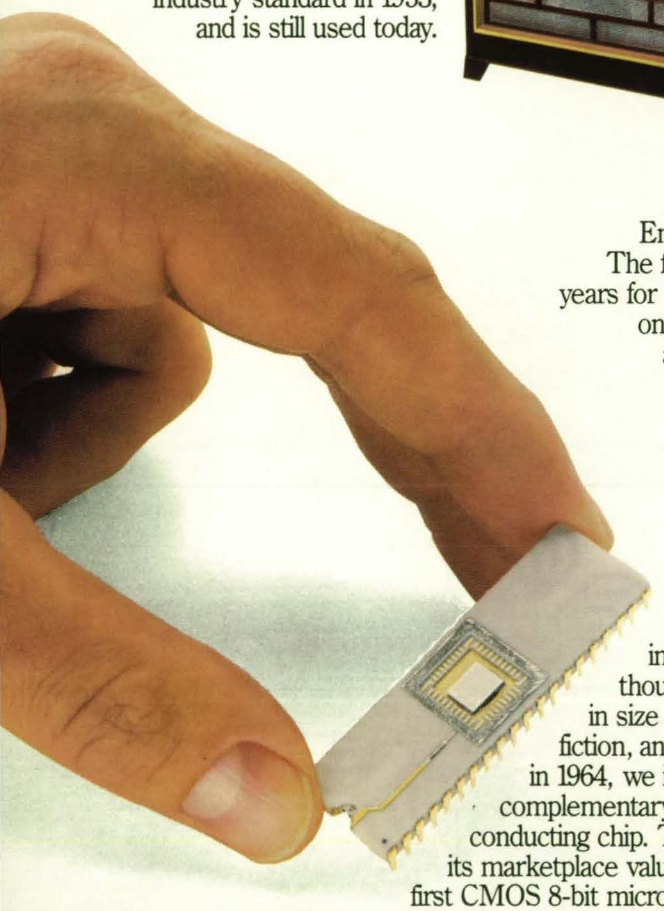

1964
In the 1950's, the concept of low-power, high-speed integrated circuits a few thousandths of a square inch in size existed only in science fiction, and the laboratory. But in 1964, we introduced the first complementary metal oxide semi-conducting chip. Then demonstrated its marketplace value by building the first CMOS 8-bit microprocessor.

For over 40 years, the David Sarnoff Research Center has been turning man's wildest flights of fancy into marketplace realities.

Now, after all those years as a proprietary R&D facility for RCA and GE, Sarnoff is an independent contract research center.

And business is growing like crazy.

Our continuing success in contracts and joint ventures ranges from computerized automobile controls and radar measurements for steel blast furnaces to plasma physics. Work in progress spans everything from high-definition TV systems to transmitting data by laser to erasable optic disks.

For our current capabilities report, contact

David Sarnoff Research Center. A subsidiary of SRI International. Emmy statuette is trademark of ATAS/NATAS.

All These Years.

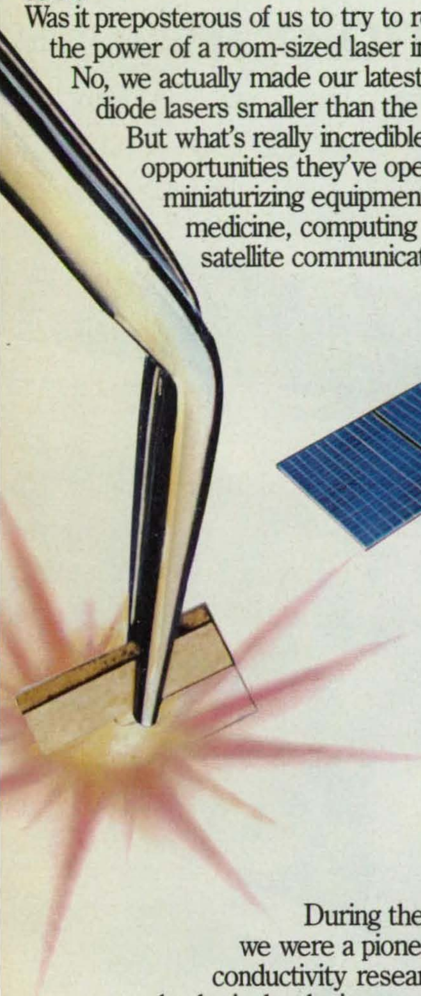

1986
Was it preposterous of us to try to reproduce the power of a room-sized laser in a smaller unit? No, we actually made our latest surface-emitting diode lasers smaller than the head of a pin. But what's really incredible are the opportunities they've opened for miniaturizing equipment in medicine, computing and satellite communications.

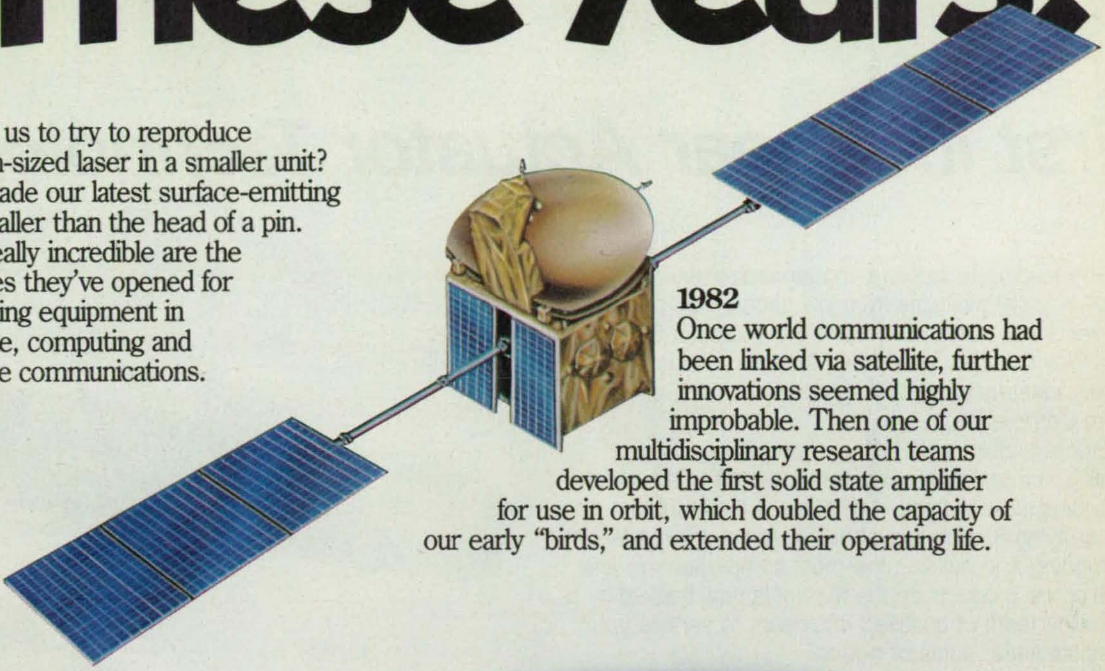

1982
Once world communications had been linked via satellite, further innovations seemed highly improbable. Then one of our multidisciplinary research teams developed the first solid state amplifier for use in orbit, which doubled the capacity of our early "birds," and extended their operating life.

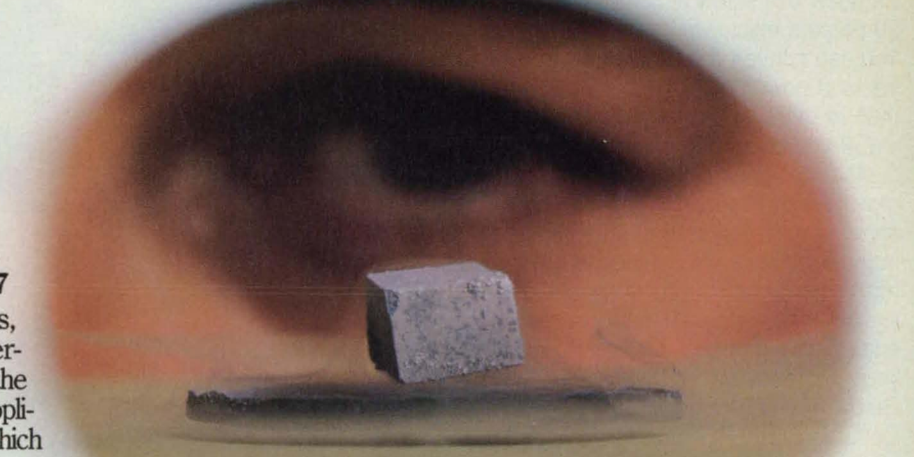

1987
During the early 60's, we were a pioneer in superconductivity research, and the leader in developing commercial applications for semiconducting wire which operated at extremely low temperatures. Modern superconductors have no resistance to electricity at twice the previous temperature and can levitate a magnet like the one shown here, but we're working on superconductive circuits that will operate at room temperature.

Joseph C. Volpe, Vice President, Marketing, at the David Sarnoff Research Center, CN 5300, Princeton, NJ 08543-5300, or call (609) 734-2178.

Then bring us *your* troublesome projects, allegedly impossible technological hurdles and unreachable goals.

Because we're crazy enough to turn them into very serious successes.

DAVID
Sarnoff
RESEARCH CENTER

Heads in the clouds, feet on the ground.

Circle Reader Action No. 604

First in Linear Actuator Technology

The leading technology in mechanical linear actuation is still available from the people who pioneered it 47 years ago. Only now, we're the Thomson Saginaw Ball Screw Company, the new name for products formerly manufactured by Saginaw Division, General Motors Corporation.

Our actuators are used in applications where reliability and quality requirements are put to the most demanding industry tests – whether in the manufacturing plant or flying 35,000 feet above it. And our experience in designing and building the most comprehensive line of ball screw products on the market is now backed by a nationwide team of qualified engineers to service your immediate linear actuator needs.

As motion transfer mechanisms, Thomson Saginaw ball screw assemblies work for you at over 90 percent efficiency in converting torque to thrust. You can convert this to your advantage by saving yourself power, money and avoid the troubles common to other inefficient actuator devices.

If you're looking for standard or custom designed linear actuators, start it moving with Thomson Saginaw. The same people that started things moving in the first place. **We welcome your inquiries.** Send us your drawings or sketches for a free estimate and/or engineering proposal. Or, write or call for your own copy of our Ball Screw Design Guide. Thomson Saginaw Ball Screw Company, Inc., P.O. Box 9550, Saginaw, MI 48608, (517) 776-4123.

Unleash The Power Of PARALLEL PROCESSING...

NEW *MODULAR* PRESSURE SCANNING SYSTEM

INTRODUCING THE MODEL 8400 PRESSURE SCANNING & ACQUISITION SYSTEM

- All Media Pressure Measurement
- Voltage, Frequency & Digital Inputs
- 100,000 + Measurements Per Second
- .05% Accuracy Full Scale

The 8400 system is a second generation approach to data acquisition. It frees the test engineer from technology of the past.

Parallel architecture lets you *simultaneously* acquire and correlate data from a variety of transducers. At high speed and high accuracy.

This acquisition system is fully integrated. So host computer software is substantially reduced. And cost of ownership is far less compared to custom data acquisition systems.

The 8400 concept uses a 32-bit 68020 microprocessor for high speed data correlation and engineering unit conversion. The 68020 interfaces your host computer to as many as 64 measurement input units *each having its own microprocessor and acquisition personality card.*

Input units include pressure scanning, calibration, analog measurement, frequency measurement, and more – allowing input from virtually any signal source.

The 8400 system is ultimately flexible. It can be configured from a low cost entry level system to ultra-high performance by your selection of modular subcomponents. This makes the 8400 specially suited for Turbine and Aerospace Testing.

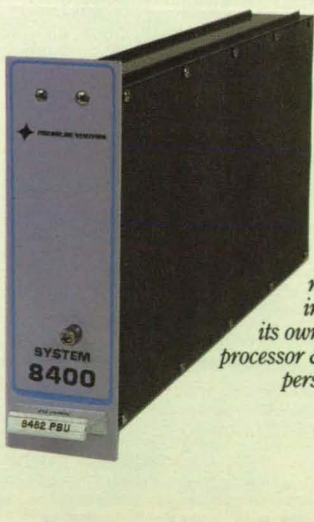

The typical measurement input unit has its own 8-bit microprocessor & acquisition personality card.

The system 8400 is specially suited for Turbine & Aerospace Testing.

All backed by the company who built their reputation on *guaranteed measurement data,* Pressure Systems, the developer of electronic pressure scanning.

Call 1-800-678-SCAN for a brochure or exciting demonstration of the 8400's capabilities.

PRESSURE SYSTEMS
34 Research Drive, Hampton, Va. 23666
(804) 865-1243 Telex 901406 Fax 804-766-2644

Circle Reader Action No. 378

NASA Tech Briefs

National Aeronautics and
Space Administration

MAY 1988
Volume 12 Number 5

SPECIAL FEATURE

TECHNICAL SECTION

ABP BPA

How will NASA's Advanced Communications Technology Satellite (ACTS), pictured above, help the U.S. maintain competitiveness in the world satellite communications market? See page 12.

DEPARTMENTS

ON THE COVER—An illustration of the ACTS satellite's deployment from the Space Shuttle. *(courtesy NASA)*

This high-burst-rate ground terminal, located at NASA's Lewis Research Center in Cleveland, OH, is a critical element in the experimental ACTS program, described in this issue beginning on page 12. The 4.72-meter terminal operates in the Ka-band (30/20 GHz), a valuable new frequency regime, and features a step-tracking system that automatically compensates for satellite movement and wind deflections. *(Photo courtesy Scientific-Atlanta Inc., Atlanta, GA)*

NASA Tech Briefs, ISSN 0145-319X, USPS 750-070, copyright © 1988 in U.S., is published monthly except July/August and November/December (10x per year) by Associated Business Publications Co., Ltd. 41 E. 42nd St., New York, NY 10017-5391. The copyrighted information does not include the individual Tech Briefs which are supplied by NASA. Editorial, sales, production and circulation offices at 41 E. 42nd Street. New York, NY 10017-5391. Subscriptions for non-qualified subscribers in the U.S., Panama Canal Zone, and Puerto Rico. $75.00 for 1 year; $125.00 for 2 years; $200 for 3 years. Single copies $15.00. Remit by check, draft, postal or express orders. Other remittances at sender's risk. Address all communications for subscriptions or circulation to NASA Tech Briefs, 41 E. 42nd Street. New York, NY 10017-5391. Second-class postage paid at New York, NY and additional mailing offices.

POSTMASTER: please send address changes to NASA Tech Briefs, 41 E. 42nd Street, Suite 921, New York, NY 10017-5391.

NASA Tech Briefs

National Aeronautics and Space Administration

NASA Tech Briefs:

Published by .... **Associated Business Publications**
Editor-in-Chief/Publisher .... **Bill Schnirring**
Associate Publisher .... **Frank Nothaft**
Associate Publisher .... **Robin J. DuCharme**
Managing Editor .... **R. J. Laer**
Associate Editor .... **Joseph T. Pramberger**
Technical Advisor .... **Dr. Robert E. Waterman**
Production Manager .... **Rita Nothaft**
Traffic Manager .... **James E. Cobb**
Circulation Director .... **Anita Weissman**
Controller .... **Neil B. Rose**
Awards Manager .... **Evelyn Mars**
Reader Service Manager .... **Arlene Berrios**

Technical Staff:
Briefs prepared for National Aeronautics and Space Administration by **Logical Technical Services Corp.**, NY, NY
Technical/Managing Editor .... **Ted Selinsky**
Art Director .... **Ernest Gillespie**
Administrator .... **Elizabeth Texeira**
Chief Copy Editor .... **Lorne Bullen**
Staff Editors .... **Dr. James Boyd, Dr. Larry Grunberger, Jordan Randjelovich, George Watson, Oden Browne, Joseph Renzler, Dr. Theron Cole, Jr.**
Technical Advisers .... **Dr. Arthur Gilman, Dr. Jay Kirschenbaum**
Graphics .... **Luis Martinez, Vernald Gillman, Charles Sammartano**
Editorial & Production .... **Bill Little, Frank Ponce, Ivonne Valdes, Paul Marcus**

ABP BPA

NASA:
NASA Tech Briefs are provided by the National Aeronautics and Space Administration, Technology Utilization Division, Washington, DC:
Administrator .... **Dr. James C. Fletcher**
Assistant Administrator for Commercial Programs .... **James T. Rose**
Deputy Assistant Administrator (Programs) .... **Henry J. Clarks**
Deputy Director TU Division (Publications Manager) .... **Leonard A. Ault**
Manager, Technology Utilization Office, NASA Scientific and Technology Information Facility .... **Walter M. Heiland**

Associated Business Publications
41 East 42nd Street, Suite 921, New York, NY 10017-5391
(212) 490-3999 FAX (212) 986-7864
President .... **Bill Schnirring**
Executive Vice President .... **Frank Nothaft**
Vice President Marketing .... **Mark J. Seltman**

Advertising:
New York Office: (212) 490-3999 FAX (212) 986-7864
Sales Manager .... **Robin DuCharme**
Regional Sales Manager (Mid-Atlantic) .... **Michelle Larsen**
Account Executive (Midwest) .... **Jack Cartwright** at (312) 501-4140
Marketing Research Manager .... **Leo D. Kluger**
Advertising Coordination Manager .... **Erving Dockery, Jr.**
Account Executives (Eastern MA, NH, ME, RI) .... **Lee Arpin** or **Brian Clerkin** at (617) 899-5613; **Bill Doucette** at (617) 278-7792
Account Executive (Western MA, CT, VT) .... **George Watts** at (413) 253-9881
Account Executives (No. Calif., UT) .... for Area Code 415—**Janice Richey King** and for Area Code 408—**Richard Cassidy** at (415) 656-3613
Account Executives (So. Calif., AZ, NV, NM) .... for Area Codes 818/213/805—**Thomas Stillman** or **Dana Gindoff** and for Area Codes 619/714—**Leslie Alley** at (213) 541-4699

NTBM-Research Center
Project Director .... **Mark J. Seltman**
Account Supervisor .... **Lourdes Del Valle**

An ant can carry a load *10X* its size...

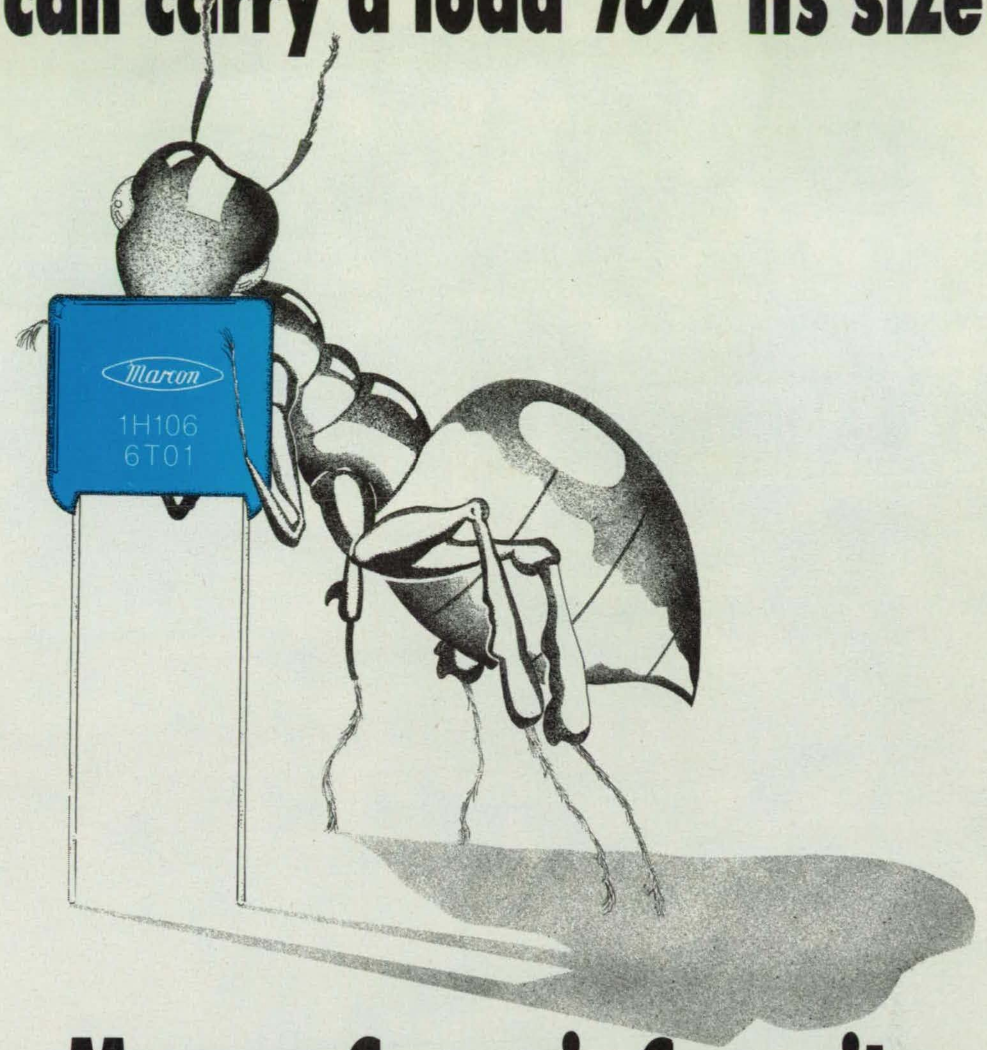

So can Marcon Ceramic Capacitors!

Small *and* powerful – Marcon's Multi-layer Ceramic Capacitors offer unprecedented advances in MLC technology. Due to our patented niobium oxide dielectric they provide:

- volumetric efficiency
- temperature stability
- low DC bias voltage dependency
- high insulation resistance
- small aging rate
- low dissipation factor
- wide range of compact sizes
- high ripple current handling capability
- ultra-low ESR
- and the highest in reliability

Marcon's MLCs also offer you a wide range of capacitance (from .10uF to 100uF) and a voltage range of 25 to 500Vdc.

Our MLCs can be used in even the most demanding of filtering assignments; especially input and

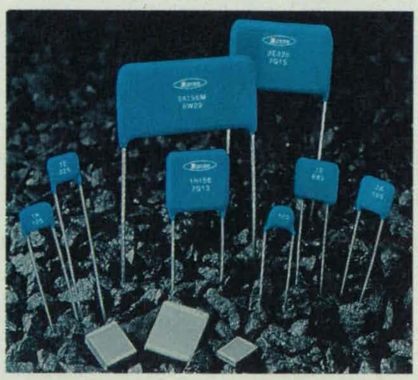

output filtering of switch-mode power supplies. Our capacitors are available in radial lead-dipped packages and surface mountable chips featuring nickel barrier or silver palladium terminations.

Start filtering your frequency with Marcon MLCs today.

Small *and* powerful – Marcon MLCs get the job done!

"Please stop and see us at Booth #2729."

MARCON
MARCON AMERICA CORPORATION
310 Era Dr., Northbrook, IL 60062
312/564-2820
Fax: 312/564-1150 GIII

Marcon

- ***Capacitors***
- ***Varistors***
- ***Humidity Sensors***

Circle Reader Action No. 597

front-end processor. Plus, the IBM Vector Facility's modular design lets you start with just the computer power you need today, and make economical in-field upgrades as your needs grow. And that gives the IBM 3090VF a big edge over more expensive and less flexible vector processors.

IBM's integrated system approach combines the power of the IBM 3090VF with the advantages of a single operating environment, low entry cost, low software and maintenance costs, a wide variety of application programs, and IBM support to create a winner in total cost-of-computing.

To find out more, or to arrange to have your IBM Marketing Representative contact you, simply call 1-800-IBM-2468, ext. 20.

IBM. The Bigger Picture

The ACTS Initiative:

Pioneering the Next Generation of Space Communications

Above is a model of NASA's Advanced Communications Technology Satellite (ACTS). Scheduled for launch in 1992, ACTS will be used to evaluate high-risk advanced technologies that fall outside the sponsorship capabilities of the private sector.

Over the last decade, United States leadership in the world communications satellite market has been increasingly threatened by foreign competition. For while U.S. satellite research and development has slowed in recent years, due in part to reduced government subsidizing of high-risk R&D projects, Europe and Japan have accelerated their satellite programs. The European Space Agency presently outspends the U.S. by a more than two-to-one margin in new satellite development, while Japan has replaced the U.S. as leading supplier of Earth stations to INTELSAT, the global satellite network that provides telecommunications services to over 170 countries.

"For years communications experts have warned us that Europe was catching up (to the U.S.) in satellite technology," said Dr. F. Michael Naderi of NASA Headquarters. "Well, now they have caught up, and it's vital that we create the advanced technology base required to meet this challenge and regain our competitive edge."

An important first step, said Dr. Naderi, is development of the Advanced Communications Technology Satellite (ACTS), an experimental satellite slated for launch aboard the Space Shuttle in May, 1992. ACTS will serve as a testing vehicle for a variety of emerging technologies that could be used on future commercial satellites. A cooperative NASA-industry endeavor, the ACTS program is sponsored by NASA's Office of Space Science and Applications (OSSA) in Washington, DC and managed by

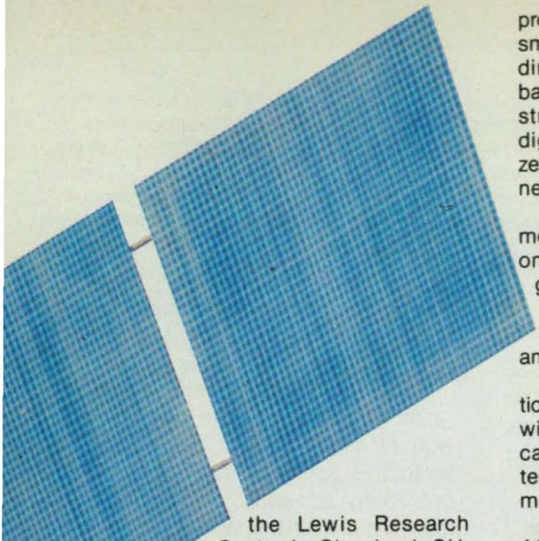

the Lewis Research Center in Cleveland, OH. Eighty contractors and suppliers from 16 states are involved in fabrication of the ACTS spacecraft and ground network, at a total cost of $499 million.

One of the key technologies ACTS will test is a multiple beam antenna system designed to expand satellite capacity. Unlike today's conventional satellites, which cover the continental U.S. (CONUS) with a single, stationary antenna coverage pattern, the ACTS multibeam antenna will concentrate communications capacity into a group of narrow spot beams, each encompassing a territory about 150 miles in diameter. The spacing of these spots across the country will allow use of the same frequency in many beams—hence frequency reuse. "With this multibeam package, we'll gain 100 times more power and ten times more bandwidth than available in current satellite systems," said Dr. Naderi, ACTS Program Manager under OSSA.

ACTS will evaluate both fixed and electronically hopped spot beams. The hopping beams will scan parts of the country every millisecond, with beam capacity divided according to the fluctuating demands of users at different locations. "By adjusting the time a hopping beam will dwell on any single location, more efficient use can be made of available satellite capacity," said Ronald Schertler, ACTS Project Experiments Manager for the Lewis Center.

The satellite's efficiency will be further enhanced by distributing beam resources through an access assignment technique called Time Division Multiple Access (TDMA). By dividing communications signals into short, compressed bursts of information, the TDMA architecture will allow several Earth stations to operate at the same frequencies through a time sharing arrangement. A master control station based at the Lewis Center will adjust the TDMA time slots to match individual user needs.

A Switchboard In The Sky

Use of multiple spot beams requires a switching system on board the satellite to interconnect the beams and route signals to their correct destinations. Two types of switching facilities will fly on ACTS: intermediate frequency (IF) matrix switching and baseband processing. The IF matrix switch will interconnect the high-volume, wide-bandwidth communications transmitted over fixed beams, while the baseband processor will route low-volume traffic from small Earth stations, such as those located directly on the customer's premises. With baseband processing, received signals are stripped down to their basic content—digital data consisting of binary ones and zeros. This data is stored and then interconnected to the proper ground antenna.

"On-board digital switching is the single most important technology advancement on ACTS" said Robert Lawton, ACTS Program Manager for General Electric's RCA Astro-Space Division, the prime contractor for the satellite. "It's a step ahead of anything the competition is doing."

In addition to permitting signal error detection and correction, the baseband processor will dynamically rout individual telephone calls, bypassing the costs associated with terrestrial switching networks and, in effect, moving the switchboard into the sky.

Baseband processing will also enable ACTS to provide multiple voice channels to very-small-aperture-terminals (VSATs) and to do so in a single satellite hop—neither of which is possible with present VSAT networks.

Solving The Orbital Jam

The ACTS communications payload will operate in the Ka-band (30/20 GHz), a virtually untapped portion of the frequency spectrum. The Ka-band's allotted frequency bandwidth is twice the size of the combined bandwidths of the C (6/4 GHz) and Ku (14/12 GHz) frequency bands presently used by commercial satellites, and therefore offers the potential to significantly increase satellite capacity.

"Implementation of the Ka-band could eliminate the potential problem of orbital congestion," said Mr. Lawton. "If we keep stacking more and more satellites at the present frequencies, we'll eventually fill all of the available orbital slots and end up with the space equivalent of a highway traffic jam. The Ka-band would expand our options considerably."

Before transmission at this higher frequency would be practical, however, researchers must solve the problem of signal fading caused by rainfall. "We could take a brute-force approach and provide a large link margin to combat fading, but that would require an extravagant, costly design," explained Dr. Joseph Campanella, Vice President and Chief Scientist for COMSAT Laboratories, contractor for the master control and ground stations. "So on ACTS we'll use an adaptive technique whereby only those terminals experiencing fade are provided additional protection." The affected terminal will send a request to the master control station for increased protection, and the station will respond by instructing the terminal and ACTS to temporarily adjust their transmission power to compensate for the uplink and downlink fades. "It's a smooth process," said Dr. Campanella. "There's no loss of data or noticeable change in transmission."

The Mission

ACTS is committed to a minimum two year mission life, during which the satellite network will be available to industry free of charge as a national testing facility. Next year, NASA will release a notice of opportunity formally soliciting proposals for experimentation. Mr. Schertler said he expects researchers to conduct more than 150 experiments, evaluating the capabilities of the flight system's advanced components, the associated ground terminals, and the overall TDMA network. Experiments will also study such aspects as satellite pointing accuracy, beam pattern and gain stability, and ground terminal antenna tracking, according to Schertler.

After ACTS

Looking beyond ACTS, Schertler envisions researchers using the Space Station platform to conduct future satellite communications R&D. "It's a natural evolution," he explained, "and it would free us from the confines of the Space Shuttle compartment."

"The important thing is that we keep pushing our research forward into the next century," added Naderi. "ACTS is a major step, but we can't stop there. We can no longer afford to sit back and watch the world go by." □

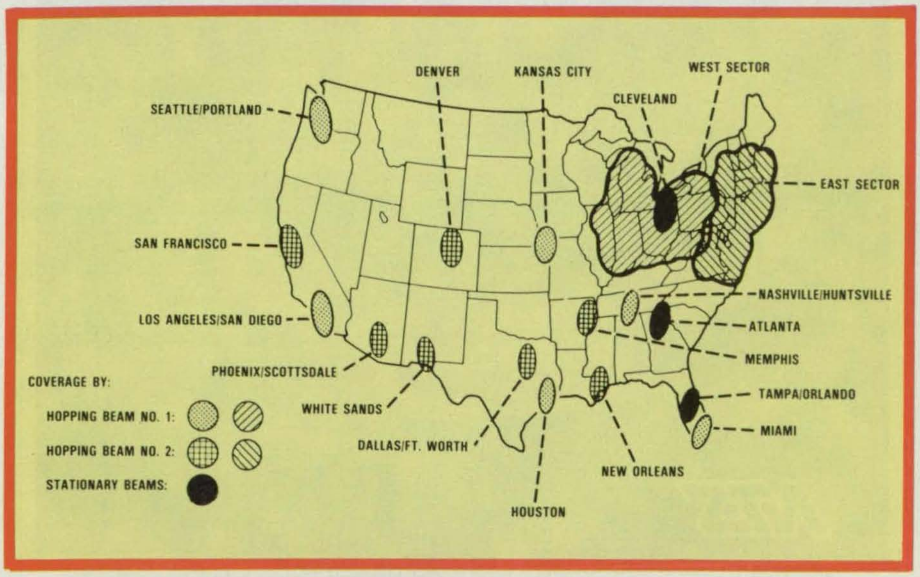

ACTS will feature three stationary and two hopping beams, providing coverage to most major metropolitan areas. Each hopping beam can hop to several discrete locations or to anywhere within a contiguous sector. Altogether, the beams will cover 20% of CONUS, which is deemed sufficient for an experimental system.

New Product Ideas

New Product Ideas are just a few of the many innovations described in this issue of *NASA Tech Briefs* and having promising commercial applications. Each is discussed further on the referenced page in the appropriate section in this issue. If you are interested in developing a product from these or other NASA innovations, you can receive further technical information by requesting the TSP referenced at the end of the full-length article or by writing the Technology Utilization Office of the sponsoring NASA center (see page 16). NASA's patent-licensing program to encourage commercial development is described on page 16.

Robotic Tool-Exchange System

A relatively simple robotic tool-exchange system consists of a tool rack, which holds such tools as screwdriver bits, sockets, or twist drills, and the mechanisms that enable a robotic end effector to pick up or replace a tool. The spring-mounted tool-rack base reduces the need for highly accurate positioning of the end effector. (See page 74).

Heat-Shrinkable, Seamless Fabric Tube

A seamless fabric tube under consideration for use in pressure suits like those worn by astronauts may also be used for protective garments in industry, rescue operations, and sports activities. The garment made from this fabric is expected to be durable and to require less manual labor than for a sewn suit. (See page 77).

Rotary Reactor Makes Large Latex Particles

A prototype chemical reactor produces latex particles up to 100 μm in diameter. Previously, such large particles could be produced only in the gravity-free environment of space. The reactor reduces the gravitational effects that interfere with particle growth and thus limit the particles to about 3 μm. (See page 76).

Handheld Controller for Robotic End Effector

A robot end-effector controller is equipped with position and force feedback. The end-effector force and position are fed back to the operator's hand through the rotation of the trigger and the rocking of the trigger guard. (See page 73).

Single-Layer, Multicolor Electroluminescent Phosphors

A new method has been conceived for the construction of a single phosphor layer composed of two or more different color phosphors for use in thin-film electroluminescent displays. The process enables the production of the single-layer, two-color phosphor layer without etching. (See page 18).

Readily Processable Polyimide

A new processable polyimide was synthesized by the reaction of a diamine, 1,3-bis 2-(3-aminophenoxy)ethyl ether, with 3,3',4,4'-benzophenonetetracarboxylic dianhydride to form the polyamic acid and subsequent conversion of it to the polyimide. Evaluation of the specimens has shown extremely high titanium-to-titanium tensile shear strength. (See page 50).

HOW YOU CAN BENEFIT FROM NASA's TECHNOLOGY UTILIZATION SERVICES

If you're a regular reader of TECH BRIEFS, then you're already making use of one of the low- and no-cost services provided by NASA's Technology Utilization (TU) Network. But a TECH BRIEFS subscription represents only a fraction of the technical information and applications/engineering services offered by the TU Network as a whole. In fact, when all of the components of NASA's Technology Utilization Network are considered, TECH BRIEFS represents the proverbial tip of the iceberg.

We've outlined below NASA's TU Network—named the participants, described their services, and listed the individuals you can contact for more information relating to your specific needs. We encourage you to make use of the information, access, and applications services offered by NASA's Technology Utilization Network.

How You Can Utilize **NASA's Industrial Applications Centers—**A nationwide network offering a broad range of technical services, including computerized access to over 100 million documents worldwide.

You can contact NASA's network of Industrial Applications Centers (IACs) for assistance in solving a specific technical problem or meeting your information needs. The "user friendly" IACs are staffed by technology transfer experts who provide computerized information retrieval from one of the world's largest banks of technical data. Nearly 500 computerized data bases, ranging from NASA's own data base to Chemical Abstracts and INSPEC, are accessible through the nine IACs located throughout the nation. The IACs also offer technical consultation services and/or linkage with other experts in the field. You can obtain more information about these services by calling or writing the nearest IAC. User fees are charged for IAC information services.

Aerospace Research Applications Center (ARAC)
Indianapolis Center for Advanced Research
611 N. Capitol Avenue
Indianapolis, IN 46204
Dr. F. Timothy Janis, Director
(317) 262-5036

Central Industrial Applications Center/NASA (CIAC)
Southeastern Oklahoma State U.
Station A, Box 2584
Durant, OK 74701
Dr. Dickie Deel, Director
(405) 924-6822

North Carolina Science and Technology Research Center (NC/STRC)
Post Office Box 12235
Research Triangle Park, NC 27709
J. Graves Vann, Jr., Director
(919) 549-0671

NASA Industrial Applications Ctr. 823 William Pitt Union
University of Pittsburgh
Pittsburgh, PA 15260
Dr. Paul A. McWilliams, Exec. Director
(412) 648-7000

NASA/Southern Technology Applications Center
P. O. Box 24
Progress Ctr., One Progress Blvd.
Alachua, FL 32615
J. Ronald Thornton, Director
(904) 462-3913
(800) 354-4832 (FL only)
(800) 225-0308 (toll-free US)

NASA/UK Technology Applications Center
University of Kentucky
109 Kinkead Hall
Lexington, KY 40506-0057
William R. Strong, Director
(606) 257-6322

NERAC, Inc.
One Technology Drive
Tolland, CT 06084
Dr. Daniel U. Wilde, President
(203) 872-7000

Technology Application Center (TAC)
University of New Mexico
Albuquerque, NM 87131
Dr. Stanley A. Morain, Director
(505) 277-3622

NASA Industrial Applications Center (WESRAC)
University of Southern California Research Annex
3716 South Hope Street, Room 200
Los Angeles, CA 90007
Radford G. King, Exec. Director
(213) 743-8988
(800) 642-2872 (CA only)
(800) 872-7477 (toll-free US)

NASA/SU Industrial Applications Center
Southern University Department of Computer Science
Baton Rouge, LA 70813
Dr. John Hubbell, Director
(504) 771-2060

If you represent a public sector organization with a particular need, you can contact NASA's Application Team for technology matching and problem solving assistance. Staffed by professional engineers from a variety of disciplines, the Application Team works with public sector organizations to identify and solve critical problems with existing NASA technology. **Technology Application Team, Research Triangle Institute, P.O. Box 12194, Research Triangle Park, NC 27709. *Doris Rouse, Director,* (919) 541-6980**

How You Can Access Technology Transfer Services At NASA Field Centers: **Technology Utilization Officers & Patent Counsels—**Each NASA Field Center has a Technology Utilization Officer (TUO) and a Patent Counsel to facilitate technology transfer between NASA and the private sector.

If you need further information about new technologies presented in *NASA Tech Briefs,* request the Technical Support Package (TSP). If a TSP is not available, you can contact the Technology Utilization Officer at the NASA Field Center that sponsored the research. He can arrange for assistance in applying the technology by putting you in touch with the people who developed it. If you want information about the patent status of a technology or are interested in licensing a NASA invention, contact the Patent Counsel at the NASA Field Center that sponsored the research. Refer to the NASA reference number at the end of the Tech Brief.

Ames Research Ctr.
Technology Utilization Officer: Laurance Milov
Mail Code 223-3
Moffett Field, CA 94035
(415) 694-6471
Patent Counsel: Darrell G. Brekke
Mail Code 200-11
Moffett Field, CA 94035
(415) 694-5104

Lewis Research Center
Technology Utilization Officer: Daniel G. Soltis
Mail Stop 7-3
21000 Brookpark Road
Cleveland, OH 44135
(216) 433-5567
Patent Counsel: Gene E. Shook
Mail Code 301-6
21000 Brookpark Road
Cleveland, OH 44135
(216) 433-5753

National Space Technology Laboratories
Technology Utilization Officer: Robert M. Barlow
Code GA-00
NSTL Station, MS 39529
(601) 688-1929

John F. Kennedy Space Center
Technology Utilization Officer: Thomas M. Hammond
Mail Stop PT-TPO-A
Kennedy Space Center, FL 32899
(305) 867-3017
Patent Counsel: James O. Harrell
Mail Code PT-PAT
Kennedy Space Center, FL 32899
(305) 867-2544

Langley Research Ctr.
Technology Utilization Officer: John Samos
Mail Stop 139A
Hampton, VA 23665
(804) 865-3281
Patent Counsel: George F. Helfrich
Mail Code 279
Hampton, VA 23665
(804) 865-3725

Goddard Space Flight Center
Technology Utilization Officer: Donald S. Friedman
Mail Code 702
Greenbelt, MD 20771
(301) 286-6242
Patent Counsel: R. Dennis Marchant
Mail Code 204
Greenbelt, MD 20771
(301) 286-7351

Jet Propulsion Lab.
NASA Resident Office
Technology Utilization Officer: Gordon S. Chapman
Mail Stop 180-801
4800 Oak Grove Drive
Pasadena, CA 91109
(818) 354-4849
Patent Counsel: Paul F. McCaul
Mail Code 180-801
4800 Oak Grove Drive
Pasadena, CA 91109
(818) 354-2734
Technology Utilization Mgr. for JPL: Norman L. Chalfin
Mail Stop 156-211
4800 Oak Grove Drive
Pasadena, CA 91109
(818) 354-2240

George C. Marshall Space Flight Center
Technology Utilization Officer: Ismail Akbay
Code AT01
Marshall Space Flight Center, AL 35812
(205) 544-2223
Patent Counsel: Leon D. Wofford, Jr.
Mail Code CC01
Marshall Space Flight Center, AL 35812
(205) 544-0024

Lyndon B. Johnson Space Center
Technology Utilization Officer: Dean C. Glenn
Mail Code EA4
Houston, TX 77058
(713) 483-3809
Patent Counsel: Edward K. Fein
Mail Code AL3
Houston, TX 77058
(713) 483-4871

NASA Headquarters
Technology Utilization Officer: Leonard A. Ault
Code CU
Washington, DC 20546
(202) 453-2119
Assistant General Counsel for Patent Matters: Robert F. Kempf, Code GP
Washington, DC 20546
(202) 453-2424

A Shortcut To Software: **COSMIC®**—For software developed with NASA funding, contact COSMIC, NASA's Computer Software Management and Information Center. New and updated programs are announced in the Computer Programs section. COSMIC publishes an annual software catalog. For more information call or write: **COSMIC®**, 382 East Broad Street, Athens, GA 30602 *John A. Gibson, Dir.,* (404) 542-3265

If You Have a Question . . . **NASA Scientific & Technical Information Facility** can answer questions about NASA's Technology Utilization Network and its services and documents. The STI staff supplies documents and provides referrals. Call, write or use the feedback card in this issue to contact: **NASA Scientific and Technical Information Facility,** Technology Utilization Office, P.O. Box 8757, Baltimore, MD 21240-0757. *Walter M. Heiland, Manager,* (301) 859-5300, Ext. 242, 243

Electronic Components & Circuits

Hardware, Techniques, and Processes

Books and Reports

Single-Layer, Multicolor Electroluminescent Phosphors

Etching is eliminated in producing phosphor layers for displays.

Langley Research Center, Hampton, Virginia

A new method has been conceived for the construction of a single phosphor layer composed of two or more different color phosphors for use in thin-film electroluminescent (TFEL) displays. In order to display the full color spectrum, including white, electronic displays must have the three primary colors red, green, and blue. Full-color TFEL displays, therefore, require red, green, and blue phosphors placed close together side-by-side in the same layer or in separate superimposed layers or in some combination of the two. The phosphor layers in a TFEL display device are formed by vacuum deposition of the phosphors, in thicknesses of 2,000 to 5,000 Å, onto a glass substrate that already has on one surface a pattern of transparent electrodes covered with a transparent insulating layer.

Prior methods for producing the single-layer, two-color phosphor layers for TFEL displays involve deposition, masking, and etching of both the red and green phosphors. The etching steps are very difficult to control and result in low yield and high cost for display production. Also, the etching leaves, on the phosphor layer, an uneven surface that promotes dielectric breakdown in the insulating layer that covers the phosphor in a TFEL display device.

The new process enables the production of the single-layer, two-color phosphor layer without etching. The method of construction, beginning with the glass substrate with electrode and insulator layers, involves the deposition of the green phosphor, $ZnS:TbF_3$; masking with a metal mask or photoresist; diffusion or ion implantation of manganese through the mask to produce the red phosphor, $ZnS:Mn:TbF_3$; and removal of the mask.

This technique can also be used to produce both single-layer, two-color phosphors of other colors and single-layer, three-color phosphors. The phosphors must be of the same host material, but with different impurities. A two-color example is $SrS:Ce_2S_3$ (red) and $SrS:CeF_3$ (blue). A three-color example is ZnS:Mg (blue),

$ZnS:Mn:TbF_3$ (red), and $ZnS:TbF_3$ (green).

This work was done by James B. Robertson of **Langley Research Center**. *For further information, Circle 121 on the TSP Request Card.*

This invention is owned by NASA, and a patent application has been filed. Inquiries concerning nonexclusive or exclusive license for its commercial development should be addressed to the Patent Counsel, Langley Research Center [see page 16]. Refer to LAR-13616.

Maser Oscillator With Dielectric Resonators

A two-resonator design should yield low phase noise.

NASA's Jet Propulsion Laboratory, Pasadena, California

A proposed sapphire-maser oscillator would exhibit phase noise intermediate between the phase noises of unstabilized microwave oscillators and those of stabilized ruby-maser oscillators with superconducting cavities. Instead of the conventional single resonator, the oscillator would contain two total-internal-reflection (TIR) dielectric resonators in a normally-conductive (that is, nonsuperconductive) copper cavity. Because the TIR resonators would not require superconductivity to achieve a relative bandwidth of 10^{-7} to 10^{-8}, the oscillator could be operated at a relatively high temperature — typically at 10 to 80 K — for which inexpensive commercial coolers are available. The oscillator would also not include the magnets that are required in ruby masers.

The two resonators would have a wheel-like ring-and-disk configuration (see figure). The upper resonator, made of sapphire doped with iron, would be sized and shaped to operate at the 31-GHz pump frequency appropriate for iron/sapphire masing at zero applied magnetic field. The pump signal would be coupled in through a coaxial cable. This resonator would be made with only as much dielectric as is

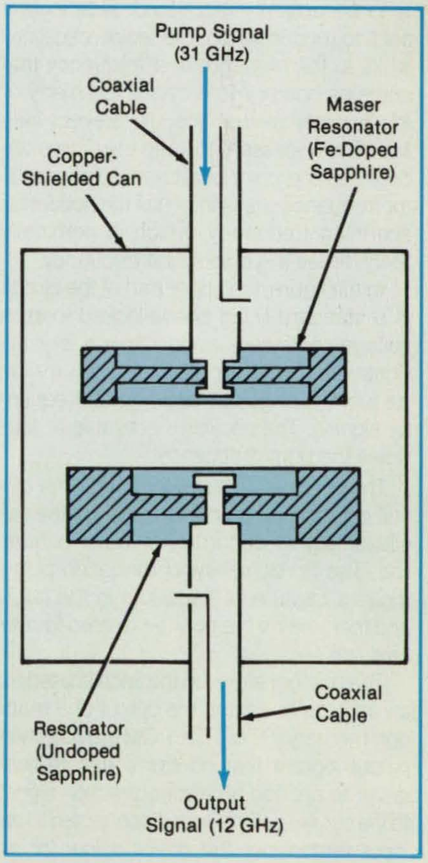

The **Two-Resonator Maser Design** would provide phase stability, isolation between the pump and output channels, and variable maser coupling.

necessary to contain the resonant electromagnetic mode, so that its entire volume could be pumped for effective regeneration of whatever signal fields are coupled to it from the lower resonator.

The lower resonator would be made of sapphire in a size and shape to resonate at the 12-GHz output-signal frequency of iron/sapphire masing. Like the upper resonator, this one is also designed to suppress the plethora of resonant modes (other than the desired one) that is ordinarily characteristic of older disk-and-cylinder resonators. The output signal would be coupled through a second coaxial cable.

Because the iron-atom maser spins are coupled to both the pump and signal frequencies via the radio-frequency magnetic field and because the fields are confined to the TIR resonators primarily by dielectric effects, the fringing magnetic fields would be used to couple the spins in the lower and upper resonators. The distance between the resonators would be adjusted by a conventional mechanical tuning mechanism to vary the degree of coupling.

This work was done by G. John Dick and Donald M. Strayer of Caltech for **NASA's Jet Propulsion Laboratory**. *For further information, Circle 132 on the TSP Request Card.*

This invention is owned by NASA, and a patent application has been filed. Inquiries concerning nonexclusive or exclusive license for its commercial development should be addressed to the Patent Counsel. NASA Resident Office-JPL [see page 16]. Refer to NPO-17157.

Burst-Locked Oscillator Avoids Side Lock

A counting circuit corrects errors when side lock occurs.

Lyndon B. Johnson Space Center, Houston, Texas

A digital error-detection-and-correction circuit in a color-television oscillator circuit provides synchronization when the color-burst frequency has drifted outside the normal tolerance. Such deviations of frequency often occur in playback from videodisk or tape records.

Each line of a color-television signal contains a short burst (the color burst) of a reference frequency to which the color oscillator of the receiver must be locked in phase if the color information in the signal is to be properly recovered. Side lock is said to occur when the color oscillator locks to the burst but at a frequency that contains one or more cycles too many or too few per picture line. To prevent side lock, it is necessary to keep the difference between the color-burst and color-oscillator frequencies less than half the horizontal scanning frequency, which is nominally 2/455 times the color-burst frequency.

In the figure, the upper part of the circuit is a standard burst phase-locked loop. A voltage-controlled, rather than a crystal-controlled, oscillator is used to allow a wide frequency range for following off-frequency signals. The oscillator operates at four times the burst frequency.

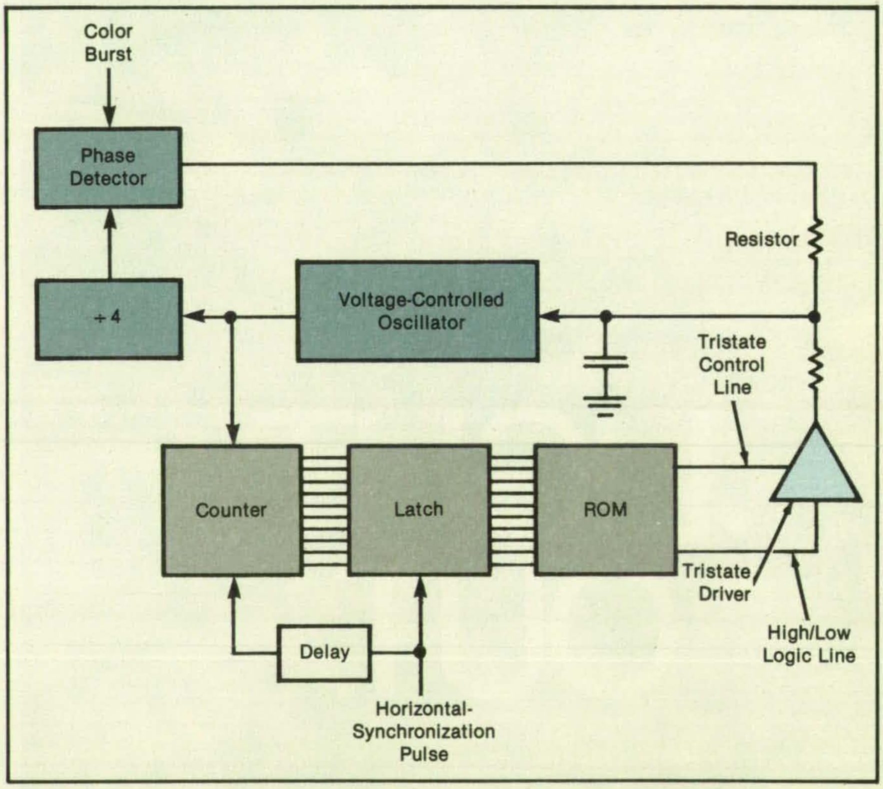

A **Digital Side-Lock-Prevention Circuit** is used in a television color-burst phase-lock-loop oscillator to provide greater tolerance of off-frequency signals than do crystal-controlled oscillators.

The counter in the lower part of the circuit counts the number of cycles of the oscillator signal occurring in each picture line. The horizontal-synchronization pulse triggers capture of the count in the latch and then resets the counter to zero for the next line.

The number stored in the latch is used as an address to control the output of a read-only memory (ROM). The ROM provides two output signals that control a tristate line-driver to provide an error-correction signal to the oscillator. One output connected to an input terminal of the driver is low for all counts (addresses) less than 909 and high for all counts above 909.

The second ROM output controls the tristate input of the driver. When the count is either 908 or 909, the oscillator is deemed to be producing the correct number of cycles per line, and the output from the ROM tristates (in effect, disconnects) the output of the driver. For other counts, side lock has occurred, and the driver provides the high or low output necessary to cause the oscillator to shift toward the frequency that will eliminate the side lock.

This work was done by Robert A. Dischert of RCA Corp. for **Johnson Space Center**. *No further documentation is available.*

Title to this invention has been waived under the provisions of the National Aeronautics and Space Act [42 U.S.C 2457(f)], to the RCA Corp. Inquiries concerning licenses for its commercial development should be addressed to

RCA Corp
Patent Operations
P. O. Box 432
Princeton, NJ 08543

Refer to MSC-21257, volume and number of this NASA Tech Briefs *issue, and the page number.*

Equations for Rotary Transformers

A common textbook problem is solved.

NASA's Jet Propulsion Laboratory, Pasadena, California

Equations have been derived for the input impedance, input power, and ratio of secondary current to primary current of a rotary transformer. The equations can be used for the quick analysis of transformer designs and are easy to set up on a programmable hand-held calculator or desktop computer.

The circuit model is one commonly used in textbooks on the theory of ac circuits (see figure). An ac voltage source of amplitude V drives the current I_1 in a primary winding of resistance R_1 and self-inductance L_1. Acting through mutual inductance M, the primary current induces a current I_2 in the secondary winding, which has self-inductance L_2. The total resistance of the secondary winding plus the load connected to the secondary winding is R_2.

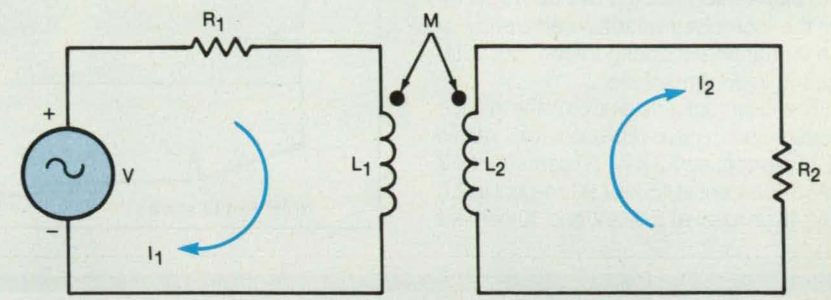

Primary Loop: $I_1 (R_1 + j\omega L_1) - j\omega M I_2 = V$
Secondary Loop: $I_2 (R_2 + j\omega L_2) - j\omega M I_1 = 0$

The **Loop Equations for a Rotary Transformer Circuit** are easily solved, resulting in the equations shown in the text.

The coupled loop equations for I_1 and I_2 are straightforward and are solved easily, yielding the following results:

(1) Input impedance =

$$Z = (R_2^2 + \omega^2 L_2^2)^{-1} \{R_1 R_2^2 + \omega^2(M^2 R_2 + R_1 L_2^2) + j\omega[R_2^2 L_1 + L_2 \omega^2 (L_1 L_2 - M^2)]\}$$

where ω is the angular frequency and j represents the imaginary axis in the complex plane.

(2) Input power =

$$P = V^2 Re(Z)/Z^2$$

where $Re(Z)$ is the real part of Z.

(3) Secondary current/primary current =

$$I_2/I_1 = \omega M/(R_2^2 + \omega^2 L_2^2)^{1/2}$$

This work was done by Phil M. Salomon, Peter J. Wiktor, and Carl A. Marchetto of Caltech for **NASA's Jet Propulsion Laboratory**. *For further information, Circle 148 on the TSP Request Card.* *NPO-17120*

Improved Charge-Coupled Imager for X Rays

Quantum efficiency and resolution would be increased.

NASA's Jet Propulsion Laboratory, Pasadena, California

A virtual-phase charge-coupled device has been proposed to improve the imaging of x rays with photon energies of 0.2 to 10 keV. The anticipated benefits of the new design include higher spatial and spectral resolution and greater quantum efficiency at low photon energies. Potential applications include imaging spectrometers for x-ray astronomy, investigations of plasmas, and x-ray crystallography.

In a conventional multiphase charge-coupled device, the sensitivity to photons of less than about 2 keV is degraded by the absorption of these photons in such "dead layers" as the oxide and gate structures. Sensitivity can be restored by the use of a virtual-phase configuration and by decreasing the thickness of the oxide in the virtual phase to 500 Å.

However, without further modification, a conventional virtual-phase charge-coupled device exhibits a loss of spatial resolution with photons of 2 to 10 keV. Such photons are absorbed below the charge-carrying and depleted regions. When charge is thus generated below the depleted region, it moves toward the charge-carrying region and spreads out. Thus, portions of the charge are detected in several adjacent picture elements whereas it is desired to detect it only in the picture element or elements struck by the photons.

In the proposed device (see figure), the depletion depth would be about 10 μm comparable to the thickness (10 to 15 μm) of the epitaxial layer on which the device is fabricated. This feature

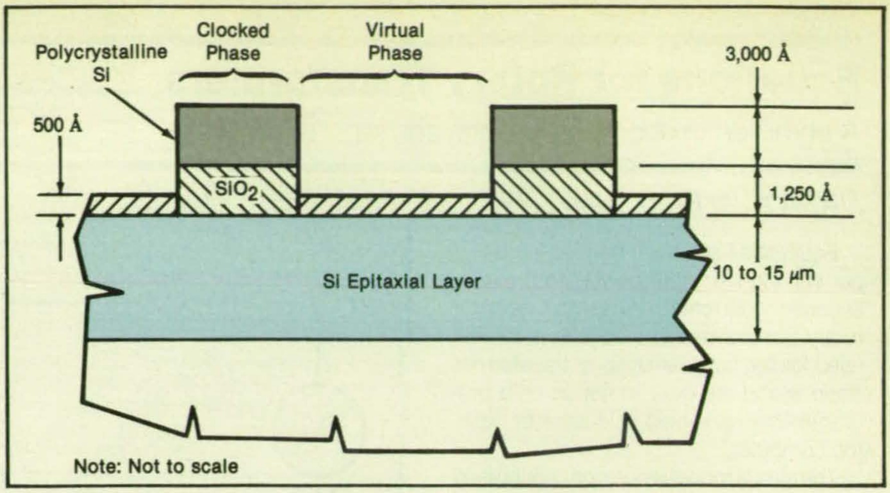

The **Improved Virtual-Phase Charge-Coupled Device** would feature a thin layer of oxide in the virtual phase to increase the quantum efficiency and a depletion layer nearly as thick as the epitaxial silicon layer to increase the resolution.

is expected to prevent the spreading of photogenerated charge to adjacent picture elements. Thus the device would offer the increased quantum efficiency of the virtual-phase configuration, but without the loss of resolution.

The quantum efficiency of the device is predicted to have representative values of 33 percent at 0.2 keV, 76 percent at 0.7 keV, 69 percent at 1.5 keV, 90 percent at 2.0 keV, 45 percent at 5.0 keV, and 10 percent at 10 keV. Numerical simulations indicate that the required deep depletion can be achieved by the use of a high-resistivity substrate doped at 1.5×10^{14} cm^{-3}, with a phosphorus implant of 1.5×10^{12} cm^{-2} at 190 keV and an arsenic implant of 3×10^{12} cm^{-2} at 25 keV.

This work was done by Mark Wadsworth of Texas Instruments, Inc., for **NASA's Jet Propulsion Laboratory**. *For further information, Circle 17 on the TSP Request Card.*

Inquiries concerning rights for the commercial use of this invention should be addressed to the Patent Counsel, NASA Resident Office-JPL [see page 16]. Refer to NPO-17312.

Microwave Transmitter With Multimode Output Section

The output-waveguide structure would transport 400 kW of continuous-wave signal power at 34.5 GHz.

NASA's Jet Propulsion Laboratory, Pasadena, California

A proposed 34.5-GHz transmitter with a unique output-waveguide section would generate as much as 400 kW of continuous-wave (CW) signal power. The microwave transmitter would include a traveling-wave-tube preamplifier that feeds a gyroklystron final amplifier operating at 100-kV, 10-A power input. Extensive monitoring and controlling circuitry would be provided, including 20 major safety interlocks associated with the gyroklystron stage alone.

The main feature of the conceptual design of this microwave transmitter is the output section (see figure), which is intended to perform multiple functions. The signal is coupled out of the gyroklystron through a window 2.5 in. (6.35 cm) in diameter, the optimum size for the gyroklystron operation. A rippled-wall mode converter and associated tapers (see figure) will convert the circularly polarized TE_{12} output mode of the gyroklystron into the required circularly polarized TE_{11} mode. The final output diameter for the waveguide system is 1.75 in. (4.44 cm). This diameter was chosen for two reasons: (1) because it was the approximate aperture size required for efficient illumination of the associated Cassegrain antenna and thus eliminated the need for a tapered feedhorn and (2) because of its ability to transport the 34.5-GHz signal with relatively low loss in the TE_{11} mode. In addition, the large diameter is required to transport the 400-kW CW signal reliably (i.e., without waveguide breakdown).

The gyroklystron output power is predominantly in the TE_{12} mode. This TE_{12} power is then converted to the TE_{11} mode with high efficiency in the mode-converter section (see figure). Propagation through the rippled-wall waveguide is described by a set of coupled wave equations. Numerical techniques are used to solve the equations, and the number of ripples, ripple amplitude, and ripple period are determined for optimum TE_{12}-to-TE_{11} mode conversion. However, neither the gyroklystron or mode-converter output will be free of spurious mode power.

Therefore, the directional couplers required for monitoring the forward and reflected TE_{11} power must be both directive and mode selective. A coupled-transmission-line analysis leads to the design of such a directional coupler, the general configuration of which is shown at the upper-right portion of the figure. Uniformly spaced, round coupling holes and an axially tapered coupling profile will provide a coupling factor of −70 dB in the forward and reverse direction, 40 dB of directivity, and spurious-mode discrimination of more than 25 dB. Two coupler arms measuring the orthogonal linear TE_{11} modes will be combined to monitor the circularity of the TE_{11} mode power.

The transmission line terminates in a multimode feed section with corrugations of varying depth. Propagation through the feed section is analyzed using mode-matching methods, and slot-depth profile is adjusted to give a suitable radiation pattern. As the signal travels along this section, the incident TE_{11} mode is transformed into the balanced HE_{11} mode, which possesses a circularly symmetric radiation pattern with theoretically no cross polarization; the HE_{11} mode is suitable for illumination of the Cassegrain subreflector. The predicted directional output pattern of this output section is shown at the lower-right portion of the figure.

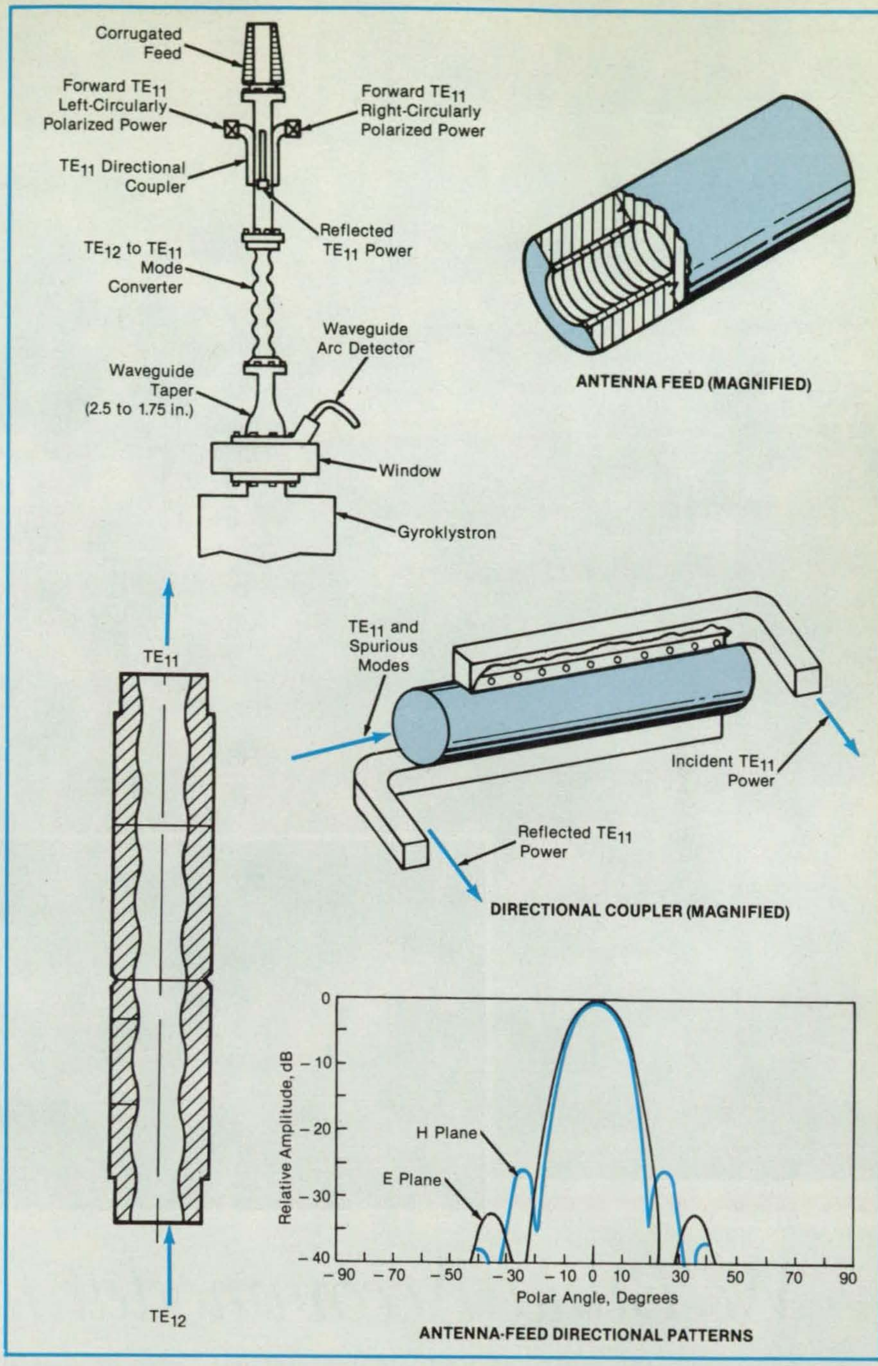

The **Output Waveguide Structure** includes a mode converter, directional coupler, polarization monitor, and a corrugated overmoded output section. The output directional pattern (bottom right) is suitable for antenna illumination without a flared feedhorn.

This work was done by Daniel J. Hoppe, Alaudin M. Bhanji, and Reginald A. Cormier of Caltech for **NASA's Jet Propulsion Laboratory**. *For further information, Circle 37 on the TSP Request Card.*
NPO-16826

Books and Reports

These reports, studies, handbooks are available from NASA as Technical Support Packages (TSP's) when a Request Card number is cited; otherwise they are available from the National Technical Information Service.

Effects of Radiation on Electronics — Additional References

A bibliography with abstracts covers literature from 1984 and 1985.

The first volume of a three-volume series of bibliographies with abstracts summarizes the literature on the effects of radiation on new electronic devices. The cited literature also includes items about sources of radiation and test facilities. The bibliography is addressed to radiation test engineers. This and the second volume cover the years 1984 and 1985. The third volume, which covers 1982 and 1983, was described previously. [See "More on Effects of Radiation on Electronics" (NPO-

17019) on page 35 of *NASA Tech Briefs,* Vol. 11, No. 7.]

The types of radiation discussed include protons, electrons, neutrons, x rays, γ rays, and ions ranging in energy from 0 to over 20 GeV. Among the semiconductor materials covered are Si, GaAs, and GaAlAs. Devices covered include transistors, integrated circuits, photodetectors, microprocessors, and dosimeters.

The abstracts are primarily from U.S. sources, including conference proceedings and research journals. The authors' original abstracts are used except where they are too lengthy or vague. The abstracts are grouped in four categories:

1. Dose-Rate Effects,
2. New Technology,
3. Post-Irradiation Effects, and
4. Test Environments.

Abstracts bearing on more than one category are repeated in each applicable category. Each abstract lists all of the categories under which it appears. Within a category, abstracts are in alphabetical order by primary author. An index of primary authors is provided.

This work was done by Frank L. Bouquet of Caltech for **NASA's Jet Propulsion Laboratory**. *To obtain a copy of the report, "Bibliography of Total Dose Radiation Effects on Electronics, Volume I," Circle 126 on the TSP Request Card. NPO-16958*

Integrated Arrays of Infrared Detectors

The state of the technology is surveyed.

A report presents an overview of the technology of integrated arrays of infrared detectors. The report covers arrays now available and those under development. It gives examples of astronomical images that illustrate the potential of infrared arrays for scientific investigations.

Integrated arrays combine detection and readout-multiplexing functions in integral packages. In principle, they can be made from a variety of intrinsic and extrinsic infrared-sensitive materials. Intrinsic materials like indium antimonide and mercury cadmium telluride are generally employed in photovoltaic detectors. Extrinsic materials like silicon doped with gallium and silicon doped with arsenic are generally employed in photoconductors or photocapacitors. Techniques for growing crystals, ensuring purity, and forming contacts are highly advanced, and integrated arrays now achieve nearly ideal performance. Limitations to sensitivity are imposed primarily by the readout circuitry, which can be based on charge-coupled devices, charge-injection devices, or switched field-effect transistors.

At present, integrated infrared arrays are made by hybrid methods. Two distinct substrates are used; by designing and processing the detector and multiplexer substrates separately and "bump bonding" them together, optimum performance can be obtained from each. Indium-bump-bonding techniques are now well established, and interconnection yields of 100 percent for 32-by-32 arrays are common.

The performances of switched field-effect transistor multiplexers, which offer the greatest sensitivity, are expected to improve further. Meanwhile, development continues on advanced detector and readout concepts like impurity-band conduction arrays, which offer the potential of superior sensitivity, linearity, and ability to withstand radiation. Also promising is an arsenic-doped silicon solid-state photomultiplier; such a device has already counted single-photon events at a wavelength of 28 μm.

This work was done by J. H. Goebel and C. R. McCreight of **Ames Research Center**. *Further information may be found in NASA TM-88357 [N87-18475/NSP], "Integrated Infrared Array Technology."*

Copies may be purchased [prepayment required] from the National Technical Information Service, Springfield, Virginia 22161, Telephone No. (703) 487-4650. Rush orders may be placed for an extra fee by calling (800) 336-4700.

Inquiries concerning rights for the commercial use of this invention should be addressed to the Patent Counsel, Ames Research Center *[see page 16].* *Refer to ARC-11787.*

Electronic Systems

Hardware, Techniques, and Processes

Books and Reports

Mobile Communication Via Satellite

A system would mix real-time and delayed-transmission channels.

NASA's Jet Propulsion Laboratory, Pasadena, California

A proposed architecture for mobile communication by satellite would enable both real-time and store-and-forward packet transmission. The real-time, or open-end, mode would be used for voice communication. The store-and-forward, or closed-end, mode would be used for data communication when a modest delay is acceptable. The system would adapt the mix of modes to user demand.

A satellite mobile system is similar to a ground-based mobile system in which users in vehicles can communicate with other users in vehicles or at fixed locations, and vice versa, when they are within line of sight of relay towers. However, in the satellite system, the "relay tower" is 36,000 km above the Earth. It will thus provide blanket coverage of an entire continent.

The traffic in such a system will not be homogeneous. Some users will need short-burst transmissions typical of interactive data transactions, while others will want open-end channel assignments for conversations or the transfer of large data files. The network design is further complicated by the uncertainty about the locations of subscribers roaming over a vast geographical area, the multipath fading that constantly works against the reliability of transmission, and the propagation delay of satellite systems.

To function successfully under these conditions, the network must conserve the frequency spectrum, maximize throughput, and minimize the end-to-end service delay and service-blocking probability. Above all, the network should be modular so that it lends itself to evolution and integration of new technologies as they become available.

A network-management center will be the most important element of the network and will coordinate service to millions of geographically dispersed subscribers. Users will gain access to the system through a mobile terminal, a base station,

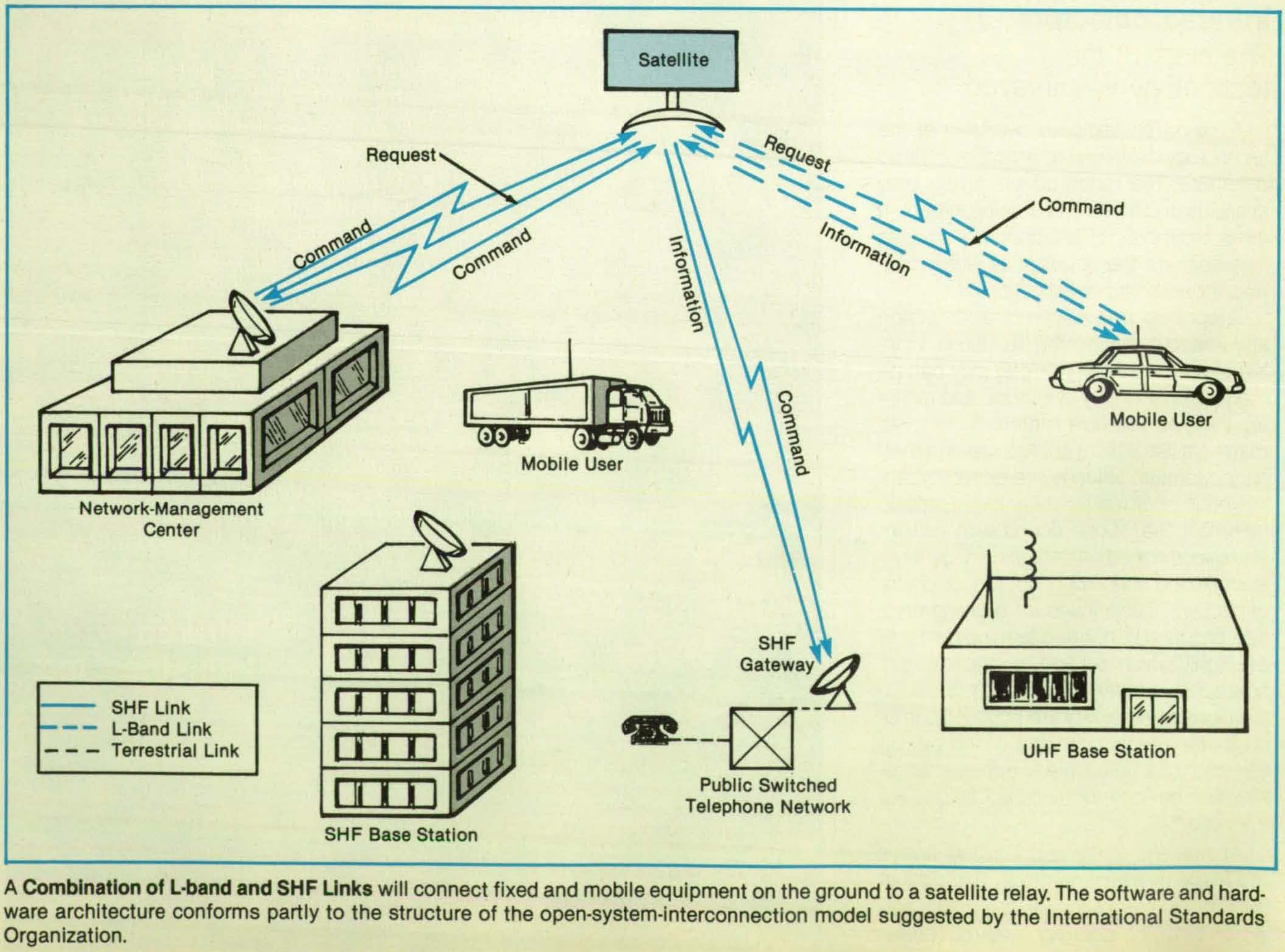

A **Combination of L-band and SHF Links** will connect fixed and mobile equipment on the ground to a satellite relay. The software and hardware architecture conforms partly to the structure of the open-system-interconnection model suggested by the International Standards Organization.

or an external switched network connected to a gateway (see figure).

The satellite will merely perform frequency translations. It will have multiple L-band beams at various frequencies so that a given frequency can be reused in nonadjacent beams, and thus will conserve the scarce frequency-spectrum resource. The backhaul communication will be provided by a single full-coverage super-high-frequency (SHF) beam. Distinct SHF bands will correspond to the multiple L-band beams.

All communications, including SHF/SHF between base stations, between gateways, and between base stations and gateways, will go through the satellite. Communications between mobile terminals will need two hops through the satellite, with an intermediate gateway or base station providing the necessary SHF/SHF translation. The mobile terminals will communicate with the satellite at L-band. The satellite will translate each 5-kHz L-band channel to or from a unique SHF channel to connect a mobile terminal to the network-management center, a base station, or a gateway.

Each L-band beam will contain two "overhead" channels. A pilot channel will enable a mobile terminal to identify the L-band beam in which it is located and to acquire the initial frequency synchronization. A wake-up channel will enable the mobile terminal to acquire the timing-reference and channel-access information.

The remaining channels are classified as either control or information channels. Control channels, in turn, are divided into the following two types:

1. Request channels, allocated to return links (L-band to SHF) only, will be used by the mobile terminals to request connections.
2. Command channels, allocated to forward links (SHF to L-band or SHF to SHF) only, will be used by the network-management center to send control information to the network elements. The information includes channel assignments and information on the status of the network.

Information channels will be used, as the name implies, for the transfer of information. They will be set up, on request, between mobile terminals and either base stations or gateways. An information channel could be either an open-end or a closed-end channel.

For each L-band beam, the network-management center will maintain a pool of request, open-end, and closed-end channels on the return links. It will maintain a similar pool of command, open-end, and closed-end channels on the forward links. It will adaptively adjust the partition of the channel types according to two performance measures: the end-to-end average delay for closed-end requests and the blocking probability for open-end requests.

This work was done by Tsun-Yee Yan and Firouz M. Naderi of Caltech for **NASA's Jet Propulsion Laboratory**. *For further information, Circle 42 on the TSP Request Card.*

Inquiries concerning rights for the commercial use of this invention should be addressed to the Patent Counsel, NASA Resident Office-JPL [see page 16]. Refer to NPO-17041.

Analog Sensor of Large-Amplitude Displacements

A noninvasive device measures large amplitudes even at low frequencies.

Langley Research Center, Hampton, Virginia

Delicate, large space structures have shown some adverse changes in motion due to the attachment of measuring devices. This problem generated a need for noninvasive measurements, at a significant number of locations, of a model subjected to large-amplitude displacements. Most devices now in use are attached electrically and/or mechanically. For example, there are devices that are on the model, such as strain gauges and accelerometers, and those that touch the model, such as linear variable-differential transformers (LVDT's). Proximity devices, laser reflectors, and optical target devices are complicated, expensive, and inaccurate. On the other hand, the model analog position sensor (see figure) is easily set up or relocated, requires little from the model to be measured, and is an inexpensive and practical solution to the problem.

Such sensors are a line of limited-view light cells attached to logic circuits that keep track of the passing dark edge and that put out a signal proportional to the change in location of the model. The output signal can be digital, or it can be converted to analog.

The model can be dark against a bright background or well lighted against a dark background. The brightness can come from sources as small as ordinary office light. The model can be as much as 6 ft (1.8 m) away and moving, and it does not have to be moving only in the plane of the sensing device. The field of view of each sensing element is a cone less than 8° wide. The output from each sensing element is interpreted by electronic latches to keep track of the moving leading edge of the model. The system can locate a model that has little mass and is as small as a human finger moving at large amplitudes, and it does not intrude on the model being measured.

While motivated by requirements for large space structures, this device could be of use in many other applications, including the opening and closing of automatic doors as far and as fast as needed. This type of low-angle, light-sensitive device can be designed as a self-contained unit to measure large amplitudes, even at low frequencies where accelerometers are not adequate.

This work was done by Robert Miserentino of **Langley Research Center** *and William C. White of Wyle Laboratories.*

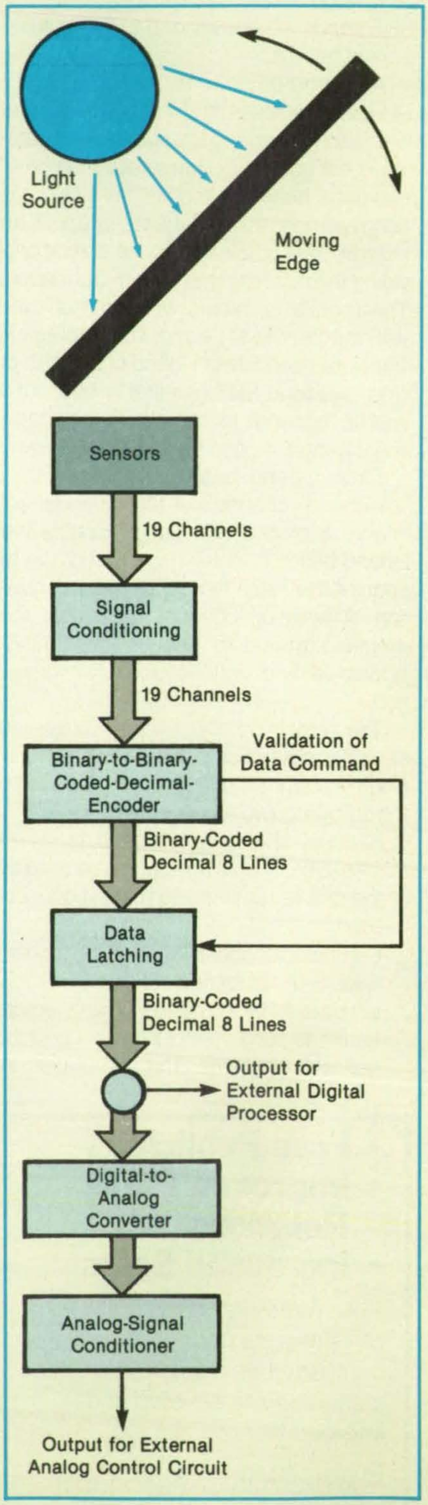

The **Low-Angle, Light-Sensitive System** can track the moving leading edge of a model.

No further documentation is available.
LAR-13731

THE BEST OF BOTH WORLDS

FROM

DATATAPE INCORPORATED

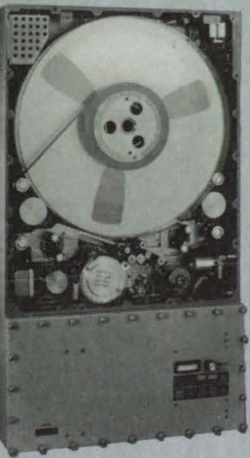

DTR-70-3
ROTARY WIDEBAND ANALOG INSTRUMENTATION RECORDER/ REPRODUCER

DDR-100
ROTARY DIGITAL AIRBORNE RECORDER

The DATATAPE DTR-70-3 fills the need for an analog portable system which can record and/or reproduce a great variety of wideband signal data such as a Serial Digital Data Stream, Radar, Communications, FLIR and Multi-line Rate Video Imagery, FDM, PSK Pre Detect and PCM Post Detect Data Signals.

- ✓ *MORE* **Record Time 5.7 Hours**
- ✓ *MORE* **Bandwidth 10 Hz - 8 MHz**
- ✓ *MORE* **Reliability, System MTBF >1600 Hrs**
- ✓ *LESS* **Power 120 Watts**
- ✓ *LESS* **Weight (Acquisition) 70 Lbs**
- ✓ *LESS* **$$, You Have to Ask to Believe It**

- Single Wideband Data Channel Plus One Voice/ Event Marking Channel
- Built-in Confidence Monitor With Go/No-Go LED Display For System Integrity
- DTR-70-3 Can Be Configured For Acquisition Only, Quick Look, or Full Up Record/Reproduce System
- Analog-Digital
- Integrity During Record Mode

The DDR-100 is DATATAPE's newest solution to high data rate recording for hostile environments. Ideally designed to provide multiple data rate acquisition for high rate digital sensors, E/O, SAR, SLAR, photo optical systems, or multiplex acoustic data.

- ✓ *MORE* **Record Time 5.5 Hours**
- ✓ *MORE* **Bandwidth 6.25 to 100 MBPS**
- ✓ *MORE* **Data Capacity 1.98 Terabits/Reel**
- ✓ *MORE* **Reliability, MTBF >2500 Hrs**
- ✓ *LESS* **Weight 76 Lbs with Tape**
- ✓ *LESS* **Power 95 Watts**
- ✓ *LESS* **$$, You Have to Ask to Believe It!**

- Single or Dual Wideband Data Plus Three Aux Tracks
- Built-in Record-Valid Monitor
- MIL-E-5400 Airborne Qualified
- Capable of Expansion up to 200 MBPS
- Auto Record for Constant Packing Density
- Up to 44 Hours at 12.5 MBPS

When you need MORE for LESS, look to DATATAPE, the complete recorder company.

360 Sierra Madre Villa • Pasadena, CA 91109-7014 • (818) 796-9381 Ext. 2597

NOTE: All specifications shown are subject to change without notice.

Kodak leading technology: the DATATAPE advantage.

DATATAPE INCORPORATED
A KODAK COMPANY

Kodak

Wideband Digital Interface Unit

Signals are converted from serial to parallel and buffered for input to a computer.

NASA's Jet Propulsion Laboratory, Pasadena, California

A wideband interface unit (see figure) receives wideband signals containing blocks of digital data, converts them to 16-bit words, and buffers them for input to the direct-memory-access (DMA) port of a host computer. The principal novel features of the unit are two very-large-scale-integrated circuits: (1) one that detects a pseudonoise-code synchronizing signal for the blocks of data and (2) a programmable random-access-memory to first-in- first-out (RAM-to-FIFO) converter, that buffers the data and releases them to the host computer when that computer is ready to receive them. Previously, many circuit chips were required to perform these functions.

The incoming signal is in blocks of 4,800 serial bits (300 16-bit words), of which 24 bits are the synchronizing pseudonoise code. Once the interface unit has found the pseudonoise code in a given block, it can synchronize and examine a sequence of bits that specify the format of that block. If the block-format code identifies the data in the remainder of the block as filler, the block is discarded; otherwise, the 16-bit status word associated with processing is appended to the block, and the resulting block of serial bits is converted into 301 16-bit words and loaded into the FIFO buffer. Any time after the first word has been placed in the FIFO buffer, data can be transferred to the host computer via the DMA adapter.

There are three operating modes: idle, command, and data acquisition. After power is applied, the interface unit waits in idle mode, until system software issues a command. When the host computer is ready to receive wideband data, it sends a "reset" command followed by the "start" command. The interface unit completes the reset cycle, synchronizes on the bits of the wideband data, and then starts transferring data to the host computer via DMA. The host computer controls the transfer of data via three program input/output registers located in the DMA adapter.

Before bits can be synchronized, the two correlator chips must be loaded with the pseudonoise code, the mask code, and the number of correlations needed for a match. This is done under microsequencer control. Data stored in the read-only memory are loaded into both correlator chips during the reset cycle. When the starting bit is received, the synchronization of bits begins.

Data are clocked into both correlator chips, which continuously search the data for the synchronization codes. Once such a code is detected and the block-format

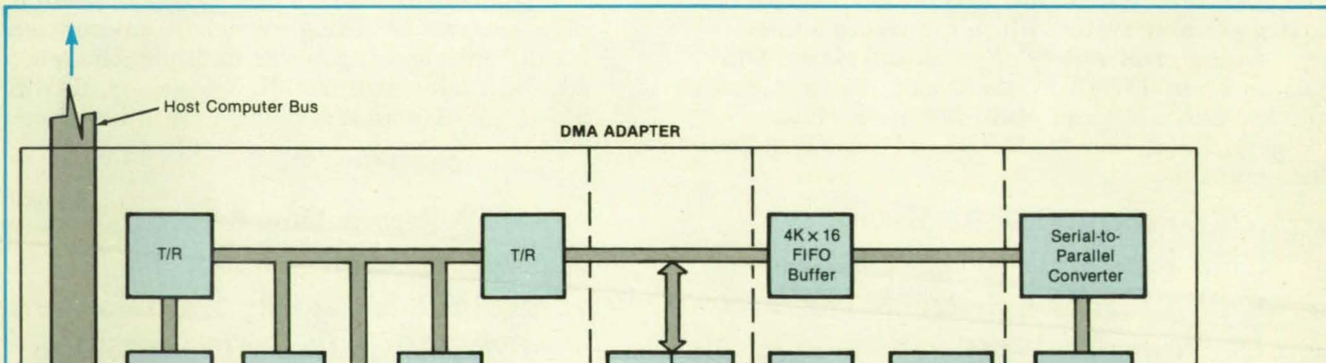

Notes:
1. "DMA" means "direct memory access."
2. "ESCR" means "external-control-and-status register."
3. "ROM" means "read-only memory."
4. "WCR" means "word-count register."
5. "T/R" means "tristate transceiver."
6. "FIFO" means "first-in/first-out."
7. "CSR" means "command-and-status register."
8. "BAR" means "buss-address register."

The **Wideband Digital Interface Unit** converts serial input data bits to 16-bit words and feeds them as needed to a host computer.

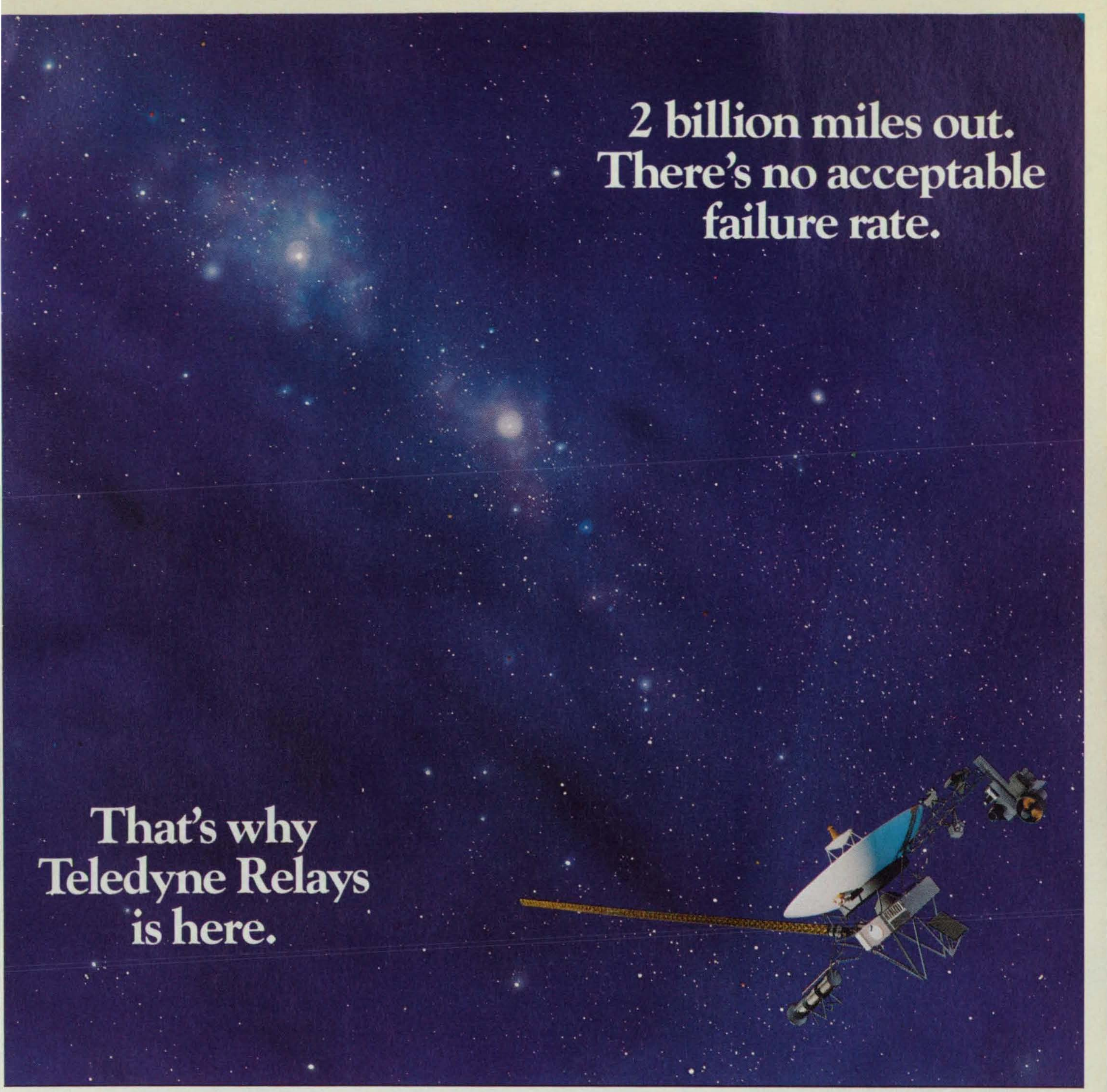

On Voyager 2, TO-5 electromechanical relays made by Teledyne Relays have spent eight years in deep space. And are still operating perfectly.

And this is only one example of the extraordinary reliability of TO-5 electromechanical relays from Teledyne Relays.

This reliability is the reason why the TO-5 has become the industry standard. And it's the reason designers keep specifying it for use in advanced technologies from space probes to weapons systems. From flight controls to test equipment.

In the 24 years since we invented the TO-5 Relay technology, we've supplied millions of relays to a very demanding market; because Teledyne's TO-5 electromechanical relays are not a compromise.

If you are working on a design which calls for unquestioned reliability, work with us. For applications on or under the sea. On or above the earth. Anywhere you need superior performance. Put our quarter century of experience to work for you.

Because—when there's no acceptable failure rate, there's only one acceptable choice—Teledyne Relays.

TELEDYNE RELAYS
Innovations In Switching Technology

12525 Daphne Ave., Hawthorne, California 90250 • (213) 777-0077
European Hqtrs: Abraham Lincoln Strasse 38-42, 6200 Wiesbaden, W. Germany • 06121-768
Belgium Sales Office: 181 Chaussee de la Hulpe, 1170 Brussels • (2) 673-99-88
U.K. Sales Office: Heathrow House, Bath Rd., Cranford, Hounslow, Middlesex, TW5 9QP • 1-897-2501
Japan Sales Office: Taikoh No. 3 Building, 2-10-7 Shibuya, Shibuya-Ku, Tokyo, 150 Japan • (3) 797-6956
France Sales Office: 85-87 Rue Anatole-France, 92300 Levallois-Perret • 1-7587160

Circle Reader Action No. 572

code checked to insure that the data are not filler, the input section forms the 16-bit words, loads them into the FIFO input register, and sends a message stating that the input buffer is filled. The input section also monitors the data clock. Should the clock stop during accumulation of data blocks, a "data clock timeout error" is posted in the external-control-and-status register (ECSR), causing an external interrupt signal, and the acquisition of data stops until the interface unit is reset by the host computer.

The FIFO buffer holds up to 13.6 wideband data blocks. Should the FIFO buffer overflow, a "FIFO overflow" status is posted in the ECSR, and an external interrupt occurs. The acquisition of data then halts until the interface is reset by the host computer. The FIFO buffer is loaded at the wideband input data rate and unloaded at the maximum DMA transfer rate. Once the FIFO buffer empties, the DMA rate is then throttled by the input data rate.

The control section is a microsequencer that includes a "next-address" control unit and an 8-bit microprogram sequencer. The sequencer controls the loading of the correlator chips, starting the serial data input cycle, loading the FIFO buffer, the posting of errors, appending the contents of the ECSR to the block of data, and unloading the FIFO buffer to the host.

Synchronized bits that have been loaded into the FIFO buffer are unloaded one word at a time and transferred directly to the memory of the host computer via the DMA adapter. Data remain synchronized in blocks as long as the 301-word boundaries are maintained. The transfer of a block can be terminated when the word-count register in the DMA adapter reads "zero," if this completion interrupt was previously enabled. The transfer of data to the host computer restarts when the system software first clears bit 10 of the control-and-status register and, after clearing that bit, sets it again. This "toggling" of the starting bit immediately starts DMA action.

The output registers are loaded with data from the FIFO buffer. When the DMA interface adapter takes control of the data bus, the output register transfers data through the tristate transceivers to the DMA adapter.

This work was done by William M. Baltau of Caltech for **NASA's Jet Propulsion Laboratory**. *For further information, Circle 34 on the TSP Request Card.*

Inquiries concerning rights for the commercial use of this invention should be addressed to the Patent Counsel, NASA Resident Office-JPL [see page 16]. Refer to NPO-17276.

Fast Data Acquisition for Mass Spectrometer

New equipment has the speed and capacity to process time-of-flight data.

Ames Research Center, Moffett Field, California

The data generated by a time-of-flight mass spectrometer are captured by a fast data-acquisition system. The system relies on a fast, compact waveform digitizer with 32-k memory that can be readily coupled to a personal computer. With this newly available digitizer, the system captures all the mass peaks on each 25- to 35-μs cycle of the spectrometer.

The computer enables the convenient control of the collection and management of data. It automates the data-acquisition process, including mass calibration, logging of pertinent experimental parameters, and presentation of the recorded spectral data in a variety of ways.

The system samples vapor plumes produced by laser-pulse heating of various materials. After the 1-ms pulse of vapor that follows each laser pulse, the system displays the following on video screens:

- a three-dimensional view of the time-resolved spectra from the vapor with the major mass peaks labeled by their ratios of mass to change and
- a presentation of laser intensity versus time and total ion current versus time.

Simultaneously, the system prints out pertinent experimental parameters, including the identity of the sample, date and time, laser-power-supply voltage, pressure in the vacuum chamber, and potential of the ion deflector. The operator can request prints and plots of data (see figure).

In addition, the system can be used to capture spectra in the averaging mode over much longer periods; for example, several tenths of a second or more. These longer measurements analyze vapors from continuous laser heating or calibration gases. Except for the three-dimensional format, the same displays and printouts are available.

The time-of-flight mass spectrometer sends out a trigger pulse at the beginning of each cycle. The microchannel-plate detector of the spectrometer produces an ac component containing the spectral signal, and a dc component — the total multiplier current — that is a measure of all the masses in the vapor. The spectral signals are fed to a transient recorder (synchronized by the trigger pulses from the spectrometer) where they are stored in a signal memory and processed by a microprocessor before being transferred to the host computer.

This work was done by K. A. Lincoln of **Ames Research Center** *and R. D. Bechtel of Santa Clara University. Further information may be found in NASA TM-88374 [N88-724538/NSP], "A Fast Data Acquisition System for the Study of Transient Events by High Repetition Rate Time-of-Flight Mass Spectrometer."*

Copies may be purchased [prepayment required] from the National Technical Information Service, Springfield, Virginia 22161, Telephone No. (703) 487-4650. Rush orders may be placed for an extra fee by calling (800) 336-4700.

Inquiries concerning rights for the commercial use of this invention should be addressed to the Patent Counsel, Ames Research Center [see page 16]. Refer to ARC-11785.

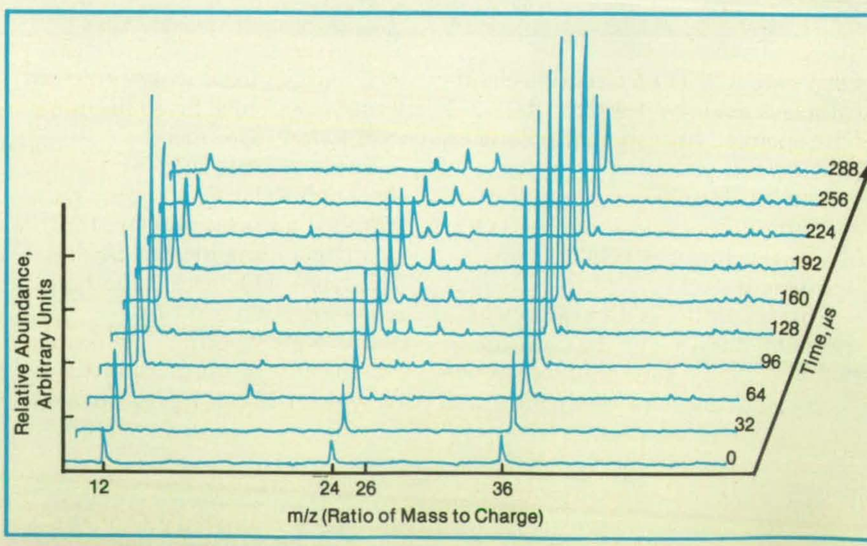

A **Pseudo-Three-Dimensional Plot** gives a time-resolved view of the mass spectra.

THE ONLY WAVEFORM DIGITIZER WITH THE BIG PICTURE...

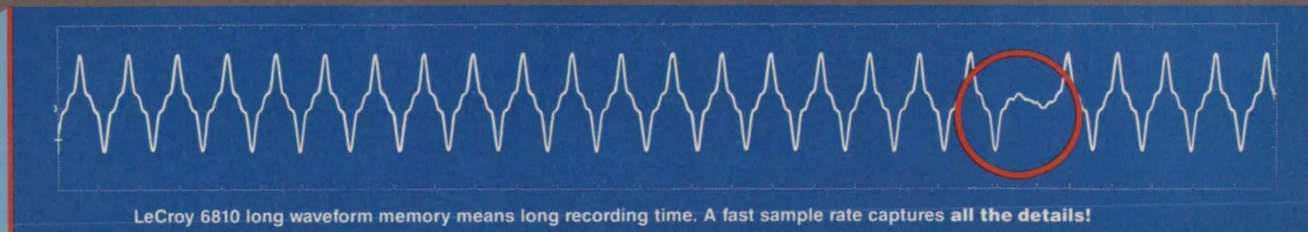

LeCroy 6810 long waveform memory means long recording time. A fast sample rate captures **all the details!**

When you want to completely understand your waveform, you need all the information you can get. LeCroy's 6810 Waveform Digitizer delivers both the BIG horizontal *and* vertical waveform picture. And the digitized data makes for simple frequency domain analysis (FFT) too.

■ The 6810's long memory, fast sample rate, and pre-trigger recording provide the BIG horizontal picture. They integrate the benefits of digitizers and strip chart recorders into one complete instrument.

The long 512k sample memory (expandable to 8M samples) means long recording time. And the fast 5Ms/sec (max) sample rate captures all the details.

It also eliminates the expense and distortion associated with antialiasing filters.

■ The 12-bit resolution and differential inputs ensure a BIG vertical picture. 12 bits means the 6810 can detect a 25 mV wiggle on a 102.4 Volt input . . . even on transient waveforms. In addition, the 67 dB SNR shows an unprecendented dynamic accuracy.

A powerhouse of features give the 6810 an exceptional degree of flexibility. These features include window and hysteresis triggering, segmentable memory with over 4800 waveforms/second throughput, trigger arrival time buffers, and dual timebases.

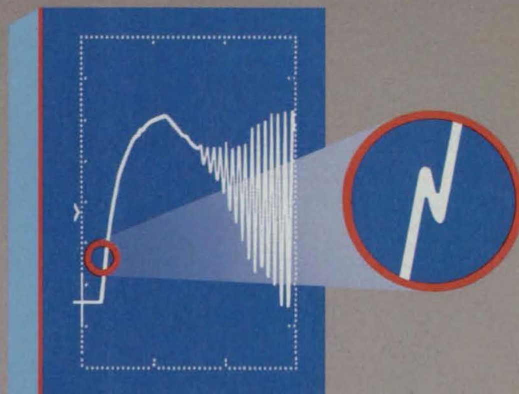

The 12-bit 6810 Digitizer captures even hidden waveform details.

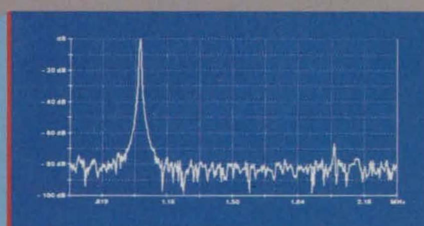

The high accuracy 6810 assures a detailed, low noise FFT display.

...LeCROY 6810.

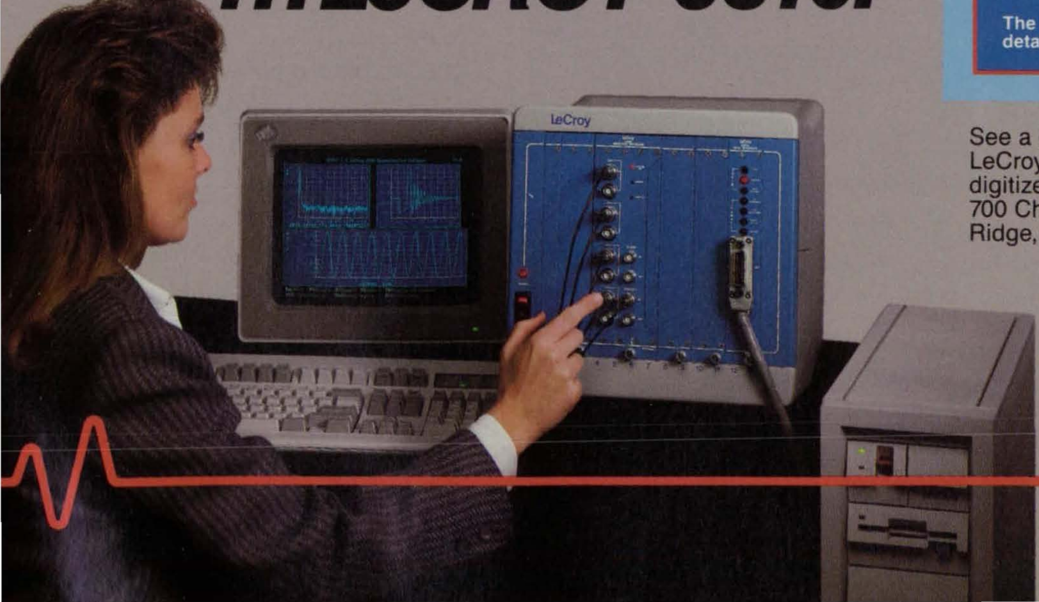

See a 6810 data sheet and a catalog on LeCroy's complete line of waveform digitizers. Circle the bingo or write us at 700 Chestnut Ridge Road, Chestnut Ridge, N.Y. 10977-6499.

For fast information on our fast instrumentation, call **(800) 5 LECROY.**

LeCroy

Innovators in Instrumentation

Circle Reader Action No. 321

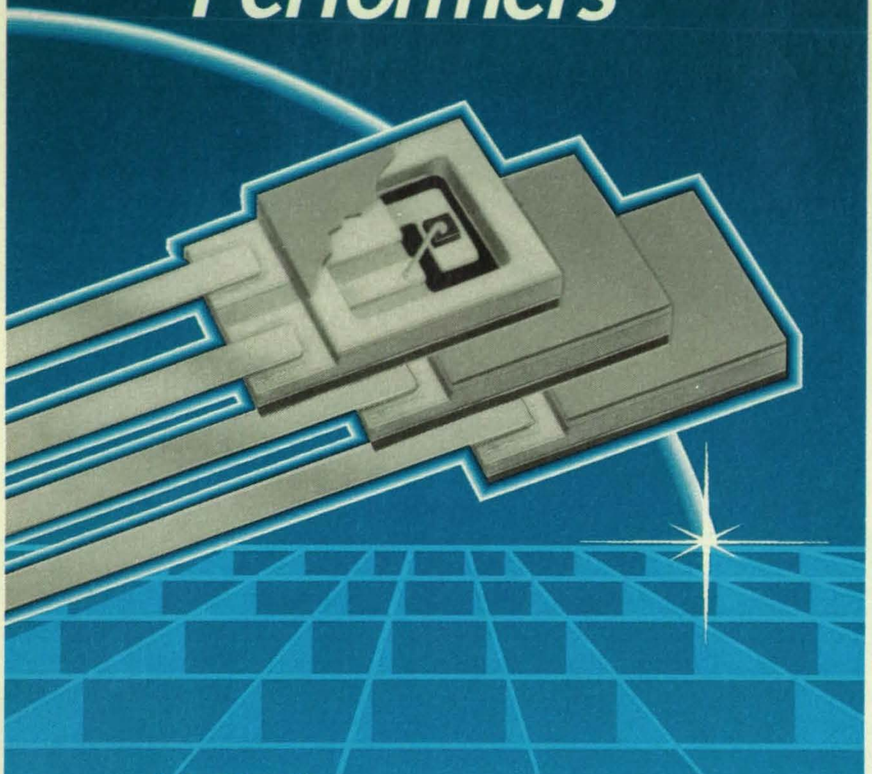

Single-Chip VLSI Reed-Solomon Decoder

Efficient utilization of computing elements reduces size while preserving throughput.

NASA's Jet Propulsion Laboratory, Pasadena, California

A real-time Reed-Solomon (RS) decoder based on a new pipeline architecture is realized on a single very-large-scale integrated (VLSI) circuit chip. The decoder architecture not only provides for error correction but also handles erasures in a pipeline manner. The new design is more efficient than previous designs and can be applied to a variety of digital communications that involve error-correcting RS codes.

Let $N = 2^m - 1$ = the length of the (N, I) RS code over $GF(2^m)$ with design distance d. Suppose that t errors and s erasures occur, and $s + 2t \leq d - 1$. Let X_i be an error location or an erasure location and $\Lambda = \{X_i | X_i \text{ is an erasure location}\}$, $\lambda = \{X_i | X_i \text{ is an error location}\}$. Let Y_i be the corresponding errata magnitude and $r = (r_0, r_1, \ldots, r_{N-1})$ be the received vector. The pipeline architecture of the decoder (see Figure 1) performs the following decoding procedure:

1. Computes the syndrome polynomial

$$S(Z) = \sum_{k=1}^{\infty} S_k Z^{-k}$$

where

$$S_k = \sum_{n=0}^{N-1} r_n \alpha^{nk}$$

$$= \sum_{i=1}^{S+t} Y_i X_i^k$$

for $1 \leq k \leq d - 1$.

2. Computes the erasure-locator polynomial

$$\Lambda(Z) = \prod_{X_i \in \Lambda} (Z - X_i)$$

from Λ.

3. Multiplies $S(Z)$ and $\Lambda(Z)$ to obtain the Forney syndrome polynomial

$$T(Z) = S(Z)\Lambda(Z)$$

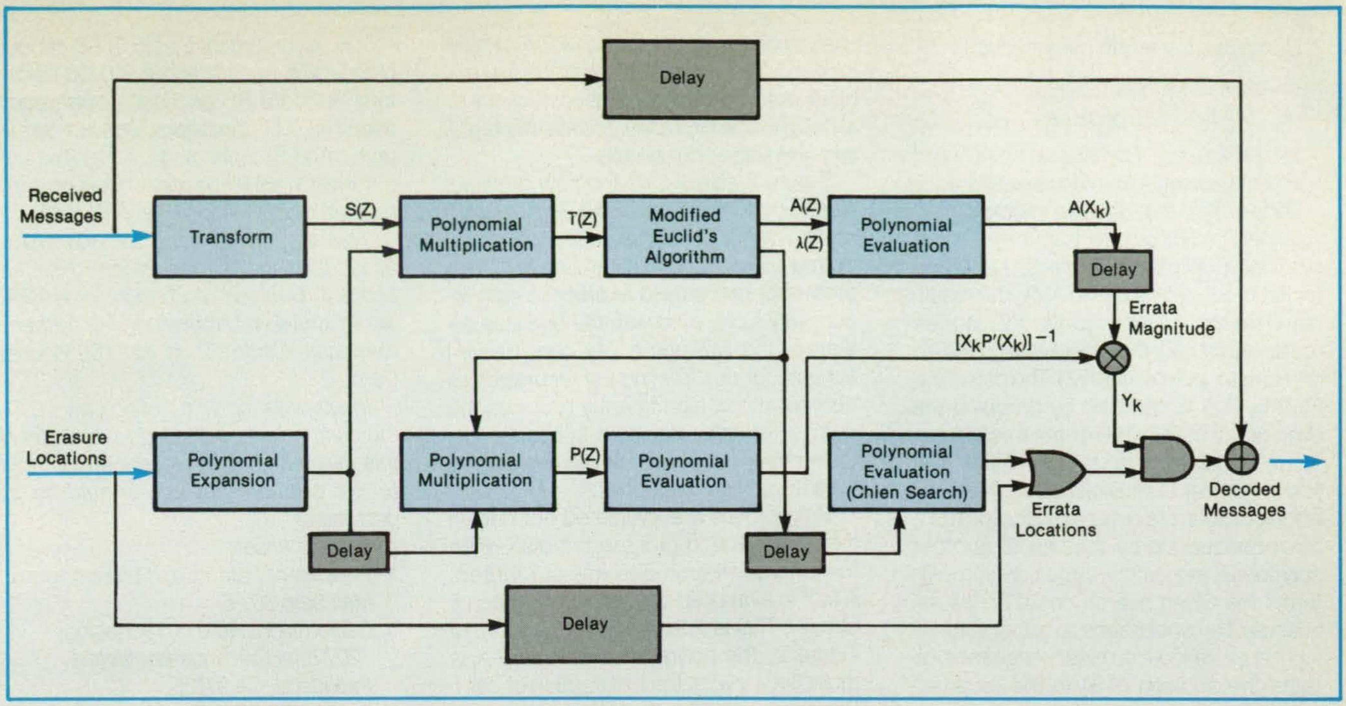

Figure 1. This **VLSI Architecture** represents a pipeline Reed-Solomon decoder for the correction of errors and erasures. The decoder uses a transform circuit to compute the syndrome polynomial $S(Z)$. The erasure information Λ enters the decoder as a binary sequence.

4. Computes the errata-evaluator polynomial $A(Z)$ and the error-locator polynomial $\lambda(Z)$ from $T(Z) = [A(Z)/\lambda(Z)]$ by the modified Euclid's algorithm.
5. Multiplies $\Lambda(Z)$ and $\lambda(Z)$ to get the errata-locator polynomial

$$P(Z) = \Lambda(Z)\lambda(Z)$$

6. Performs a Chien search on $\lambda(Z)$ to find the error-location set λ.

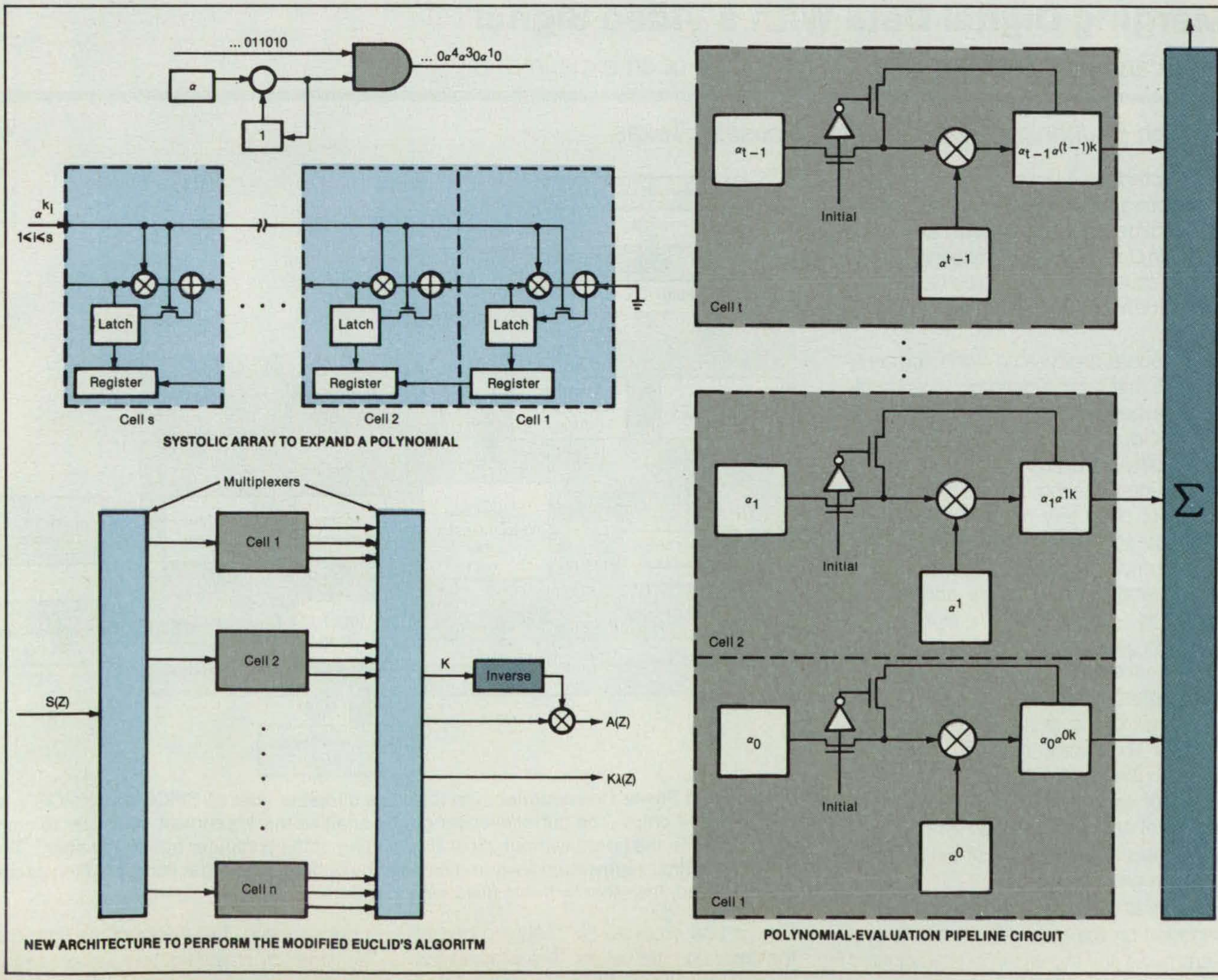

Figure 2. These **Details of the Decoder Architecture** of Figure 1 illustrate the principle features responsible for its improved performance.

7. Computes the errata magnitudes

$$Y_k = \frac{A(X_k)}{X_k P'(X_k)}$$

for $1 \leq k \leq s + t$ by evaluating $A(Z)$ and $P'(Z)$. Uses sets λ and Λ to direct the additions of Y_k to the received vector r.

A new architecture implements the modified Euclid's algorithm by operating on the product of $S(Z)$ and $\Lambda(Z)$. The resulting error-locator polynomial $\lambda(Z)$ is then multiplied by $\Lambda(Z)$, thereby obtaining the errata-locator polynomial $P(Z)$. The derivative $P'(Z)$ of $P(Z)$ is obtained by dropping the even terms of $P(Z)$. The errata magnitudes Y_k are calculated then by a field inversion and a number of multiplications. Next the error locations are obtained in the form of a binary sequence by the use of another polynomial-evaluation circuit, which performs the Chien search on $\lambda(Z)$. This sequence of error locations, together with the input erasure-location binary sequence, directs the addition of Y_k to the received message.

The multiplications of $(Z - \alpha^k)$ can be implemented by the systolic array shown in Figure 2. Since it contains zeros as well as α^k's (where $\alpha^k \in \Lambda$), the input stream is used to control the updating of the latches in each basic cell. At the end of the arrivals of the erasure locations, the coefficients of $\Lambda(Z)$ are loaded from the latches into registers and shifted out serially.

Figure 2 also shows the new architecture to perform the modified Euclid's algorithm. The input multiplexer directs the syndrome polynomials to different cells. Each processor cell is used to process data recursively. Compared with the previous design of the systolic array, the present scheme for multiplexing the recursive cell computations significantly reduces the number of cells and, as a consequence, the number of circuits. The cell reduction is greater for high-rate codes.

Polynomials are evaluated not only in the Chien search process but also when the errata magnitudes are computed. $A_i(\alpha^i)^k$ is evaluated sequentially for each k at cell i. This is illustrated at the bottom of Figure 2. The polynomial coefficient A_i is multiplied by α^i at the initialization of cell i. From then on, a feedback loop computes the quantities $A_i(\alpha^i)^k$ for $k = 1, 2, 3, \ldots, N-1$. The summation shown at the right in Figure 2 is implemented quite simply since all quantities are binary.

It is estimated that a (15,9) RS decoder chip would require about 29,000 transistors. A (31,15) RS decoder would require about 88,000 transistors. Considering the present VLSI technology, a high-throughput 5-bit (31,15) RS decoder could be implemented readily on a single VLSI chip.

This work was done by Howard M. Shao, Trieu-Kie Truong, In-Shek Hsu, and Leslie J. Deutsch of Caltech for **NASA's Jet Propulsion Laboratory**. *For further information, Circle 52 on the TSP Request Card.*

In accordance with Public Law 96-517, the contractor has elected to retain title to this invention. Inquiries concerning rights for its commercial use should be addressed to

Edward Ansell,
Director of Patents and Licensing
Mail Stop 301-6
California Institute of Technology
1207 East California Boulevard
Pasadena, CA 91125

Refer to NPO-16854, volume and number of this NASA Tech Briefs *issue, and the page number.*

Merging Digital Data With a Video Signal

Data can be displayed on a television image of an experiment.

Lyndon B. Johnson Space Center, Houston, Texas

An interface circuit board combines data from a computer with a video signal. Video images of an experiment can thus be sent with digital data on the experiment to a remote station. The digital data can be raw and unformatted or in the form of characters.

The board contains its own microprocessor so that it can function independently of the experiment computer (see figure). The microprocessor relieves the experiment computer of timing and control tasks on the interface board; the experiment computer need only fill the board buffers with data and occasionally communicate with the interface board. The microprocessor generates the address and control signals to read the memory, synchronize loading of data into shift registers, track the data-word count, swap buffers, and control the programmable timer, which is an integral part of the digital video-generation circuitry. The microprocessor software is unique in that the timing of the reading and writing of digital data is governed by the horizontal and vertical video synchronization signals, which are two of the inputs to the microprocessor.

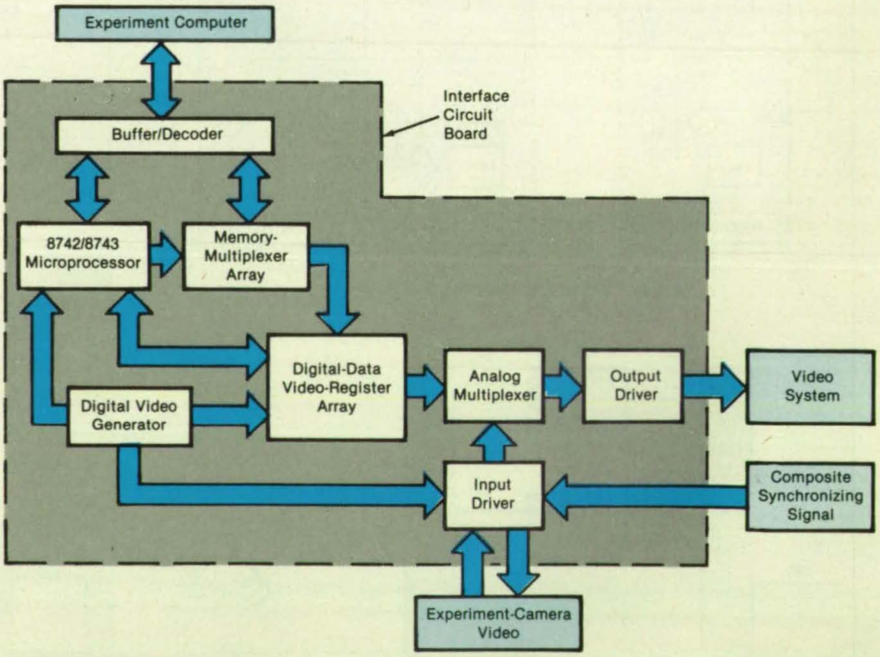

For Minimal Power Consumption, the interface circuit is built of CMOS and HMOS integrated-circuit chips. The buffer/decoder circuit enables the experiment computer to communicate with the board without excessive loading of the computer bus by the board. The memory multiplexer/memory array implements the buffer-swapping scheme in which as one buffer is read, the other buffer is filled with new data.

The position at which the digital data are displayed on the receiving screen is programmable and therefore can be adjusted for a given application. The horizontal position can be changed by changing one of the timer counter values. The width of the data can be changed by changing another counter value. The height of the data can be varied by changing the number of scan lines over which the data are written in a video field. The position and size functions are part of the microprocessor software.

The overall system uses combined memory and input/output mapping in the address space of the experiment computer. This feature partitions data and control functions so that the experiment computer can operate more efficiently.

Analog-multiplexer/bypass circuitry on the board attenuates and shifts the level of the digital data for mixing with the video signal. The timer output controls the multiplexer for proper mixing of the digital and camera video signals on each horizontal scan line. The bypass mode allows the video signal to pass unaltered to the transmitter in case of a failure of the digital subsystem.

The board can be used with any IBM PC or compatible computer and can readily be integrated with other hardware and software. It is normally in an idle state, during which the experiment computer can examine either of the board buffers or cause the board to place a digital test pattern on the video screen. When the time comes to send data, the experiment computer sends an initialization word and a command word to the board. The initialization word configures the board for transmission; and after one of two buffers has been filled with data, the command word swaps buffer availability.

The swap action starts reading of the newly acquired data in one buffer, and the data words are written to a shift register. The register serially transmits the digital data on a horizontal line scan at a 2.048-MHz rate. The board can send data acquired in 1 second in only thirty-two sixtieths of a second. It therefore waits for the experiment computer to swap buffers and continue transmission into the other buffer. The waiting periods prevent overfilling of the buffers, the subsequent loss of data, and the loss of synchrony between digital and camera data.

This work was done by Thomas J. Collins III, William G. Crosier, and William H. Paloski of Technology Inc. for **Johnson Space Center**. *For further information, Circle 3 on the TSP Request Card.*
MSC-21248

Books and Reports

These reports, studies, handbooks are available from NASA as Technical Support Packages (TSP's) when a Request Card number is cited; otherwise they are available from the National Technical Information Service.

Integrated Displays for Helicopter Pilots

Concepts that combine a variety of sensor data are evaluated.

A report describes an evaluation of three similar video displays for the guidance of helicopter pilots in low-level flight at night in adverse weather. The evaluation was done by piloted simulation in a vertical-motion simulator.

In all three displays, a computer produces guidance information for the pilot by integrating data from terrain-following radar, forward-looking infrared (FLIR) imagery, and data from such autonomous navigation instruments as inertial navigation systems and Doppler radar. The FLIR imagery, information on the status of the helicopter, and command symbols were incorporated in one head-down display.

In all displays, the FLIR imagery is aligned with the flight path of the aircraft. In display 1, the pitch attitude is conformal to the FLIR imagery. In display 2, the pitch attitude is also conformal to the FLIR imagery, but the pitch scale is increased. In display 3, the pitch attitude is nonconformal to the imagery, and the pitch scale is the same as in display 2.

The pilots performed three kinds of tasks in the simulator:

1. Following the terrain at an altitude of 100 ft (30 m) above the local ground level while traveling along a prescribed course at a speed of 60 knots (31 m/s);
2. Following the terrain in a similar manner, but at a speed of 90 knots (46 m/s); and
3. Deceleration to hover while following the terrain along a prescribed course.

The pilots carried out the tasks over various simulated terrain profiles during simulated day and night, with and without simulated wind and turbulence.

All three display concepts were rated acceptable by the pilots. However, the pilots expressed a preference for display 3 because it provided them with greater awareness of the pitch attitude of the helicopter, thereby enabling them to control the attitude more precisely.

This work was done by Harry N. Swenson and Clyde H. Paulk, Jr., of **Ames Research Center** *and Robert L. Kilmer and Frank J. Kilmer of IBM Corp. Further information may be found in NASA TM-86779 [N86-31551/NSP], "Simulation of Display/FLIR Concepts for Low Altitude Terrain-Following Helicopter Operations."*

Copies may be purchased [prepayment required] from the National Technical Information Service, Springfield, Virginia 22161, Telephone No. (703) 487-4650. Rush orders may be placed for an extra fee by calling (800) 336-4700.

Inquiries concerning rights for the commercial use of this invention should be addressed to the Patent Counsel, Ames Research Center [see page 16]. Refer to ARC-11699.

Research on the CH-47B Helicopter

Although it is not new, this helicopter continues to yield valuable information.

A report describes new equipment added to, and the research capabilities of, the CH-47B helicopter. This variable-stability aircraft has been used in flight research for more than 15 years. The helicopter continues to be a source of unique flight research, much like a wind tunnel or large ground-based simulator.

Two new installations on the helicopter are a programmable force-feel system for the evaluation pilot's conventional cyclic stick and a four-axis side-stick controller. They permit a range of in-flight investigations of manipulator characteristics and augmentation-system features.

A new color electronic display system with a programmable symbol generator will provide display formats for a variety of missions — those of vertical-takeoff-and-landing aircraft as well as helicopters. In addition, a powerful new general-purpose flight computer is in operation. The computer is programmable in high-level languages and will support research more efficiently. Moreover, flight-control software has been developed to improve the capability of the helicopter to perform simulations in flight.

Over the past several years, the CH-47B has been used as an in-flight simulator, as a research facility for control systems, and for gathering data on handling qualities. The recent uses of the helicopter include the following:

- Research in high-bandwidth flight controls,
- Testing a translational-velocity-command and position hold system for maneuvering near hover,
- Investigating vertical-response handling qualities criteria, and
- Developing model-following control laws.

Although some of the research equipment in the CH-47B helicopter has become outdated over the years, this limitation has been offset by major advances in analytical tools, fundamental modeling, and research capabilities that result from advances in computer equipment and programs.

This work was done by Kathryn B. Hilbert, George E. Tucker, Robert T. N. Chen, and Emmett B. Fry of **Ames Research Center** *and William S. Hindson of Stanford University. To obtain a copy of the report, "New Capabilities and Recent Research Programs of the NASA/Army CH-47B Variable-Stability Helicopter," Circle 49 on the TSP Request Card.*

Inquiries concerning rights for the commercial use of this invention should be addressed to the Patent Counsel, Ames Research Center [see page 16]. Refer to ARC-11759.

Physical Sciences

Depolarization-Measuring Device

The knowledge of radiation in a lidar channel enables the determination of the depolarization ratio.

Langley Research Center, Hampton, Virginia

The depolarization-measuring device is used at Langley Research Center to measure the relative gain and the depolarization of light in a lidar system. The device rotates the lidar return prior to detection, thereby introducing a known amount of radiation into the perpendicular lidar channel. Knowledge of the amount of this radiation can be readily interpreted in terms of the relative optical/electronic gain ratio between data collected by the parallel and perpendicular channels and the depolarization that the scattering medium introduced into the linearly-parallel-polarized incident beam.

The operation of the device is shown schematically in the figure. The half-wave plate is positioned on a rotatable mount. When the mount is rotated by angle θ from the zero position, where it transmits a parallel-polarized beam without rotating it, the electric field of the beam is rotated by angle 2θ. It can be easily shown that the ratio of the outputs of the detection system is given by the following equation, assuming that the incident beam is linearly polarized

$$S_1/S_{11} = G_1\,(\delta + \tan^2 2\theta)/G_{11}\,(1 + \delta \tan^2 2\theta)$$

where S_1 and S_{11} are the perpendicular and parallel output signals, respectively, G_1 and G_{11} are the optical/electronic gains through the perpendicular and parallel channels, and δ is the polarization ratio. If the backscattering is constant during the experiment and measurements are taken at two angles, the two resulting equations can be solved for the gain ratio G_1/G_{11} and for δ.

The half-wave plate can also be put at the output of the laser, and the polarization plane of the laser rotated before it is scattered. The half-wave mount can be rotated continuously to provide data continuously at all angles. These data can probably be used to determine unique signatures for different scattering media.

This work was done by Jose M. Alvarez of **Langley Research Center**. *No further documentation is available.*

This invention is owned by NASA, and a patent application has been filed. Inquiries concerning nonexclusive or exclusive license for its commercial development should be addressed to the Patent Counsel, Langley Research Center [see page 16]. Refer to LAR-13621.

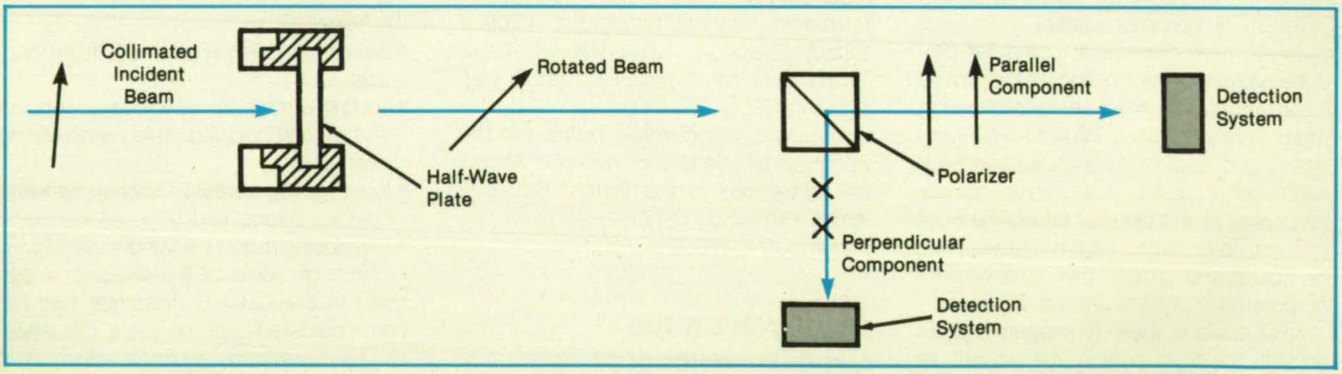

The **Half-Wave Plate Is Rotated** to introduce a known amount of radiation to the perpendicular channel.

Low-Threshold, Solar-Pumped C_2F_5I Laser

Laser threshold of 100 solar constants has been achieved.

Langley Research Center, Hampton, Virginia

Since the conversion of Sunlight into high-power laser light in space could have a number of important applications, including space manufacturing and propulsion, research on solar-pumped lasers could lead to large, orbiting solar collectors that concentrate Sunlight on an appropriate lasant, producing megawatts of continuous power. Up to now, most of research has focused on the alkyl iodides, which absorb solar light near 280 nm and then photodissociate into radicals and excited iodine atoms that lase at 1.315 μm. A number of alkyl iodides, including i-C_3F_7I, C_2F_5I, n-C_4F_9I, and CF_3I, have been investigated with the goal of defining the most appropriate lasant for closed-cycle, low-threshold operation.

A unique solar-laser experiment was devised to evaluate the above-mentioned and other candidate lasants. Using two xenon-arc solar simulators, lasing was achieved with pentafluoroethyl iodide, C_2F_5I, a new alkyl iodide, at a laser threshold of only 100 solar constants (1 solar constant = 1.35 kW/m^2). This solar laser had the lowest threshold observed to date. Its output power and energy were 350 mW and 45 mJ, respectively. The duration of lasing of this static-gas-fill system has provided important kinetic information on the recombination rates of radicals and ground-state iodine atoms; these rates are important parameters for closed-cycle operation.

Completed studies of the scaling with pressure, solar intensity, parent-molecule species, and beam shape are leading to a fuller understanding of the alkyl iodide lasants. These studies of threshold-pumping requirements and laser kinetics are valuable contributions toward the development of convenient, efficient solar-pumped lasers.

This work was done by Russell J. De Young and Willard R. Weaver of **Langley Research Center**. *No further documentation is available.* *LAR-13677*

Short-Cycle Adsorption Refrigerator

Each adsorption unit includes a long-lived nonmechanical heat switch.

NASA's Jet Propulsion Laboratory, Pasadena, California

A modular adsorption/Joule-Thomson-effect refrigerator offers fast regeneration; when fully developed, its adsorption/desorption cycle time is expected to be only 1 minute, as compared with 15 minutes in previous versions. The refrigerator is smaller and lighter than the previous units of equivalent capacity. A modular configuration makes it relatively easy to build refrigerators that have capacities from milliwatts to watts, according to cooling needs.

The refrigerator is intended for the long-term cooling (up to 10 years) of infrared sensors and other equipment in space to temperatures ranging from 4 to 80 K. The only moving parts are small check valves. The refrigerator is designed to be powered mostly by waste heat. A prototype containing 12 compressor modules connected in banks of 4 provides one-quarter watt of cooling at 25 K. Operating under the control of a computer, the four banks of compressor modules are operated in a phased heating/cooling sequence so that nearly steady cooling is provided for the external heat load.

In the refrigerator, pressurized hydrogen generated by a bank of compressor modules during its heating phase passes through a system of check valves and expands in a Joule-Thomson junction as it enters a refrigeration chamber. There, the

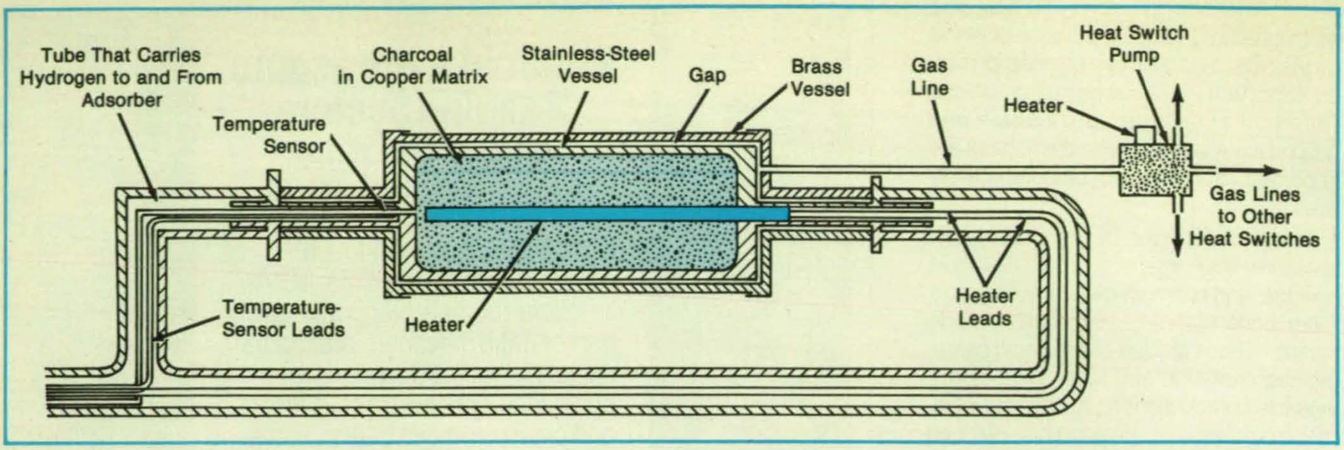

The **Heat Switch Is a Gap** between concentric cylindrical vessels. For rapid heating and cooling of the core, the gap must be less than about 50 μm.

hydrogen absorbs heat from the load before it is sucked out by another bank of compressor modules in its cooling phase.

In each compressor module, adsorbing charcoal is contained in an inner pressure vessel of stainless steel (see figure). An open-foam copper matrix holds the charcoal and enhances the transfer of heat. A brass outer vessel surrounds the stainless-steel cylinder, and the gap between inner and outer vessels constitutes the heat switch. When the gap is filled with hydrogen, the heat switch exhibits high heat conductance (is on). When the gap is empty, the switch exhibits low heat conductance (is off). A miniature charcoal adsorption pump supplies the gas for the switches in each bank of four compressor modules.

To demonstrate the refrigerator, an electric heater was used to supply heat to each module to cause the desorption of hydrogen from the charcoal in its core. (In a practical model, the heat for desorption would come from waste heat such as that from electronic equipment.) With the heat switch turned off, the adsorber was heated. The adsorber gave off hydrogen as it heated up. When the pressure reached about 80 atm (8.1 MPa), the heater was turned off, and the heat switch was turned on. The adsorber transferred its heat to a liquid-nitrogen bath surrounding the module, readsorbing hydrogen as it cooled and eventually becoming saturated with the gas, ready for another heating cycle. Cooling from 165 K to 85 K took only 50 seconds.

This work was done by C. K. Chan of Caltech for **NASA's Jet Propulsion Laboratory**. *For further information, Circle 46 on the TSP Request Card.*
NPO-16571

Generating Hyperthermal Atomic Oxygen

Atomic oxygen diffused through silver is desorbed by low-energy electron impact.

Langley Research Center, Hampton, Virginia

The velocity of spacecraft through the rarefied atmosphere in orbit results in the impingement of hyperthermal atomic oxygen on spacecraft surfaces. The high chemical reactivity of the oxygen flux has caused substantial degradation of organic materials onboard the Shuttle; as a result, materials on the proposed Space Station, composites used in large space structures, and exterior coatings on optical systems and laser communications systems may have substantially reduced lifetimes. It is therefore essential to study the reactivity of these materials with atomic oxygen in laboratories on the ground.

To simulate the flux of hyperthermal atomic oxygen on spacecraft surfaces, there is a need for an atomic-oxygen-beam generator in which the mean energy of the O atoms is about 5 eV, and the flux is about 10^{15} cm^{-2}s^{-1}. In conventional methods for obtaining such fluxes, it is difficult to achieve these parameters while maintaining a ratio of O to O_2 greater than 90 percent.

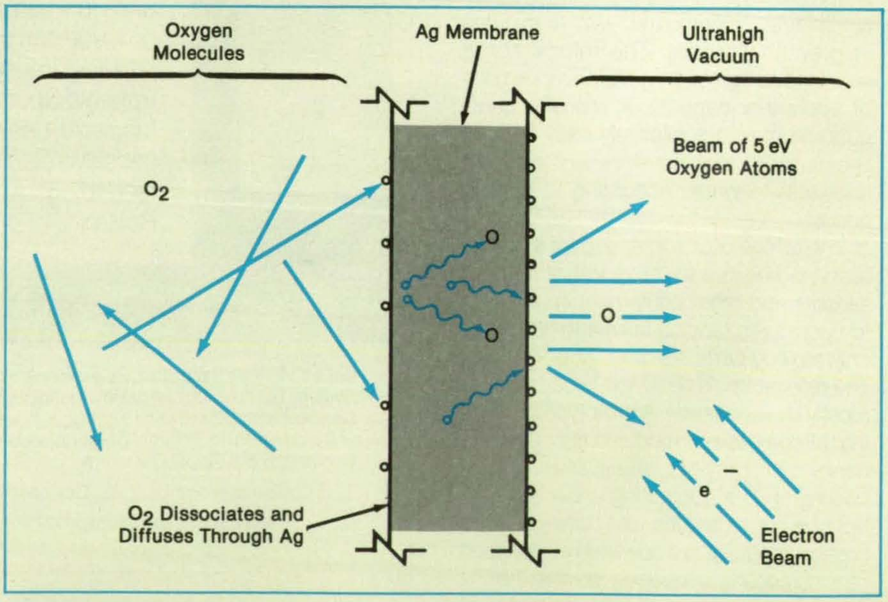

Oxygen Atoms Diffuse Through Silver Foil and emerge on the high-vacuum side, aided by electron-stimulated desorption. Atomic-oxygen flux levels range up to 10^{12} cm^{-2}s^{-1}, and kinetic energies range from 1 to 10 eV. O^+ and O^- ions can be swept aside by charged cylindrical grids.

A promising approach exploits two unique phenomena. The first is the unusually high permeability of oxygen through silver, which occurs by the sequential adsorption of O_2, surface dissociation into O atoms, dissolution, and subsequent diffusion of O atoms through a thin silver membrane to a vacuum interface.

The second phenomenon is electron-stimulated desorption. Normally, O atoms

For critical structural test . . . a total solution

For mechanical design verification and vibration troubleshooting, the new 1202 Structural Analyzer does it all . . . from advanced FFT signal processing with zoom and integrated signal generation, to versatile modal analysis with interactive geometry and enhanced animation that simplifies the interpretation of complex structures. ONLY the 1202 does it all in a *single, user friendly,* portable, cost-effective package.

The 1202 is a complete 4-channel analysis system with integrated software for FFT signal processing, modal analysis, structural modification and forced response simulation. When combined with Schlumberger's 1250 series Frequency Response Analyzer, the 1202 can be expanded to 36 parallel channels for large complex projects. Fast graphics on a built-in display features unique hidden line animation of mode shapes, surface strain contours and flexible stack plots. Internal 20 Megabyte fixed drive with a 3-1/2 inch floppy backup, IEEE-488 and RS232 are all standard.

All this capability is available, fully integrated, from one source. . .Schlumberger Instruments. Ask for our application oriented brochure for the full story.

Schlumberger Instruments

20 North Avenue, Burlington, MA 01803
Telephone: (617) 229-4825
Toll Free (outside MA): 1-800-225-5765

Schlumberger Technologies

on the silver are in an adsorbed state, unless the surface temperature exceeds 450 °C, then surface diffusion results in O-atom collisions and the subsequent desorption of O_2. When there is a flux of low-energy electrons incident upon this surface, the O atoms are excited to antibonding states before they can recombine, and they desorb as hyperthermal O neutrals and O^+ ions. The figure illustrates a combination of these two phenomena.

In this technique, the oxygen molecules are dissociated on the higher-pressure silver surface into atomic oxygen, which then diffuses through to the ultra-high vacuum side [10^{-11} torr ($\sim 10^{-9}$ Pa)]. On the ultra-high-vacuum surface, the atomic oxygen remains adsorbed if the surface temperature is maintained below 450 °C and is bombarded with low-energy ($\sim$100 eV) electrons, causing electron-stimulated desorption of O atoms before substantial recombination can take place. Atoms so desorbed have energies in the 5-eV range, and the gas produced has an O-to-O_2 ratio greater than 90 percent.

This work was done by Ronald A. Outlaw of **Langley Research Center**. *Further information may be found in NASA TP-2668 (N87-18621/NSP) "Electron Stimulated Desorption of Atomic Oxygen from Polycrystalline Ag and Ag (110)."*

Copies may be purchased [prepayment required] from the National Technical Information Service, Springfield, Virginia 22161, Telephone No. (703) 487-4650. Rush orders may be placed for an extra fee by calling (800) 336-4700.

Inquiries concerning rights for the commercial use of this invention should be addressed to the Patent Counsel, Langley Research Center *[see page 16].* *Refer to LAR-13652.*

Books and Reports

These reports, studies, handbooks are available from NASA as Technical Support Packages (TSP's) when a Request Card number is cited; otherwise they are available from the National Technical Information Service.

Infrared Attenuation of Thallium Bromoiodide Fibers

Theory and measurements are discussed.

A report presents measurements of attenuation of infrared signals in unclad 381-μm-diameter optical fibers of thallium bromoiodide [Tl(Br,I)], a polycrystalline thallium halide. There is interest in developing materials for the transmission of light at wavelengths longer than the 1.3 to 1.5 μm currently in use: losses due to Rayleigh scattering would be lower, and larger single-mode fibers could be produced. Metal halides and fluoride glasses have shown the most promise as candidates for optical fibers useful at wavelengths around 10 μm.

Measurements of attenuation in Tl(Br,I) fibers in the wavelength ranges of 1.2 to 3.4 μm and 3 to 11 μm are compared with those of two other groups of researchers. That Tl(Br,I) shows promise as a future fiber material is indicated by attenuations in the range of 0.1 dB/cm observed at wavelengths approaching 10 μm. However, further improvements will have to be made in chemical purity and in such mechanical properties as flexibility and strength. The data from the fiber and bulk samples show various attenuation peaks due to impurities (e.g., water) that prevent attenuation from reaching the theoretical minimums. The attenuation in the best of the fibers tested is inversely proportional to the square of the wavelength; with such a dependence on the wavelength, the scattering may be caused by long surface grooves on the fiber.

When attempts were made to polish the end of a fiber, the fiber broke repeatedly, in part due to the large sizes of the crystals in the polycrystalline matrix. However, recent research shows that these early-generation fibers suffer a deterioration of mechanical stability with age, perhaps caused by residual strain from fiber extrusion leading to separation at grain boundaries.

The report also reviews the physics of fiber optics in the geometrical-optical limit. This simplified theory is sufficient for the description of transmission in fibers that have diameters much larger than the wavelength. The fundamental loss mechanisms in fibers and their relative importances in fibers of different types (glass, crystalline, and polycrystalline) are described. An appendix describes the physical and chemical characteristics of Tl(Br,I). The material is lethally toxic when vaporized, and even small amounts in the human body may cause serious neurological damage.

This work was done by John Goebel of **Ames Research Center** *and Beryl Magilavy of Sterling Software. Further information may be found in NASA TM-86817 [N86-32268/NSP], "Infrared Attenuation of Thallium Bromo-Iodide Fibers."*

Copies may be purchased [prepayment required] from the National Technical Information Service, Springfield, Virginia 22161, Telephone No. (703) 487-4650. Rush orders may be placed for an extra fee by calling (800) 336-4700.

Inquiries concerning rights for the commercial use of this invention should be addressed to the Patent Counsel, Ames Research Center *[see page 16].* *Refer to ARC-11752.*

THE CHALLENGE: "DEMONSTRATE HOW HIP WILL ENHANCE THE PERFORMANCE AND IMPROVE THE FATIGUE STRENGTH OF OUR COMPONENTS."

This is a challenge our Thermatech Division meets every day. As one of the largest toll Hot Isostatic Pressing facilities in the United States, it provides this service to the entire aerospace industry. Avco Lycoming, for example, has instituted HIP as bill of material for the AMS 4225 aluminum cylinder heads for all their reciprocating aircraft engines.

EXTENSIVE APPLICATIONS FOR HIP.
HIP subjects components to a high gas pressure and elevated temperature sufficient to reduce shrinkage porosity by closing internal voids. Many engineers are learning that HIP'ed cast components deliver the consistency and mechanical properties expected of forgings. In addition to titanium and superalloys, performance improvements are also seen in steel, bronze, cast iron, ceramics and aluminum. Our Thermatech Division is licensed to HIP aluminum under the Alcoa patented 359 process. We also HIP powder metal components.

HIP lowers life cycle costs, and not just for the aerospace industry. HIP is used for high performance automotive pistons, rods, crankshafts and engine blocks. It also has applications for medical implants and pump and valve components for the oil, food and chemical industries.

HIP PIONEERS.
We began production HIP'ing in 1975 and now have one of the largest capacities in the United States with capabilities from small developmental-size presses to 55″ in diameter and 80″ in height, pressures to 45,000 psi and temperatures to 4000°F.

This extensive range enables us to answer virtually any challenge.

IMPOSSIBLE? CHALLENGE US.

HOWMET CORPORATION

THERMATECH DIVISION, WHITEHALL, MI

THE IMPOSSIBLE MADE POSSIBLE.
Another service that sets Howmet apart is our 80,000 square foot research, development and engineering center. Here metallurgical teams and laboratory specialists come up with breakthrough solutions to seemingly impossible challenges. They are always available to you as a Howmet customer.

WE INVITE YOUR CHALLENGES.
At Howmet, we will work closely with you, engineer to engineer, from concept through design to finished product. Whether your problem requires a cost-effective solution or state-of-the-art technology for complex applications, you'll find Howmet able to help.

For more information on HIP and the potential it holds for you, write our Marketing Department, Howmet Corporation, 475 Steamboat Road, Greenwich, CT 06836-1960. Or phone the manager of the Thermatech HIP Department at (616) 894-5686.

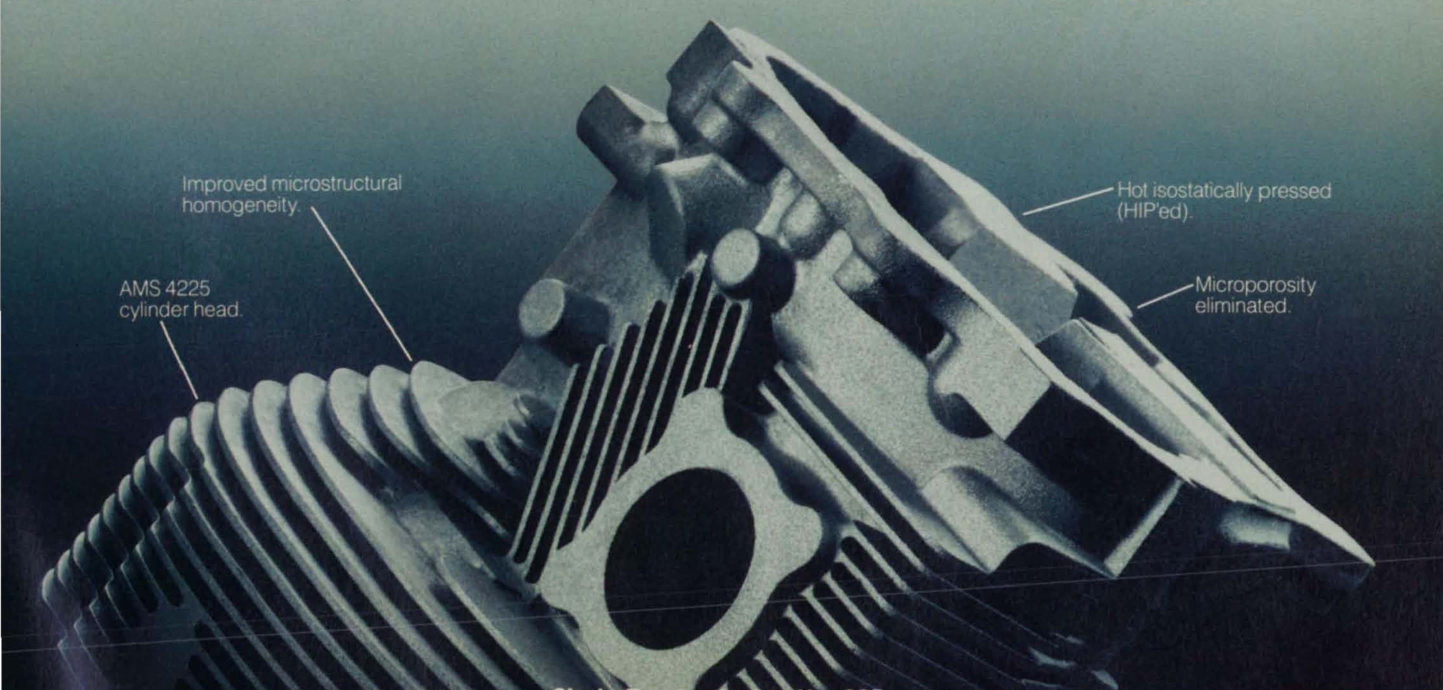

Circle Reader Action No. 335

SIMPLY THE BEST DEFENSIVE LINE IN THE GAME.

When it comes to depth, diversity, and a proven winning record, no other line of circuit breakers can compare with ours. The Airpax team is your source for fast response and reliable performance in your choice of more styles, configurations and ratings to meet your specific needs.

We've been tackling the toughest applications for more than thirty years. Chalking up milestone victories such as twenty years of uninterrupted MIL-C-39019 approval in Type AP electromagnetic circuit breakers. Blitzing international markets with the VDE-approved and rail-mount magnetic circuit breakers. Continually striving through innovation to keep you, the Airpax customer, at the forefront of circuit breaker technology.

Draft the best defensive players into your design. Contact Airpax Corporation, Cambridge Division, Woods Road, Cambridge, MD 21613. (301) 228-4600. Telex: 6849138, Fax: (301) 228-8910. A North American Philips Company.

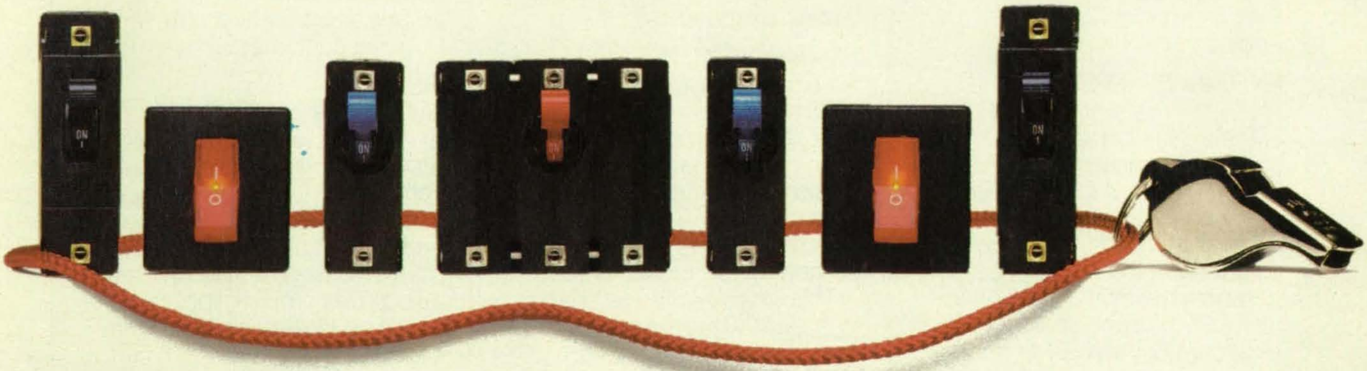

See us at ELECTRO '88 booth #1351.

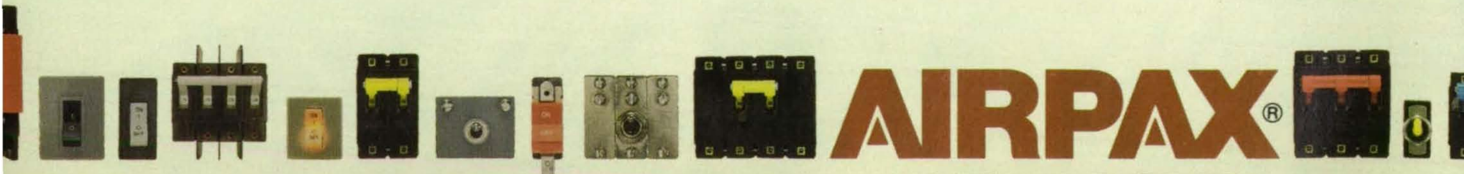

AIRPAX®

CAMBRIDGE DIVISION

Circle Reader Action No. 566

Reliability of Inspection by SLAM

Scanning laser acoustic microscopy finds flaws in ceramic specimens.

A report describes an evaluation of scanning laser acoustic microscopy (SLAM) in the detection of surface voids in silicon nitride and silicon carbide. SLAM is an attractive technique for the nondestructive inspection of these ceramics because it can image surface and subsurface microflaws in real time. The detection of such flaws is important because they limit the strengths and fracture toughnesses of ceramic parts in advanced high-temperature heat engines.

In SLAM, a laser light is used to detect distortions, on an angstrom scale, produced on the surface of a specimen by ultrasonic waves transmitted through the specimen. From the distortion, SLAM creates a picture on a video monitor of such defects as voids, inclusions, and cracks.

In the evaluation, specimens of sintered Si_3N_4 and SiC were examined by SLAM at an ultrasonic frequency of 100 MHz, in both the as-fired condition and after polishing. The specimens were intentionally impressed with styrene microspheres during firing to introduce voids of known size, shape, number, and location in the surface.

The evaluation concentrated on the statistical reliability of the detection of voids by SLAM. In the polished specimens, SLAM detected surface voids as small as 100 μm in diameter with 0.90 probability at a confidence level of 0.95. However, the reliability of detection was substantially less for voids in unpolished, as-fired specimens. Moreover, inspection of the as-fired specimens took 10 times as long as the inspection of the smooth specimens. If ceramic engine parts are smoothly finished, as they are likely to be, the SLAM technique should detect surface and near-surface flaws quickly and reliably.

This work was done by Don J. Roth, Stanley J. Klima, and James D. Kiser of **Lewis Research Center** *and George Y. Baaklini of Cleveland State University. Further information may be found in NASA TM-87035 [N85-32337/NSP], "Reliability of Void Detection in Structural Ceramics Using Scanning Laser Acoustic Microscopy."*

Copies may be purchased [prepayment required] from the National Technical Information Service, Springfield, Virginia 22161, Telephone No. (703) 487-4650. Rush orders may be placed for an extra fee by calling (800) 336-4700.
LEW-14633

Materials

Hardware, Techniques, and Processes

Extending Fatigue Lives of Selected Alloys

Rejuvenating treatments have been demonstrated.

Marshall Space Flight Center, Alabama

Experiments with three alloys have shown that some combinations of heat treatment, hot isostatic pressing, and/or surface treatment can extend the cycle lives of fatigue-damaged or fatigue-precracked specimens. Successful rejuvenation tests were conducted on MAR-M246(Hf)(DS) — a directionally solidified, high-strength, nickel-based superalloy — and on the nickel-based alloy Inconel* 718. The results of tests of the titanium-based alloy Ti/5Al/2.5Sn ELI are inconclusive.

For each alloy, tests were first done to determine the "baseline" high-cycle-fatigue lives and high-cycle-fatigue failure modes over a range of test conditions. Next, controlled fatigue damage was introduced into specimens, either by fatigue testing to a specified number of cycles or by growing a fatigue crack from a starting notch. Following this, the damaged specimens were subjected to candidate rejuvenating treatments, then tested to failure. The effectiveness of each such treatment was judged by comparing the fatigue data of the damaged and treated specimens to the "baseline" fatigue data taken at the same test conditions.

The high-cycle-fatigue life of fatigue-damaged MAR-M246(Hf)(DS) was significantly extended by a solution reheat treatment at 1,221 °C for 2 h followed by aging at 871 °C for 16 h. Transmission electron microscopy provided evidence that the heat treatment reduced the density of dislocations caused by fatigue cycling.

Inconel* 718 containing a single, large fatigue precrack was partly rejuvenated by electron-beam welding to seal the crack at the surface, hot isostatic pressing at a temperature of 982 °C and pressure of 200 MPa for 3 h to heal the crack, and solution and aging reheat treatment identical to the standard heat treatment during manufacture.

Annealing at 816 or 927 °C may extend the fatigue life of fatigue-damaged Ti/5Al/2.5Sn ELI: transmission electron microscopy shows that this treatment reduces the dislocation density. However, the rejuvenation results are clouded by large variations in the tests-specimen properties.

*Inconel is a registered trademark of the Inco family of companies.

This work was done by D. E. Matejczyk of Rockwell International Corp. for **Marshall Space Flight Center**. *For further information, Circle 153 the TSP Request Card. MFS-27131*

Electrochromic Variable-Emissivity Surfaces

Temperature could be controlled by altering infrared radiative properties.

Marshall Space Flight Center, Alabama

Experimental radiative-thermal-control coats have been made by vacuum deposition of thin films that include electrochromic layers. The absorptivity, emissivity, and reflectance of a suitably coated surface at various wavelengths can be

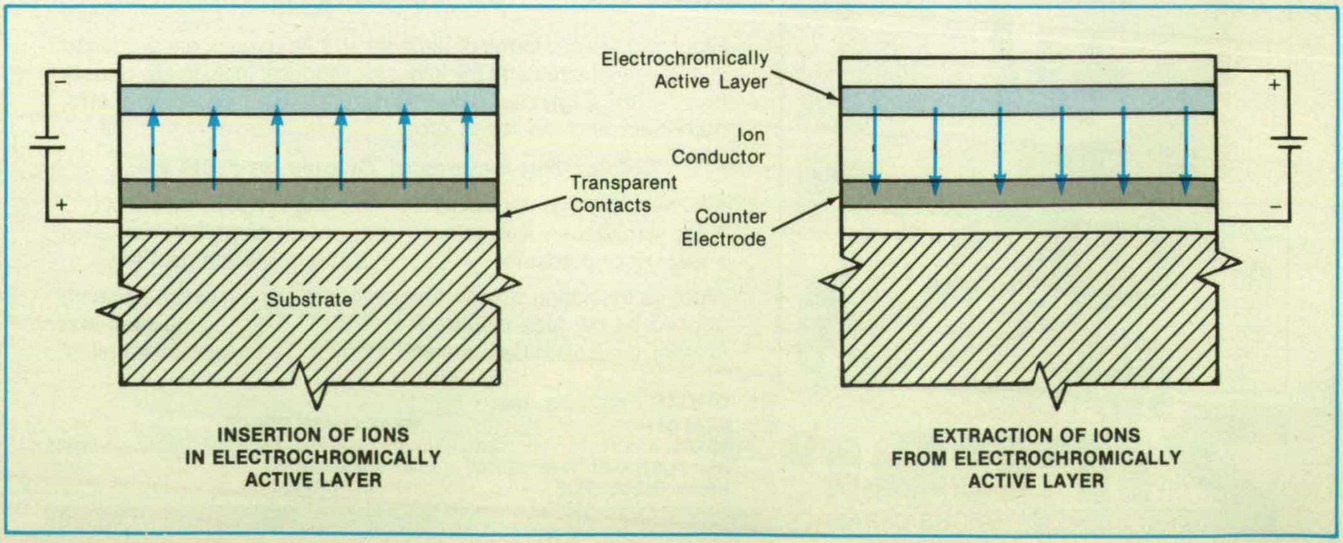

The **Infrared Emissivity** of the electrochromically active layer would be changed by applying a voltage to insert or remove Li atoms electrochemically. The change would be reversible and continuously variable between the specified limits of the layered structure.

changed reversibly by the application of a suitable voltage between two of its layers. When fully developed, such variable-emissivity surfaces could be useful for the controlled radiative (for example solar) heating and radiative cooling of equipment or of inhabited rooms.

The electrochromic materials of interest are the insertion compounds, in which small atoms can be inserted or from which small atoms can be extracted reversibly. One such compound is tungsten oxide, which interacts with lithium in the reversible electrochemical reaction

$$WO_3 + xLi^+ + xe^- \underset{\text{extraction}}{\overset{\text{insertion}}{\rightleftharpoons}} Li_xWO_3$$

The insertion of Li causes a change in optical properties due to the donation of an electron from Li to the WO_3 host material. A host material without long-range crystalline order (for example, amorphous WO_3) becomes more absorptive, while a crystalline material tends to become more reflective. The wavelength dependence of the enhanced reflectivity or absorptivity (and, therefore, emissivity) depends on the nature and thickness of the host material.

A typical coat might include an electrochromically active layer of Li_xWO_3, a transparent ion-conducting (but otherwise solid and electrically insulating) layer of $LiAlF_4$, and an electrochromically passive counterelectrode of TiO_2 or Nb_2O_5. The voltage would be applied to the active and counter layers through amorphous In_2O_3 contact layers, which are nearly transparent to infrared radiation.

Thus far, three versions have been tested:

1. A structure of polyethylene terephthalate/Al/a-Li_xWO_3/liquid electrolyte/a-Nb_2O_5/In_2O_3, which is switched between a state of high solar absorptivity with high infrared emissivity and a state of moderate solar absorptivity with low infrared emissivity;
2. A structure of glass/In_2O_3/c-Li_xWO_3/liquid electrolyte/a-Nb_2O_5/In_2O_3, which can be switched between a state of low solar absorptivity with low infrared emissivity and a state of low solar emissivity with high infrared emissivity; and
3. A structure of infrared-transmissive As_2S_3/In_2O_3/c-Li_xWO_3/liquid electrolyte/a-Nb_2O_5/In_2O_3, which can be switched between thermally reflecting and thermally transmitting (blackbody) states.

The experiments show that a device can be adjusted continuously to a state between its two extreme states. The energy density required for a complete transition between extreme states is less than 0.2 Wh/m^2 (720 J/m^2). No holding voltage is required because a device remains in its optical state until voltage is applied to change it.

This work was done by R. David Rauh and Stuart F. Cogan of EIC Laboratories, Inc., for **Marshall Space Flight Center**. *For further information, Circle 90 on the TSP Request Card.*

Inquiries concerning rights for the commercial use of this invention should be addressed to the Patent Counsel. Marshall Space Flight Center [see page 16]. Refer to MFS-26032.

PMR Composites of Increased Toughness

Toughness is increased without sacrificing processability or hot strength.

Lewis Research Center, Cleveland, Ohio

Addition-curing polyimide resin (PMR) polyimides are now gaining wide acceptance as matrix resins in composites destined for high-temperature applications in engines. Considerable cost and weight can be saved by the use of fiber-reinforced polyimide composites in place of the metals currently used in the moderately-high-temperature zones [up to 550 °F (288 °C)] of jet engines.

The technology for the application of these advanced composite materials to jet engines is developing rapidly. A graphite/PMR polyimide air-bypass duct has recently been developed to replace the titanium duct currently used on the F-404 engine that powers the Navy's F-18 fighter. Other components currently under consideration for composite applications include engine-inlet guide vanes, first- and second-stage stators, and anti-icing leading-edge wing panels.

A major concern in all of these applications is the resistance of the material to damage by impacts at low velocities. Such impacts can cause hidden internal damage in composite structures. While initially the damage may not degrade the structural integrity of the component, load reversals from vibrations induced in the structure under flight conditions can cause the damage to grow until the structure fails. This type of damage, which can result from dropped tools, runway debris, and the like, can occur in both the airframe structures and in the engine itself.

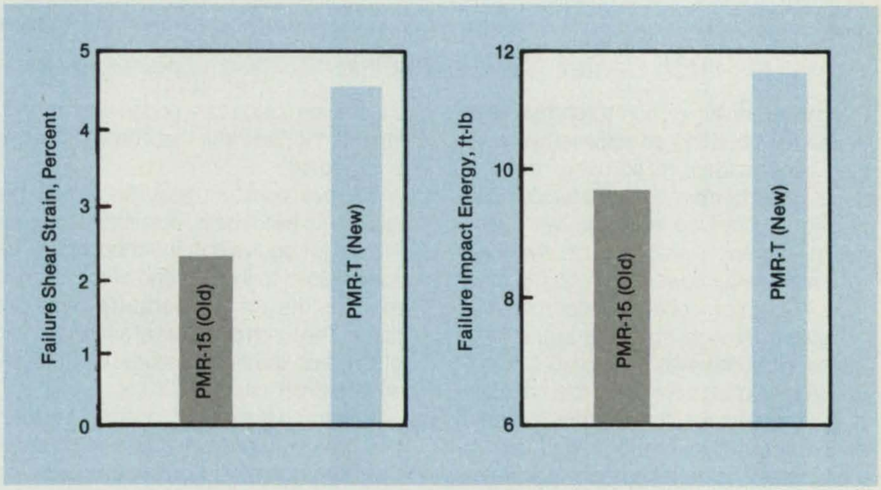

The **Toughnesses of Old and New Composites** were measured under impact.

PMR polyimides, which exhibit excellent resistance to oxidation at high temperatures, are inherently brittle matrix resins. With the broadening interest in the use of composites to improve the performances of engines, there is an obvious need for a tougher PMR polyimide material more tolerant to damage.

Some newly identified PMR resin compositions provide significant improvements in composite-shear-strain and low-velocity-impact properties. The resin composition that provided the best overall balance of composite toughness and retention of mechanical properties at 600 °F (316 °C) with processability was obtained by substituting 20 mole percent of the diamine used in PMR-15 resins with a diamine containing twice the number of flexible phenyl connecting groups.

The figures compare the properties of Celion 6000 graphite-fiber-reinforced composites, prepared from state-of-the-art PMR-15 resin, with those of the new PMR-T resin. The shear strain to failure and energy absorbed during low-velocity impact shown for the PMR-T composites are 85 and 25 percent higher, respectively, than the values shown for the PMR-15 composites. While the glass-transition temperature of the composites was approximately 50 °F (28 °C) lower than that of the PMR-15 composites, only a minimal difference in flexural strength of the two materials at

600 °F (316 °C) [135 ksi (93 MPa) for the PMR-15 composite and 128 ksi (88 MPa) for the PMR-T composite] was observed after exposure to air at a temperature of 600 °F (316 °C) for 1,500 h. The increased ductility offered by PMR-T resins provides PMR composite materials with better resistance to impacts at low velocities, without sacrifice of processability or long-term mechanical properties at 600 °F (316 °C).

This work was done by Raymond D. Vannucci and Kenneth J. Bowles of **Lewis Research Center**. *Further information may be found in NASA TM-87081 [N85-32148/NSP], "Graphite/PMR Polyimide Composites With Improved Toughness."*

Copies may be purchased [prepayment required] from the National Technical Information Service, Springfield, Virginia 22161, Telephone No. (703) 487-4650. Rush orders may be placed for an extra fee by calling (800) 336-4700.
LEW-14574

High-Emissivity Coatings for High-Temperature Surfaces

Plasma-sprayed coatings increase cooling by thermal radiation.

NASA's Jet Propulsion Laboratory, Pasadena, California

High-emissivity coatings on high-temperature refractory surfaces greatly increase their rates of heat radiation. In radiatively cooled engines and heat pipes, such coatings can prolong life and allow operation at higher powers.

A coating of zirconium diboride on tungsten or molybdenum increases the emissivity of a surface to more than 0.6 at 2,000 °C — more than twice that of the uncoated material. The coating is applied by plasma-arc spraying after the surface has been thoroughly cleaned and roughened to ensure adhesion.

On the electrode of an experimental high-power radiation-cooled electric thrustor, the coating causes the operating temperature in a typical case to decrease by 100 to 200 °C, preventing overheating and the resultant damage. The coating may also have potential applications in automotive engines: it could allow critical engine parts to operate cooler than they normally would, by enhancing radiative heat transfer.

This work was done by William D. Deininger and David Q. King of Caltech for **NASA's Jet Propulsion Laboratory**. *For further information, Circle 56 on the TSP Request Card.*

This invention is owned by NASA, and a patent application has been filed. Inquiries concerning nonexclusive or exclusive license for its commercial development should be addressed to the Patent Counsel, NASA Resident Office-JPL [see page 16]. Refer to NPO-17122.

Hydrogen/Air-Ignition Torch

The torch is simple, reliable, and economical.

Lewis Research Center, Cleveland, Ohio

A hydrogen/air-ignition torch has been devised for burning off excess hydrogen that accumulates in scrubber exhaust ducts. The torch consists of a welded concentric double-tube assembly with gaseous hydrogen flowing through the inner tube and the air flowing through the outer tube. The airflow cools the inner tube prior to flowing through openings in the inner tube and mixing with the gaseous hydrogen. A spark plug connected to a constant-duty simple ignition transformer is threaded into the side of the torch and into the inner tube. The transformer is used to excite the spark plug for a period long enough to ignite the gas. After that, the transformer is turned off.

To give constant assurance that the torch is lit, two type-K, open-ball, Chromel/Alumel (or equivalent) thermocouples are spot welded to the exit end of the torch to monitor the air temperature near the flame. The torch operates at a mixture ratio of 6:1, and the flame leaves the torch at subsonic velocities.

This torch is simple to operate, inexpensive, and very reliable. The burning of excess hydrogen by means of this torch has proven to be more economical than the previous carbon dioxide insertion technique.

This work was done by George A. Repas of **Lewis Research Center**. *Further information may be found in NASA TM-88882 [N87-13470/NSP] "Hydrogen Air-Ignition Torch."*

Copies may be purchased [prepayment required] from the National Technical Information Service, Springfield, Virginia 22161, Telephone No. (703) 487-4650. Rush orders may be placed for an extra fee by calling (800) 336-4700. *LEW-14552*

Readily Processable Polyimide

A polymer exhibits resistance to hydraulic fluid, excellent processability, and extremely high adhesive strength.

Langley Research Center, Hampton, Virginia

As part of an effort to develop tough, solvent-resistant thermoplastics for potential use as structural resins on aerospace vehicles, a new processable polyimide was evaluated. The synthesis involved the reaction of a new diamine, 1,3-bis 2-(3-aminophenoxy)ethyl ether, with 3,3′,4,4′-benzophenonetetracarboxylic dianhydride to form the polyamic acid and subsequent conversion of it to the polyimide. Various physical properties of the polyimide were measured. Films, moldings, adhesive specimens, and composite specimens were prepared and evaluated. Of particular interest is the extremely high titanium-to-titanium tensile shear strength of this polyimide.

The polyimide was semicrystalline with a crystalline-melt temperature (T_m) of 242 °C and a glass-transition temperature (T_g) of 150 °C. After the T_m had been exceeded, thermal annealing for several hours at 210 °C was unsuccessful in inducing crystallinity. Thermogravimetric analysis showed 5 percent weight loss in air and in nitrogen at 373 °C and 408 °C, respectively. The melt viscosity of fully-imidized amorphous polyimide measured at 210 °C was 6×10^6 P at a frequency of 0.1 rad/s and 1×10^5 P at 100 rad/s.

Transparent yellow films cast from N-methylpyrrolidone solutions of 95 percent imidized polymer and subsequently dried at 210 °C gave tensile strength, tensile modulus, and elongation at 25 °C of 12,500 psi (86.2 MPa), 391,400 psi (2.67 GPa), and 4.0 percent, respectively; and at 93 °C of 9,500 psi (65.5 MPa), 291,000 psi (2.01 GPa), and 5.0 percent, respectively. Film specimens were bent back upon themselves and placed in this stressed condition in jet fuel, deicing fluid, and hydraulic fluid. After 24 h of immersion, no detectable sensitivity was observed. However, after only a few minutes of exposure in methylene chloride (a component of paint stripper), pronounced crazing was observed.

Transparent orange moldings were fabricated at 260 °C under 100 psi (0.69 MPa) and cut into compact tension specimens. The fracture toughness (K_{Ic}) at 25 °C was 2,670 psi-in.$^{1/2}$ (2.93×10^6 N/m$^{3/2}$), and the fracture energy (G_{Ic}) at 25 °C was 18.2 in.-lb/in.^{2} (3.19×10^3 N/m). The surface of the failed specimens was highly crazed and moderately rough due to yielding.

Standard Ti/Ti tensile shear specimens were fabricated at 260 °C under 100 psi (0.69 MPa) and tested. The average Ti/Ti tensile shear strength of 7,850 psi (54.1 MPa) at 25 °C was exceptionally high, possibly the highest value ever reported for single lap specimens. The failure mode was essentially 100 percent cohesive. Strengths at other conditions were also excellent except after immersion in boiling water for 72 h. The problem, however, was at the interface (adhesive failure) and not with the polyimide. Powdered aluminum filler reduced the strength somewhat at 25 °C and increased the strength slightly at 121 °C.

Small graphite fabric composites fabricated at 260 °C under 200 psi (1.38 MPa) have flexural strength, flexural modulus, and short-beam shear strength of 70,500, 7,300,000, and 4,100 psi (486 MPa, 50 GPa, and 28 MPa) at 25 °C, respectively. No testing was done at elevated temperature because of the low values obtained at 25 °C. The significant finding of extremely high Ti/Ti tensile shear strength for this polyimide in addition to its other properties indicates a high potential for such aerospace applications as the adhesion of Ti/Ti substrates.

This work was done by Paul M. Hergenrother of **Langley Research Center** *and Frank W. Harris and Mark W. Beltz of the University of Akron. For further information, Circle 72 on the TSP Request Card.*

Inquiries concerning rights for the commercial use of this invention should be addressed to the Patent Counsel. Langley Research Center [see page 16]. Refer to LAR-13675.

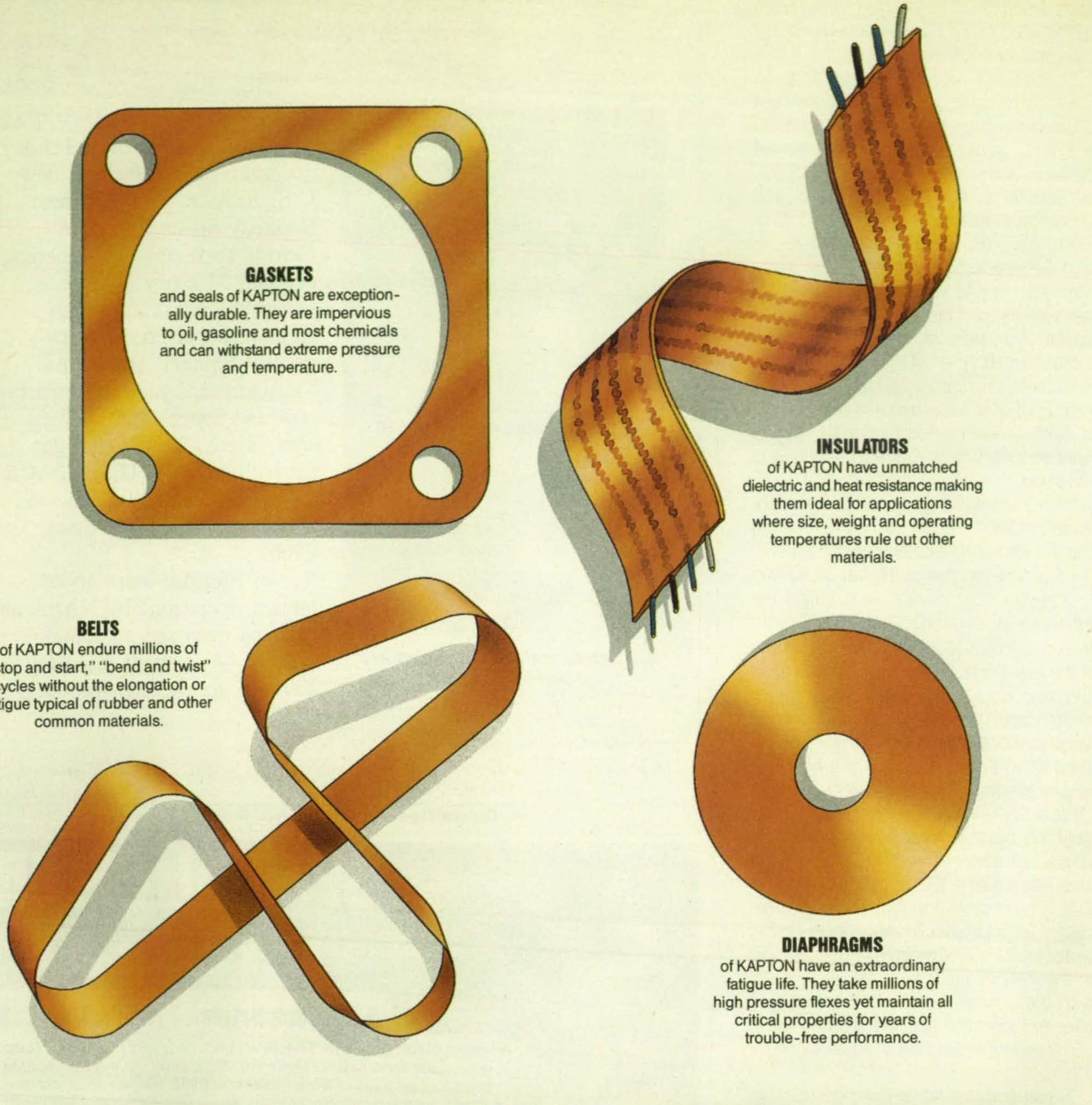

These parts made of KAPTON® have one thing in common. They survive where other materials fail.

Du Pont KAPTON[1] is an ultra-tough engineering material suited for uses where other materials such as polyester, rubber and even metals are prone to fail.

KAPTON survives extreme temperatures (-269° to 400°C). It won't melt, drip, or propagate flame. It has remarkable tensile strength yet remains flexible over a broad range of temperatures. And it is impervious to most chemicals.

With these unique properties, KAPTON can take real punishment. It is tough enough for "under-the-hood" automotive uses. It is used in well-drilling and mining equipment where intense heat destroys lesser materials. KAPTON has even ventured to the moon as a radiation shield on the Lunar Excursion Module.

For some thought-provoking ideas on how you might use KAPTON, please see the news clips on the following page. And for more information, write for our free brochure or call:

Du Pont Company
Room G50714
Wilmington, DE 19342
1-800-527-2601

DU PONT
REG. U.S. PAT & TM OFF

Circle Reader Action No. 577

[1] KAPTON is Du Pont's registered U.S. trademark for its proprietary polyimide film.

Process Makes High-Grade Silicon

Reactants and electrolyte are recycled to yield a relatively pure product.

Lyndon B. Johnson Space Center, Houston, Texas

A process produces metallurgical-grade silicon from quartz sand. In contrast with some conventional processes, the process does not involve odorous or toxic substances and proceeds at a lower temperature.

Like conventional processes, the new process is based on the reaction of silicon dioxide with aluminum, which yields silicon and aluminum oxide: $3\ SiO_2 + 4\ Al \rightarrow 3\ Si + 2\ Al_2O_3$. However, the aluminum for the new process is taken from an operating aluminum-electrolysis cell, and the Al_2O_3 product is returned to the same cell. The aluminum is thus continually recycled and purified, and the purity of the silicon is therefore high as well.

One of the starting materials for the process is 99.5-percent-pure silica sand from natural deposits. (Sand of lower purity can be used, but must first be beneficiated.) The sand is introduced into a holding furnace that contains aluminum and electrolyte (molten cryolite) from the electrolysis cell (see figure), and the resulting mixture is heated to a temperature of 1,000 to 1,050 °C. A molten aluminum/silicon alloy accumulates in the furnace. The alloy is transferred to a precipitator, and the electrolyte, now rich in Al_2O_3, is returned to the electrolysis cell.

In the precipitator, the alloy is cooled to 700 °C, causing globules rich in silicon to solidify, leaving a melt rich in aluminum. The mixture is transferred to a separator, where the solid silicon is extracted and passed to a purifier. The molten aluminum, containing about 12.6 percent silicon — close to the eutectic composition — is returned to the electrolysis cell.

In the purifier, the solid silicon is treated with molten cryolite that contains SiO_2. The residual aluminum in the solid silicon reacts with the SiO_2 to form additional solid silicon. The Al_2O_3 thus produced dissolves in the electrolyte and is returned with it to the electrolysis cell. The electrolyte also contains some silicon, but the material is not wasted because it is recycled. The solid silicon can be recovered directly by remelting at 1,410 °C or purified further by a salt that is more readily removable than cryolite, by leaching or by a vacuum treatment.

This work was done by Rudolf Keller of EMEC Consultants for **Johnson Space Center**. *For further information, Circle 9 on the TSP Request Card.*

In accordance with Public Law 96-517, the contractor has elected to retain title to this invention. Inquiries concerning rights for its commercial use should be addressed to

EMEC Consultants
R.D. 3 Roundtop Road
Export, PA 15632

Refer to MSC-21323, volume and number of this NASA Tech Briefs *issue, and the page number.*

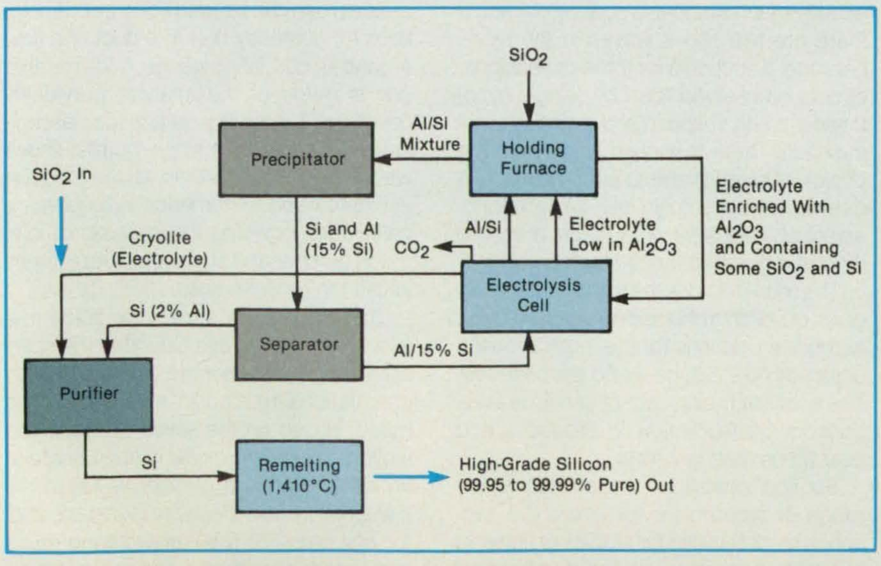

Aluminum and Electrolyte flow to and from an aluminum-electrolysis cell at various stages of the silicon-producing process. The electrolyte is molten cryolite.

Computer Programs

COSMIC: Transferring NASA Software

COSMIC, NASA's Computer Software Management and Information Center, distributes software developed with NASA funding to industry, other government agencies and academia.

COSMIC's inventory is updated regularly; new programs are reported in *Tech Briefs*. For additional information on any of the programs described here, circle the appropriate TSP number.

If you don't find a program in this issue that meets your needs, call COSMIC directly for a free review of programs in your area of interest. You can also purchase the 1988 *COSMIC Software Catalog*, containing descriptions and ordering information for available software.

COSMIC is part of NASA's Technology Utilization Network.

COSMIC® — *John A. Gibson, Director,* (404) 542-3265
The University of Georgia, 382 East Broad Street, Athens, Georgia 30602

Computer Programs

These programs may be obtained at a very reasonable cost from COSMIC, a facility sponsored by NASA to make computer programs available to the public. For information on program price, size, and availability, circle the reference number on the TSP and COSMIC Request Card in this issue.

Mechanics

Unsteady Flow in a Supersonic Cascade With Shocks

The operating range of turbomachinery for which stability can be calculated is extended.

The computer program TIPS (Two In-Passage Shocks) calculates unsteady lifts and moments on a compressor blade if the relative mach number is supersonic and if there are two shock waves in the blade passage. It accounts for three-dimensional effects in observed flows by using a hypothetical blade shape in a two-dimensional cascade. There is enough flexibility in the choice of blade shape to accommodate a desired entrance angle, exit angle, boundary-layer thickness, and stage pressure ratio at a given entrance mach number.

The model divides the mean flow into regions of uniform or one-dimensional flow in which the solutions for the superimposed unsteady flow can be found successively. The analysis makes use of previous solutions for unsteady flow in cascades and over an oscillating wedge.

Six flow conditions are chosen in the range of parameters for which the two-shock model is valid for studies of flutter in torsion and bending. It is found, in keeping with previous results from a single-shock model, that in each case the instability increases with decreasing frequency.

The analysis of unsteady flows in blade rows has been facilitated by the use of models for the underlying steady flow that permit the governing differential equations to be written with constant coefficients. This has been true for both supersonic flows and mixed flows with single shock waves in which the mean flows were assumed to be uniform. Numerous experiments, using both pressure sensors and laser anemometers, have shown that multiple shock waves are common in the tip regions of the blades, especially near the operating point of the compressor. One of the frequent patterns observed in the experiments includes an oblique shock wave at the leading edge of each blade and a nearly-normal shock wave at the trailing edge. It is that flow this program addresses.

A model for the mean flow incorporates the two shock waves and modifies the actual blade surfaces to account for the effects of three-dimensional flows. Three mean-flow domains are modeled as either uniform or one-dimensional flow so that the greatest use can be made of previous solutions for unsteady flow in a duct and flow around an oscillating wedge. Considerable use is made of the analysis previously developed for the flow in a blade passage in the presence of a single normal shock wave. The range of validity of the model is estimated, and six numerical examples are calculated, covering the intervals of inlet mach number and stage pressure ratio for which the model is valid.

This model for a supersonic blade row with shock waves has extended the operating range of turbomachinery for which calculations related to stability can be made. Based on the single configuration explored here, the model is appropriate at an entrance mach number ≤ 1.3 at the lowest applicable stage pressure ratio and, for any pressure ratio, at entrance mach numbers higher than those of the single-shock model. The calculations for specific cases show that in this operating region

The way some companies build their positioners, could give you the creeps.

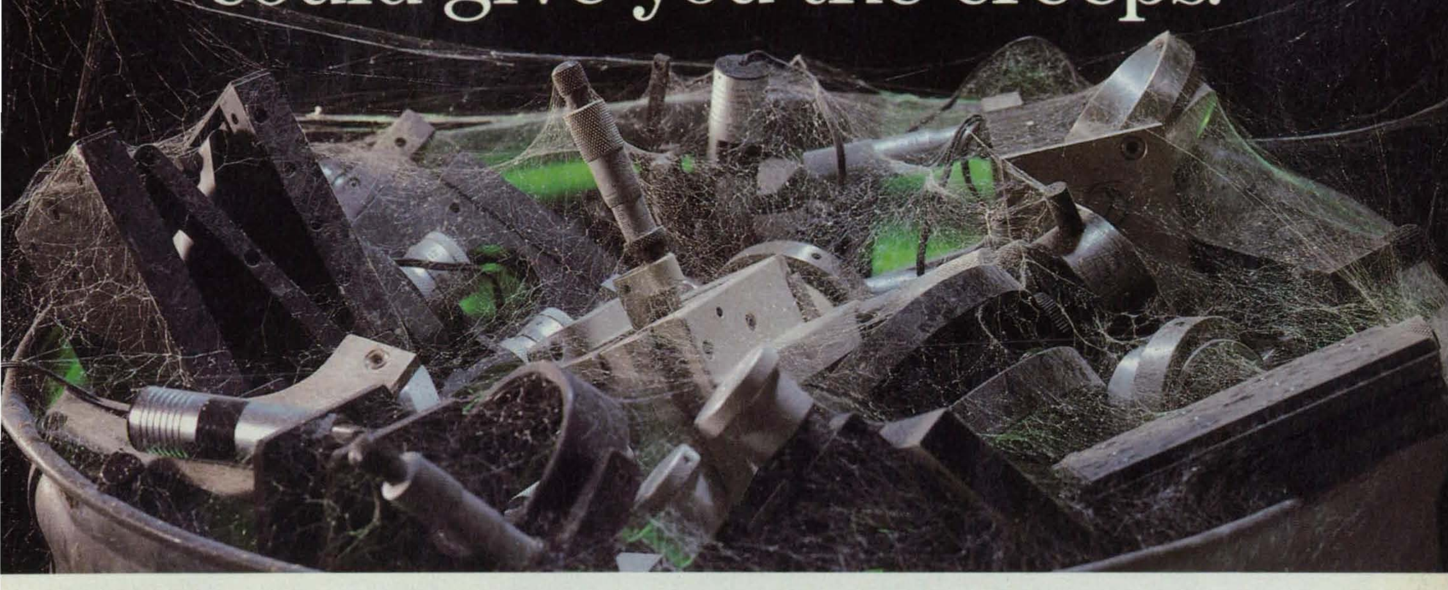

Have you ever set up an experiment and had the test results drift over time? We call this mysterious phenomenon "creep." It could be caused by something as seemingly insignificant as minute changes in temperature at the test area.

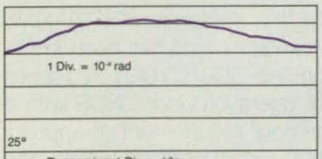

As temperatures change, differences in the coefficients of expansion of the various materials can cause the positioners to wander off from their initial positions.

At Klinger Scientific, we know why other manufacturers build their positioners of aluminum. It can be easier and less expensive. But we just can't bring ourselves to do it.

All our stages are made of thermally matched materials, stainless steel and hardened tool steel. Rockwell Grade 60, to be exact.

ONLY HARDENED TOOL STEEL CAN STAND UP TO OUR WAY OF WORKING.

We use just one type of material, the best, because it's the best way yet devised to keep the creeps out of our stages and your tests and measurements.

Tool steel has another important advantage. Because it's so incredibly hard, we can grind the guide bearing V-ways absolutely flat and straight.

So our carriages move smoothly on their ball bearing slides with essentially zero trajectory error.

Klinger stages are sensitive to better than one micron. With repeatability to one micron.

NOW YOU CAN AFFORD KLINGER PRECISION.

Klinger manufactures over 200 linear stages, with travel ranges up to 1.5 meters, and over 100 precision rotational stages. Every one is compatible with every standard optical table. And we provide adaptor plates if you need to convert from metric to English mounting surfaces.

Best of all, we've made our products more price competitive without compromising, in any way, the highest standards our customers expect from Klinger Scientific.

So you no longer have to settle for less than the finest. You can build your systems with Klinger parts and never worry about errors creeping into your work again.

To find out more about the complete Klinger line of micropositioning systems, call or write Klinger Scientific Corporation, 999 Stewart Avenue, Garden City, NY 11530. (516) 745-6800. We'll tell you more about our new pricing structure and send you a free copy of our micropositioning handbook.

KLINGER SCIENTIFIC

Building better positioning systems, piece by perfect piece.

U.S.A. Headquarters: 999 Stewart Avenue, Garden City, NY 11530 (516) 745-6800.
Regional Offices: Northern California (415) 969-0247; Southern California (714) 999-5088. Worldwide distribution network: Contact Micro-Controle, Z.I. de St. Guenault, B.P. 144, 91005 Evry Cedex, France. Tel.33(1)64.97.98.98. FAX 33(1)60.79.45.61.

Circle Reader Action No. 368

the presence of shock waves has a strong influence on the unsteady flow and that the tendency for instability at low frequencies observed in the single-shock model persists in the two-shock model. The thickness ratio appears to have significant influence on the stability of the flow at high frequencies.

The program is written in FORTRAN IV and run on an IBM 3033 with 370TSS operating system.

This program was written by Frank B. Molls of **Lewis Research Center** *and Willis H. Braun. For further information, Circle 84 on the TSP Request Card.*
LEW-14339

Computing Flows Over Wavy Surfaces

Wind/wave interactions, drags, and related phenomena can be predicted.

WAVEGEM is a package of algorithms developed to study two-dimensional turbulent flow past wavy surfaces. The component programs include (1) PROFILE — a program that creates initial equilibrium turbulent flat-plate profiles for a given flow condition, (2) CONMAP — a conformal-mapping program, and (3) WAVY — the two-dimensional Navier-Stokes equation solver, which simulates flow over a wavy surface. The WAVEGEM package can be used to estimate the effects of waviness introduced through fabrication and to study interactions between wind and waves. It can also be applied to the examination of the reduction of drag on wavy walls.

The typical problems studied with WAVEGEM are flows over stationary wave trains, the amplitudes of which are much smaller than the wave number. The geometrical coordinates of a wavy surface over 1 wavelength are fed to CONMAP. CONMAP uses fast and efficient conformal-mapping techniques to develop an orthogonal grid system. The mapping coefficients and physical grid coordinates are held in mass storage. CONMAP also performs a linear interpolation of the input velocity field using measured data or values calculated from PROFILE to create a velocity field in the computational domain at time zero.

The evolution of flow at subsequent times is determined by WAVY, which solves the Reynolds-averaged Navier-Stokes equations with higher-order Fourier/Chebyshev spectral techniques. The primary input to the programs includes the free-stream velocity, viscosity, skin-friction coefficients, thickness of the boundary layer, and the geometrical specification of the wave. The output of WAVY consists of short-cycle printed tables containing pressure at the wall, velocity at a point above the wall, friction drag, pressure drag, and Reynolds number.

WAVEGEM is written in FORTRAN 66 for batch execution and has been implemented on the CDC CYBER 170-series computers operating under NOS with a central-memory requirement of approximately 200K (octal) of 60-bit words. The program was developed in 1986.

This program was written by John C. Lin and Barbara H. Pitts of **NASA's Langley Research Center** *and R. Balasubramanian of Cambridge Hydrodynamics, Inc. For further information, Circle 26 on the TSP Request Card.*
LAR-13659

Space-Station-Interior Noise-Analysis Program

The intelligibility of speech is evaluated for specified acoustical environments.

The Space Station Interior Noise Analysis Program (SSINAP) predicts the noise levels and the associated interference to speech that will occur in a space station. SSINAP is an analysis tool for optimizing the acoustic design of a space station with respect to communication by speech. The program makes a systematic prediction of the noise and vibration environment of a craft defined by the user and evaluates the relative acceptability of the predicted environment for effective communication by speech. Although designed for a space station, SSINAP can be applied to any system of rectangular or cylindrical acoustical spaces contained by known structures.

The user describes the space station as a group of physical subsystems. SSINAP performs a statistical energy analysis (SEA) of the total vibroacoustic system for each of nine octave bands centered at frequencies ranging from 31 to 8,000 Hz. This is coupled with a model for predicting the intelligibility of speech on the basis of a speech-transmission index (STI). SSINAP computes the STI for any room in the space station.

The space station is defined as a series of structural elements and airspaces. A connectivity matrix describes the complex transmission paths in terms of acoustical and vibrational power conveyed between coupled elements of the system. The acoustical and vibrational input to each subsystem can be entered directly by the user or can be calculated by the choice from a menu of equipment sources, including heating, ventilating, and air-conditioning systems; ac and dc motors; pumps; and a variety of fans.

SSINAP calculates the power lost in each subsystem due to the absorption of sound, internal damping, and friction. A set of SEA linear equations is solved to produce the unknown panel velocities and acoustic pressures. The STI is then calculated, given the geometrical specification of the room, directivity factors, and the listener's age and location.

SSINAP is menu-driven with an extensive data-checking/editing facility. The input can be stored as a file for future use, saving time and enabling easy alteration of such data as absorption coefficients, power levels, and impedances.

SSINAP is written in MicroSoft FORTRAN Version 3.3 for interactive execution and has been implemented on an IBM PC operating under PC DOS Version 2.1 with a central-memory requirement of approximately 175K of 8-bit bytes. The program was developed in 1987.

This program was written by Eric Stusnick of Wyle Laboratories for **Langley Research Center**. *For further information, Circle 24 on the TSP Request Card. LAR-13766*

Spectrum-Analysis Program

Minerals can be identified in geological images.

The Spectral Analysis Manager (SPAM) computer program was developed to enable easy qualitative analysis of multidimensional data from imaging spectrometers. Imaging spectrometers provide sufficient spectral sampling to define a unique spectral signature for each pixel. Thus, the direct identification of materials for geological studies becomes possible.

SPAM provides a variety of capabilities for interactive analysis of the massive and complex sets of data associated with multispectral remote sensing. In addition to normal image-processing functions, SPAM provides multiple levels of online help, a flexible command interpretation, graceful recovery from errors, and a program structure that can be implemented in a variety of environments. SPAM was designed to be oriented visually and friendly to the user, with the liberal employment of graphics for rapid and efficient exploratory analysis of data from imaging spectrometry.

SPAM provides functions to enable such arithmetical manipulations of the data as normalization, linear mixing, band ratio discrimination, and low-pass filtering. SPAM can be used to examine the spectrum of one pixel or the average spectrum over a number of pixels. SPAM also supports the segmentation of images, fast matching of spectral signatures, the use of a library of spectra, the analysis of mixtures, and the extraction of features. Fast matching of spectral signatures is performed by use of a binary spectrum-encoding algorithm to separate and identify mineral components present in the scene.

The same binary encoding enables the automatic clustering of spectra. Spectral data can be entered from a digitizing tablet, stored in a user library, compared to the master library containing mineral spectral standards, and then displayed as a time-sequence spectral movie. The output plots, histograms, and stretched histograms produced by SPAM can be sent to a line printer, stored as separate red, green, and blue files on disks, or sent to a quick color recorder.

SPAM is written in C for interactive execution and is available for three different computing environments. There is a DEC VAX/VMS version with a central-memory requirement of approximately 242K of 8-bit bytes, a DEC VAX/TAE version, and a machine-independent UNIX 4.2 version. The VAX/TAE implementation is designed to interact with the TAE program supplied by the user and includes standard VICAR-labeled sets of image data. (Both TAE, Transportable Applications Executive, and VICAR, Video Image Communication and Retrieval, programs are available separately from COSMIC.) The display devices currently supported are the De Anza and Raster Technologies display processors. Other 512 × 512 resolution color display devices may be added with minor code modifications. The program was developed in 1986.

This program was written by J. E. Solomon, M. Lee, A. S. Mazer, and M. Martin of Caltech for **NASA's Jet Propulsion Laboratory**. *For further information, Circle 30 on the TSP Request Card. NPO-17180*

Mathematics and Information Sciences

NASKERN Program Tests Computers

A "benchmark" program exercises computers on a set of standardized problems.

A test computer program, NASKERN, has been developed for use by the Numerical Aerodynamic Simulation (NAS) project to aid in the evaluation of the performances of supercomputers. NASKERN consists of seven test-kernel programs that perform computations typical of supercomputer calculations at NASA Ames Research Center. It is expected that the performances of supercomputers when running this program will provide accurate projections of the performances of these computers on the actual computer codes of the NAS program.

The seven programs all emphasize the vectorized performance of a modern computer system. Each program is independent and consists of various looped floating-point operations. The programs include the following:

1. A matrix product;
2. An in-place, complex, radix-two, fast Fourier transform;
3. Parallel Cholesky decomposition;
4. Block tridiagonal matrix solution;
5. Gaussian elimination;
6. Creation of vortexes from boundary conditions; and
7. Simultaneous inversion of three matrix pentadiagonals.

NASKERN calculates performance statistics based on checks of accuracy, the number of operations performed, running times on the central processing units, and the resulting rates of calculation in terms of the number of floating-point operations per unit time.

NASKERN is written in FORTRAN 77 for batch execution and can be implemented on any machine with 64-bit precision. It has been run on a CRAY supercomputer under COS with a central-memory requirement of approximately 500 K of 64-bit words. NASKERN requires a machine-dependent clock-timing subroutine. The program was developed in 1986.

This program was written by David H. Bailey of Sterling Software for **Ames Research Center**. *For further information, Circle 138 on the TSP Request Card. ARC-11726*

Subroutines for Image Processing

Dozens of functions and test programs are included.

The Image Processing Library computer program, IPLIB, is a collection of subroutines that facilitate the use of a COMTAL image-processing system driven by an HP 1000 computer. IPLIB uses an HP driver to direct all communications between the HP and a COMTAL Vision One/20 system. Dozens of functions are supplied, along with a test program for each function. Each IPLIB function takes the form of a FORTRAN subroutine invocation with appropriate parameters.

The functions include the addition or subtraction of two images with or without scaling, display of color or monochrome images, digitization of the image from a television camera, display of a test pattern, manipulation of bits, and clearing of the screen. IPLIB also provides the capability to read or write points, lines, and pixels from an image; read or write at the location of a cursor; and read or write an array of integers into COMTAL memory. The documentation catalogs the subroutines alphabetically and hierarchically for use as a cross-reference guide.

IPLIB is written in FORTRAN 77 for interactive execution and has been implemented on an HP 1000 computer operating under RTE VI with a central-memory requirement of approximately 64K. IPLIB is intended for use by those familiar with the COMTAL Vision One/20 image-processing system. The program was developed in 1985.

This program was written by Nettie D. Faulcon and James H. Monteith of **Langley Research Center** *and Keith W. Miller of the College of William and Mary. For further information, Circle 57 on the TSP Request Card. LAR-13620*

Network Queueing System

This program directs traffic in a UNIX-based network.

The Network Queueing System (NQS) computer software provides batch and device queueing facilities for various computers comprising a networked UNIX environment. Running as a collection of user-space programs, NQS provides facilities for remote queueing, request routing, remote status, queue-access controls, batch-request resource-quota limits, and remote output return. NQS was developed as part of an effort aimed at tying together diverse UNIX-based machines into NASA's Numerical Aerodynamic Simulator Processing System Network.

The NQS architecture was designed with the following 10 goals:

1. Provide full support for both batch and device requests;
2. Support all of the resource quotas enforceable by the underlying UNIX kernel implementation that are relevant to any particular batch request and its corresponding batch queue;
3. Support remote queueing and routing of batch and device requests throughout the NQS network;
4. Modularize request-scheduling algorithms so that schedulers can be easily modified at individual installations;
5. Support restrictions on access to the queue through user- and group-access lists for all queues;
6. Enable networked output return of both output and error files to possibly remote machines;
7. Allow mapping of accounts across machine boundaries;
8. Provide friendly configuration-modification mechanisms for each installation;
9. Support status operations across the network, without requiring a user to log in on remote target machines; and
10. Provide "hooks" for the possible future implementation of file staging (i.e., copying specific files to the execution machine).

Three types of queues (batch, device, and pipe) are supported by NQS. Batch queues do not require a specific device other than the CPU resource of the machines; that is, they consist merely of shell scripts executed without any associated terminal. A device queue is for requests that require the direct services of a specific device, such as a line printer. A pipe queue exists to transport requests to other batch, device, or pipe queues at possibly remote machine destinations. The pipe-queue mechanism is responsible for routing and delivering requests to other queues in spite of machine failures, lack of owner authorization at some destinations, insufficient space, disabled queues, and other rejections. All NQS network conversations are performed by use of the Berkeley socket mechanism as ported into the respective vendor kernels.

NQS is written in the C language and runs under both System V and Berkeley UNIX, and has been ported to various hardware environments, including DEC VAX, Silicon Graphics IRIS, Amdahl 5840 mainframes, and the CRAY-2 and CRAY-XMP machines. NQS has a central-memory requirement of approximately 160K of 8-bit bytes on a DEC VAX computer. The NQS daemon must reside on every computer in the network. NQS requires the nmap utility, which is supplied as part of the NQS package. The program was developed in 1986.

This program was written by Brent Kingsbury of Sterling Software, Inc., for **Ames Research Center**. *For further information, Circle 21 on the TSP Request Card.*

Inquiries concerning rights for the commercial use of this invention should be addressed to the Patent Counsel, Ames Research Center [see page 16]. Refer to ARC-11750.

Calculating Numbers to Arbitrarily High Precision

The PITEST program is a package of fast routines for performing multiprecision arithmetic.

The PITEST program is a package of subroutines that perform arithmetic on floating-point numbers of arbitrarily high precision. PITEST can also work on very large integers by treating them as floating-point numbers with enough precision to represent their integral values exactly. Multiprecision computations are important in public-key cryptography, Bessel-function evaluation, and as tests for the integrity of scientific computer systems (testing both equipment and FORTRAN compilers).

The main program of PITEST calculates the value of π, the ratio of the circumference of a circle to its diameter, using two algorithms recently discovered by the Borweins. PITEST is capable of calculating π to several billion digits, although the program as delivered will calculate only 25,000 digits.

Once the multiprecision package has been verified by obtaining the same result for π by the two supplied calling programs, then it may be used confidently for application programs. This package contains subroutines to perform multiplication, division, and the extraction of square roots by use of subroutines based on such sophisticated techniques as fast Fourier transforms. The use of these subroutines can dramatically reduce the demand on computational resources when arithmetic of high precision is required.

PITEST is written in FORTRAN 77 for batch execution and can be implemented on any computer with 60-bit or 64-bit floating-point arithmetic. PITEST has been implemented on a CRAY-XMP supercomputer under COS with a central-memory requirement of approximately 160K of 64-bit words. It has also run on an IBM PC with a math coprocessor. PITEST requires a machine-dependent clock-timing subroutine. The program was developed in 1986.

This program was written by David H. Bailey of Sterling Software for **Ames Research Center**. *For further information, Circle 22 on the TSP Request Card.*
ARC-11725

Liquid-Seeding Atomizer

Particles are sprayed in drops of evaporating liquid.

Ames Research Center, Moffett Field, California

An improved atomizer for use in a wind tunnel (see Figure 1) generates a well-defined spray of uniformly sized liquid drops and solid particles for use in laser Doppler velocimetry or visualization of the airflow about a model. The atomizer does not disturb the airflow measurably at the model. In contrast with conventional atomizers, the new one is less bulky and can therefore be inserted through a small access hole in the wind-tunnel wall.

The major structural component of the atomizer is an air-supply tube that spans the wind tunnel (see Figure 2). Orifices for air are placed at evenly spaced locations along the downstream side of the tube, wherever a spray is required. A liquid-feed tube is silver soldered or otherwise fastened along its entire length to the air-supply tube on each side of the line of orifices for air. Orifices for liquid are drilled in the sides of the liquid-feed tubes facing each other, adjacent to the orifices for air.

The distance between the liquid-feed tubes is about 70 percent of the diameter of the orifices for air, so that the air flowing out of the orifices creates a venturi effect. Because the liquid-feed tubes are restrained from vibrating away from the air-supply tube, the fluid jets do not become distorted and form large droplets, as they can in some conventional atomizers.

The liquid-feed tubes are joined at one end; they could be made by suitably bending one piece of stainless-steel tubing. With this shape, the tubes can be cleaned by circulating a cleaning fluid through them, without having to remove the atomizer from the wind tunnel.

For proper seeding of the wind-tunnel airflow, the sprayed mixture should consist of uniformly sized microscopic particles in a liquid that evaporates quickly before the spray reaches the wind-tunnel test section. One such mixture is 0.2 weight percent of ½-μm-diameter polystyrene-latex spheres in alcohol or an alcohol/water solution. A typical air-supply pressure, air-orifice diameter, and liquid-orifice diameter are

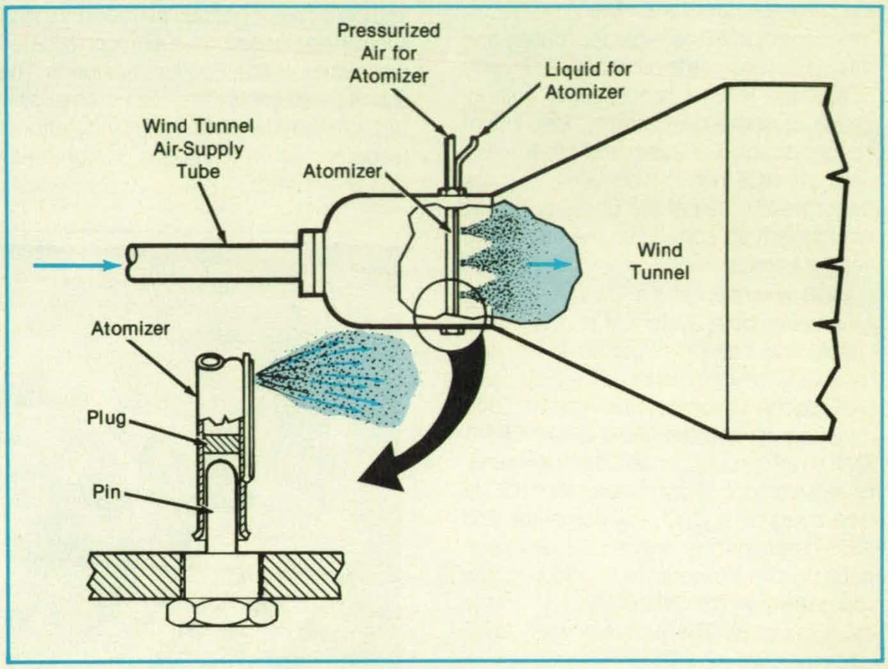

Figure 1. **Placed Near the Wind-Tunnel Inlet,** the atomizer sprays evaporating liquid containing solid particles into the wind-tunnel airflow. The particles are entrained in the flow and scatter light, thus enabling the flow to be observed optically. One end of the atomizer slides on a stationary pin to accommodate thermal expansion and contraction.

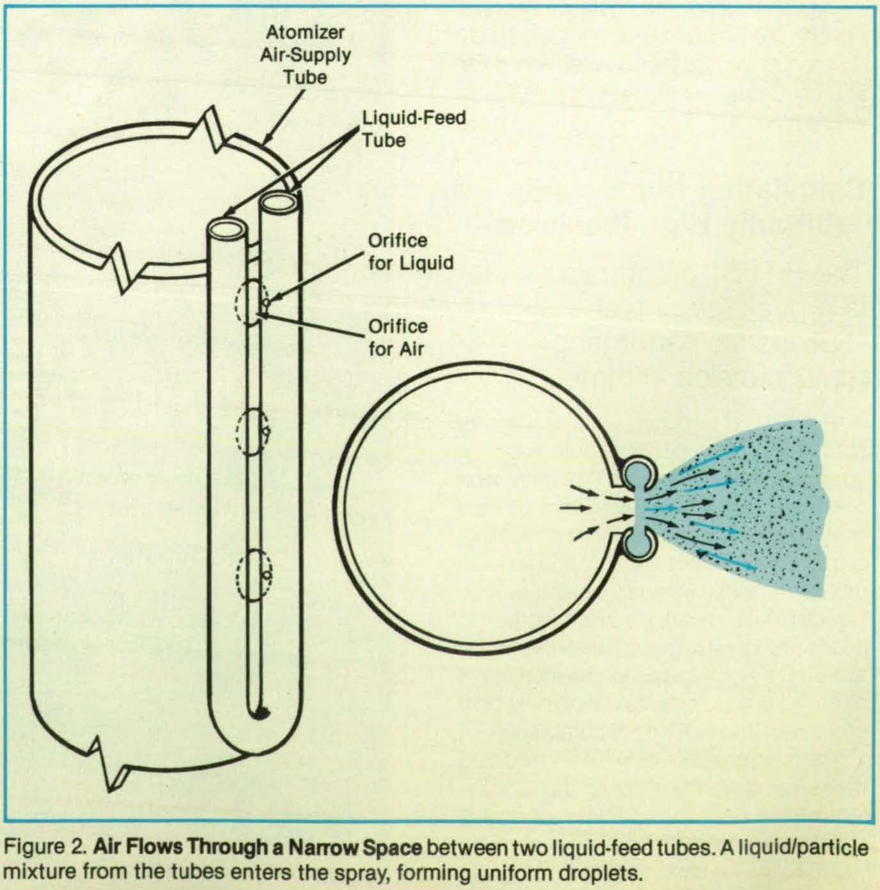

Figure 2. **Air Flows Through a Narrow Space** between two liquid-feed tubes. A liquid/particle mixture from the tubes enters the spray, forming uniform droplets.

400 psi (2.8 MPa), 0.180 in. (4.57 mm), and 0.015 in. (0.38 mm), respectively.

The atomizer can be used in supersonic and transonic wind tunnels. With suitable spacing of the orifice groups, the sprays from the separate groups consolidate into one large fan-shaped spray. The width of the spray can be chosen via the number and spacing of orifice groups. The thickness of the spray can be altered by changing the distance between tubes, the air pressure, and/or the orifice size. Thus, the spray can be configured so that it does not deposit obscuring particles on the observation parts and does not clog the porous boundary-layer suction plates of the wind tunnel.

This work was done by Henry L. B. Seegmiller of **Ames Research Center**. *For further information, Circle 15 on the TSP Request Card.*

Inquiries concerning rights for the commercial use of this invention should be addressed to the Patent Counsel. Ames Research Center [see page 16]. Refer to ARC-11631.

Designing Shafts for Long Life

Fatigue lives are affected by many factors.

Lewis Research Center, Cleveland, Ohio

An improved method has been developed for choosing the sizes of power-transmitting shafts for limited or unlimited service lives under a variety of operating conditions. In essence, the method replaces some traditional simplifying approximations and guesswork by more-refined design equations based on considerations of metal fatigue. The method will be especially beneficial where critical compromises have to be made between shaft weights and reliabilities or where the penalties of shaft failure are severe.

The basic problem is to estimate the diameter required for a shaft to survive a specified number of cycles under an expected sequence of steady or variable-amplitude loads. Preferably, the analysis for a given shaft would begin with the experimental determination of its curve of stress amplitude versus number of stress cycles to failure under the appropriate mean loading condition (see figure). However, in the absence of full fatigue-life data, the analysis is based on a nominal-stress-life approximation, in which a straight line on a log-log plot connects the true fracture strength at 1 cycle to the fatigue limit of the shaft at 10^6 or 10^7 cycles.

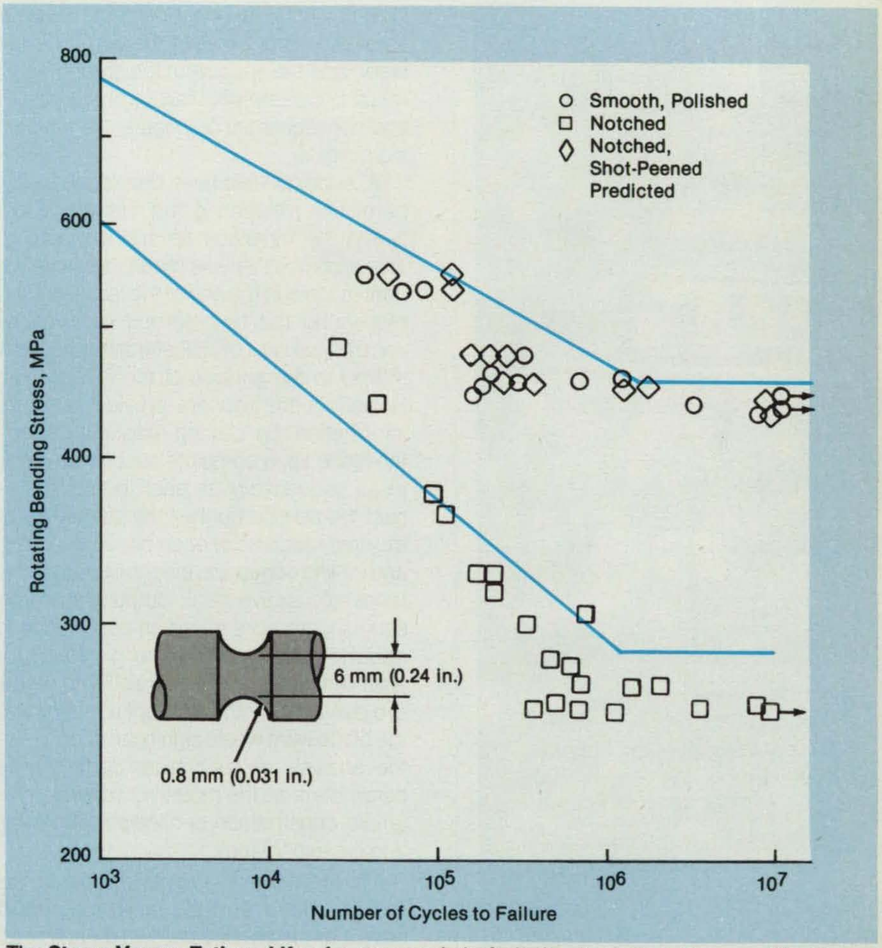

The **Stress Versus Fatigue Life** of a proposed shaft design is plotted, then modified to account for expected operating conditions and used to calculate a shaft diameter required for a given fatigue life. If the diameter of the shaft represented by the plot equals or exceeds the required diameter, the shaft is considered adequate.

A number of factors are introduced to modify the stress levels and slopes on the log-log fatigue-life plot for the effects of environmental, geometrical, and loading conditions likely to be encountered in service. These factors are based on previous experimental and theoretical determinations of the effects of surface finishes, temperatures, the inclusion of more inherent defects with increases in size, stress concentrations at splines and keyways, press-fitted collars, residual manufacturing stresses, and corrosion.

The effects of variable-amplitude loading are treated by expressing a complicated, irregular loading history as a series of constant-amplitude events and by invoking the Palmgren-Miner linear-damage rule. This rule assumes the accumulation of damage at a linear rate without regard to the sequence of loading and in some cases may have to be replaced by more-complicated cumulative-damage theories that express the effects of different load sequences.

In some applications of the new design method, it was shown that occasional cyclic overloads reduce the fatigue strength considerably or else require the use of a much larger shaft diameter. The sensitivity of shaft fatigue life to bending stress was found to depend primarily on the tensile strength and the overall fatigue-life-modifying factor: the life might vary with stress to the −14th power for a small, smooth, high-strength-steel shaft or to the −5th power for a large, rough, heavily notched, low-strength-steel shaft.

This work was done by Stuart H. Loewenthal of **Lewis Research Center**. *Further information may be found in NASA TM-87354 [N86-27661/NSP], "New Methodology for Shaft Design Based on Life Expectancy."*

Copies may be purchased [prepayment required] from the National Technical Information Service, Springfield, Virginia 22161, Telephone No. (703) 487-4650. Rush orders may be placed for an extra fee by calling (800) 336-4700.
LEW-14517

Measuring Fan-Blade-Tip Displacements

Magnets and Hall-effect transducers are used to monitor tip-to-shroud clearances.

Langley Research Center, Hampton, Virginia

The fan blades in a wind tunnel are subjected to a myriad of forces during service. The material, construction, and age of the blades and the temperature, humidity, and density of the tunnel fluid combine with the turning speed and the resultant centrifugal loads to influence the size of the space between the fan blades and the wind-tunnel shroud. If this space becomes critically small, scuffing between the tip of the fan blade and the surface of the shroud could result in catastrophic failure of the fan set and consequential damage to the fan-driving system.

A technique has been developed for dynamically measuring the clearance between the fan-blade tip and the shroud. This technique entails mounting a permanent magnet in the end of the fan blade and monitoring the tip-to-shroud distance by use of the output of Hall-effect transducers affixed to the surface of the shroud. The Hall-effect transducers provide real-time information. By placing magnets in each fan-blade tip, a complete set can be monitored sequentially as each blade rotates past the sensor. Further, the placement of multiple magnets in each blade at leading and trailing edges and the monitoring of the times of relative peak outputs at corresponding sensors afford an opportunity to ascertain dynamically the presence of twist within the blade. This ability to measure dynamically the tip displacement and the blade twist would significantly enhance the analysis of such blade-performance parameters as the mounting scheme, materials, construction, service performance, and life expectancy.

The permanent magnet affixed to the radial-tip surface of the fan blade should have a low mass and positive means of attachment because the magnet and capture assembly are subjected to centrifugal forces commensurate with the mass and the rotary speed. Also, the field of the magnet must be sufficient to traverse the tip (magnet)-to-shroud distance and excite the transducer. These criteria are satisfied by a small, commercially-available rare-earth magnet that has a mass of only 2.59 g and produces a magnetic-flux density of 350 G at a distance of 0.200 in. (5.08 mm).

The Hall-effect displacement transducer should have a stable, accurate, and linear output at relatively high levels. It should be small and easily configured, both electrically and mechanically. Again, a commercially available model was found to satisfy the requirements. This sensor has a linearity of ±1.5 percent and a sensitivity of 7.5 ± 0.2 mV/G.

The displacement-measurement technique is based on a transducer output proportional to the sensed magnetic-flux density and to the corresponding separation. This information can be used in two basic ways. First, the level of the output is monitored to ascertain the displacement, and this signal is usable as a real-time alarm parameter to prevent scuffing of the blade tip and resultant catastrophic failure. Second, the time of peak sensor excitation can be compared between multiple blade-magnet/sensor sets to ascertain dynamically changes in the aerodynamic shape.

This technique has already been successfully demonstrated on a laboratory prototype. Although the technique was developed for wind tunnels, it should have potential application in many rotating machines, provided that the surrounding materials are nonmagnetic and that the temperatures are not severe.

This work was done by Robert F. Berry, Jr., of **Langley Research Center**. *No further documentation is available.*

This invention is owned by NASA, and a patent application has been filed. Inquiries concerning nonexclusive or exclusive license for its commercial development should be addressed to the Patent Counsel, Langley Research Center [see page 16]. Refer to LAR-13722.

Simplified Drag Analysis for Nozzles

Measurements, graphs and calculations are combined to give realistic and convenient estimates.

Marshall Space Flight Center, Alabama

A hybrid empirical/analytical method gives a fast, fairly accurate estimate of the viscous-flow loss caused by wall friction in a nozzle. Purely analytical assessments, in

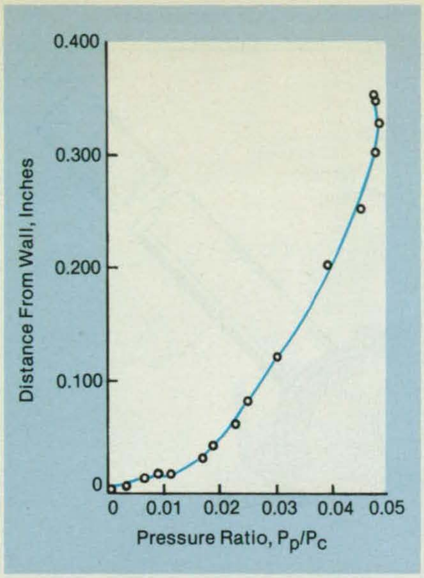

Figure 1. **Making a Pressure Survey** of the nozzle is the first step in determining drag. The quantity p_p/p_c is the ratio of the pressure measured by a pitot tube to the chamber pressure. For this graph, the gas is air, and p_c is 149 lb/in.^{2} (1.03 MPa).

contrast, are inexact; and detailed point-by-point measurements to obtain temperatures, velocities, and densities are time consuming and costly.

The hybrid method can be applied to jet-expansion devices in turbines, compressors, and a variety of other equipment. The medium may be liquid, vapor, or gas moving at speeds ranging from subsonic to supersonic. The results can be used to predict the performance of a nozzle, to determine the effects of design changes, and to verify computer solutions.

First, pitot-tube measurements are made at various distances from the wall to obtain the pressure distribution in the viscous boundary layer (see Figure 1). Next, the pressure readings are converted to mach numbers, and an analytical expression for the mach-number profile of the boundary layer is fitted to the mach numbers derived from the pressure (see Figure 2) by adjusting a shape factor (a) in this expression.

Other quantities that must be measured or calculated include the boundary-layer thickness (δ), the nozzle exit radius (R_e), the ideal-thrust coefficient (C), the gas-dynamic nozzle-throat area (A), the wall pressure (p_w), the chamber pressure (p_c), and the mach number at the edge of the boundary layer (M_δ). The ratio of the drag loss (ΔT) to the ideal thrust (T) is then given by

$$\Delta T/T = (2\pi\delta R_e^2/aCA)(p_w/p_c)M_\delta^2 \, [1 - \exp(-\delta/R_e)]$$

This work was done by W. R. Wagner of Rockwell International Corp. for **Marshall Space Flight Center**. *For further information, Circle 129 on the TSP Request Card. MFS-29060*

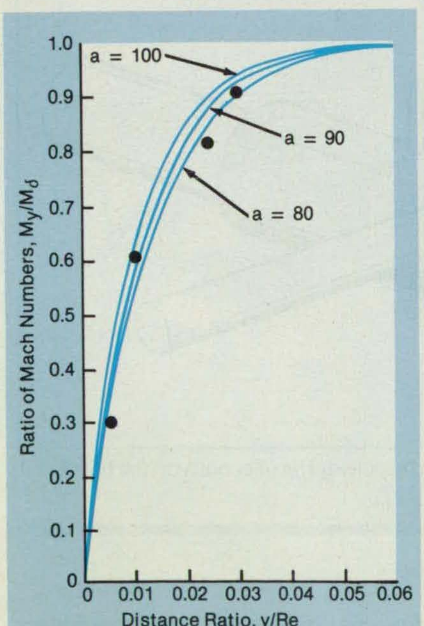

Figure 2. This **Mach-Number Profile** is a graph of the ratio of squares of the local mach number (M_y) to that at the edge of the boundary layer (M_δ), plotted against the ratio of distance from the wall (y) to the nozzle exit radius (R_e). The curves represented by three different values of the shape factor (a) are fitted to the data points.

Tool Extracts Smooth, Fragile Tubes

When a laterally compressible tube is too slippery to pull, a simple tool does the job.

Marshall Space Flight Center, Alabama

A handtool grasps a smooth, laterally compressible tube so that it can be pulled from a retainer without slippage and without damage. The tool consists of three linked sections of steel tube with sticky rubber on the inside and handles on the outside (see figure).

With the sections open, the user places the tool around the tube to be pulled. The user closes the tool and latches it. With the tool locked around the tube, the user gently pulls on the handles. The rubber lining grips the part without slipping so that the pulling force exerted by the user extracts the part. The lining applies pressure uniformly around the circumference of the part and thus prevents even thin-walled tubes from being crushed.

This work was done by Fred G. Sanders of **Marshall Space Flight Center**. *For further information, Circle 139 on the TSP Request Card.*

Inquiries concerning rights for the commercial use of this invention should be addressed to the Patent Counsel, Marshall Space Flight Center [see page 16]. Refer to MFS-28185.

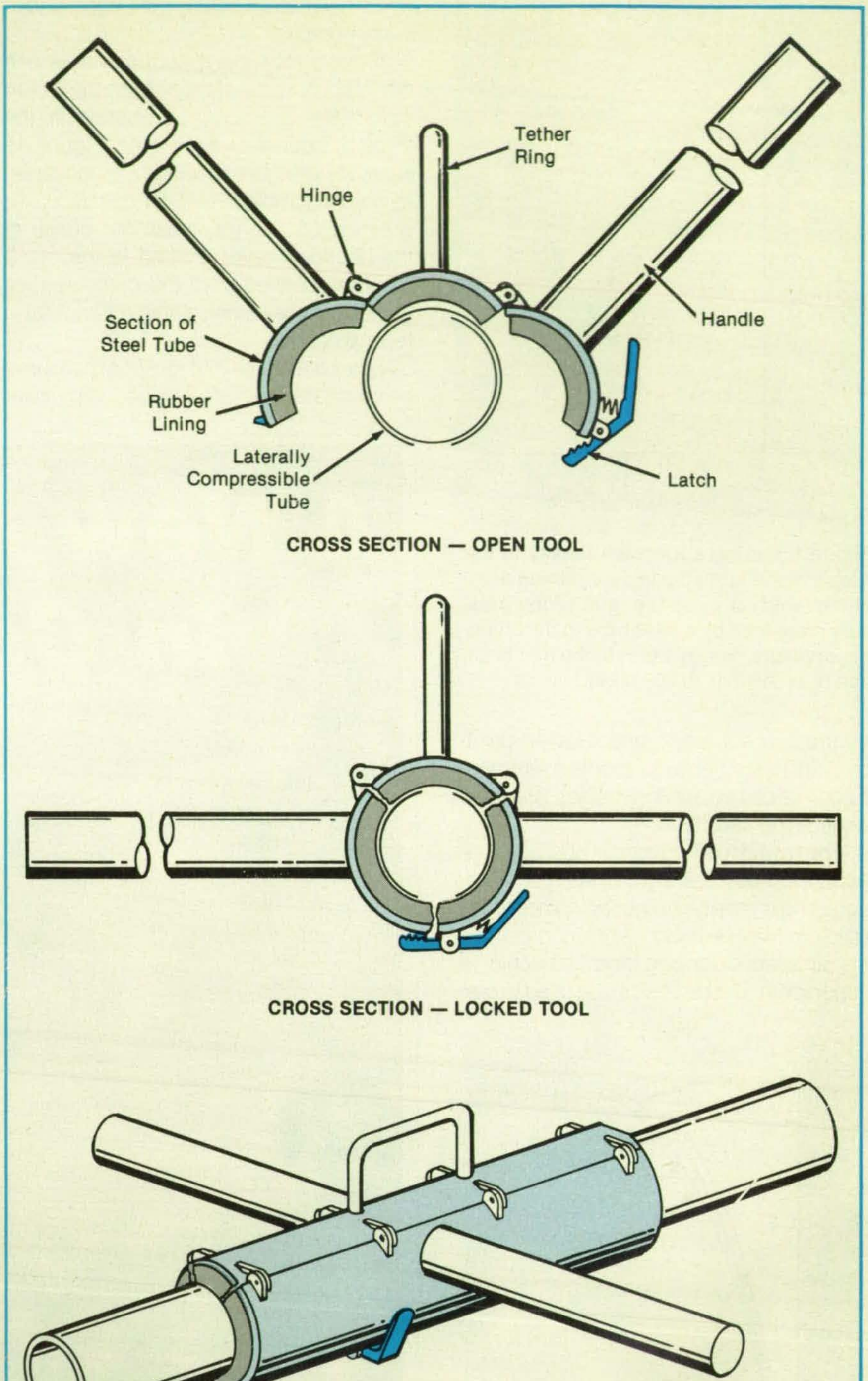

Hinged Sections of the Tool encircle the tube to be pulled. The user pulls on the handles to extract the tube.

Books and Reports

These reports, studies, handbooks are available from NASA as Technical Support Packages (TSP's) when a Request Card number is cited; otherwise they are available from the National Technical Information Service.

Coupled Aerodynamic/ Acoustical Predictions for Turboprops

Acoustical predictions agree fairly well with measurements.

A report discusses the use of coupled aerodynamic/ and acoustical computer codes to predict the noise emitted by turbopropeller blades turning at supersonic tip speeds. Because the pressures for fuel-efficient flight have forced the reconsideration of propeller-driven airplanes, there is an increasing need for such computations to evaluate the potential impact of noise on passengers and on communities along flightpaths.

To predict the noise field, an existing turboprop-noise computer code by Farassat was modified to accept blade-pressure inputs from a three-dimensional turbofan aerodynamical computer code by Denton. The unmodified Farassat code includes both the near- and far-field contributions from the blade panels, using blade-surface dipoles as the sources of noise, and using separate formulations of the Ffowcs-Williams-Hawkings equation for the subsonic and supersonic portions of the blades. Separate integrations are done for the surface-pressure-dependent, surface-drag-dependent, and shape-dependent contributions to the total noise.

The unmodified Denton code solves the Euler equations by use of a finite-volume, time-marching solution of the equations of continuity, momentum, and energy. An input mesh must be sufficiently fine to resolve gradients near the leading and trailing edges of a blade and to resolve shocks wherever they might occur. The flow quantities propagate downstream, while pressure propagates upstream.

The Denton code was modified by extending the calculation mesh to about twice the blade radius and by applying circumferentially-periodic rather than solid-wall boundary conditions in the region between the blade tip and the outer shroud. Outputs were added to serve as inputs to the Farassat code and to generate color contour plots of flow variables.

In the modified, combined code, the file of mesh points and corresponding normalized blade-surface pressures generated by the Denton code are read in the Farassat input subroutine for pressure—a two-dimensional linear interpolation routine is used to obtain the normalized pressure at the particular locations required by the Farassat code. The interpolated normalized pressures are converted to the proper dimensions by multiplying them by the local relative-velocity head on the blade.

The modified, combined code was tested by applying it to a representative modern, highly swept turbopropeller of eight blades and a diameter of 0.622 m. Results are compared with corrected acoustic data measured in Jetstar flights. Predictions of the first and second harmonics are within 3 dB in directions within 20° of the propeller plane.

This work was done by Bruce J. Clark and James R. Scott of **Lewis Research Center**. *Further information may be found in NASA TM-87094 [N87-23598/NSP], "Coupled Aerodynamic and Acoustical Predictions for Turboprops."*

Copies may be purchased [prepayment required] from the National Technical Information Service, Springfield, Virginia 22161. Telephone No. (703) 487-4650. Rush orders may be placed for an extra fee by calling (800) 336-4700.
LEW-14588

 Circle Reader Action No. 500

Behavior of Joint Seal in Solid Rocket Booster

A combination of high pressure and large or rapid gap opening can cause failure.

A report analyzes the behavior of the O-ring seals in the case of the Solid Rocket Booster. Numerical simulations of the transient response of a seal are presented with measurements of relevant mechanical properties of O-rings to show that there is a range of operating conditions in which the seal can fail.

The O-ring, made of a copolymer of vinylidene fluoride and hexafluoropropylene, has nominal major and minor diameters of 12 ft (3.66 m) and 0.280 in. (7.11 mm), respectively. It is seated in a rectangular groove 0.216 in. (5.49 mm) deep in a steel clevis and is compressed into the groove by a steel tang. When the tang and clevis are in contact, the O-ring is fully compressed by 0.064 in. (1.63 mm), sealing against the tang and all three sides of the groove.

The effects of out-of-roundness of the case and the initial pressurization upon ignition (which causes a jump that restores roundness) combine to increase the separation between the tang and the clevis. With regard to the performance or failure of the seal, the issue is whether the resiliency of the O-ring can keep the O-ring pressed against the clevis or whether a gap will form between the O-ring and clevis, allowing the pressurized exhaust gas to escape.

The behavior of the O-ring seal was simulated numerically with the SPAR finite-element computer code. Although the viscoelastic behavior of the seal is highly nonlinear and changes with time, the linear SPAR code contributes to an understanding of the dynamic response. The first condition studied was the sudden separation of the tang and clevis after full compression, with various gas pressures from 0 to 936 psi (0 to 6.45 MPa) applied to the O-ring cross section along the top 180°. The transient response was modeled as a superposition of 30 uncoupled vibrational modes of the O-ring in the frequency range of 2,000 to 8,000 Hz. The numerical results showed that the gas pressure tends to force the seal back into the groove, preventing the O-ring from maintaining a seal.

The next condition investigated involved some changes in the model and involved the sudden separation of the tang and clevis to a gap of 0.048 in. (1.22 mm) after initially compressing the O-ring by 0.046 in. (1.17 mm). A sonic condition with a pressure of 400 psi (2.76 MPa) was used to calculate the pressure distribution over the top of the O-ring, and again a superposition of vibrational modes was used to model the transient response. Although the linear elastic analysis shows a fast response, tests of O-rings indicated that at a temperature of 25 °F (−4 °C), the material does not respond rapidly enough to maintain a seal.

The numerical simulation of a freely floating O-ring showed that it can translate to a sealing position faster than the gap-opening transient. Unfortunately, freely floating seals are not recommended by the manufacturer for operating pressures over 200 psi (1.38 MPa). Additional tests of mechanical properties at various temperatures show that the ability of a compressed O-ring to respond to the tang/clevis separation decreases markedly with a decrease in temperature from 75 to 25 °F (24 to −4 °C).

This work was done by Carleton J. Moore of **Marshall Space Flight Center**. *Further information may be found in NASA TM-86580 [N87-17039/NSP], "Solid Rocket Booster Joint Seal Analyses."*

Copies may be purchased [prepayment required] from the National Technical Information Service, Springfield, Virginia 22161, Telephone No. (703) 487-4650. Rush orders may be placed for an extra fee by calling (800) 336-4700.
MFS-28257

Heating Distributions for Aeroassisted Vehicles

Predicted and measured distributions are similar for two proposed shapes.

The report discusses the anticipated distributions of temperature on symmetric and asymmetric large-angle blunt nose-cone space vehicles re-entering the atmosphere. The report is based on both measured data and data predicted by a mathematical model.

The cone configurations are being considered for use as possible aeroassisted orbital-transfer vehicles. Such vehicles will use aerodynamic forces to decelerate and to maneuver from high to low orbits. The aerodynamic environment during a transfer, although lasting only 10 minutes, will encompass several computationally complex flow regimes and phenomena.

The report considers three cone angles: 100°, 120°, and 140°. The experimental surface-temperature data were obtained on specimens made of thermal-protection materials proposed for the vehicles. The experimental data are compared with predictions from a boundary-layer integral matrix procedure with surface kinetics to determine how well the heating distribution over an asymmetric cone could be approximated by axisymmetric solutions for a cone and spherical segment. In addition, the report discusses a relationship between the stagnation-point heat-transfer rate and the bow-shock standoff distance for the cones.

The temperature-distribution data from the symmetric and asymmetric cones are quite similar, the report notes. Predicted temperatures compare well with the measured wall temperatures at the stagnation point but are slightly lower than the measured temperatures over the conical portion. Bow-shock standoff distances in front of the asymmetric blunt cones are closer to the body than for the asymmetric cones because of the sonic-point location on the edge of the spherical segment. The rates of heat transfer to blunt cones at stagnation points are easy to estimate by use of the bow-shock standoff distance.

This work was done by David A. Stewart of **Ames Research Center** *and Paul Kolodziej of Sterling Software. To obtain a copy of the report, "Heating Distribution Comparison between Asymmetric and Symmetric Blunt Cones, Circle 101 on the TSP Request Card.*

Inquiries concerning rights for the commercial use of this invention should be addressed to the Patent Counsel, Ames Research Center [see page 16]. Refer to ARC-11754.

Machinery

Test Apparatus for Oversize Ball-Bearing Models

A see-through machine enables direct observation and indirect measurements at moderate speeds.

Marshall Space Flight Center, Alabama

Enlarged scale models of ball bearings show the flow of lubricant and heat around the bearings. The scale models, used in a moderate-speed rotary test machine, obviate difficult direct measurements on real, small, high-speed bearings.

A combination of visual observation, infrared measurement, and thermocouple mapping shows the flow and heating patterns on the inner and outer races, the cage, and the balls. The rotary test machine (see figure) has transparent walls and working fluid.

In the machine, the inner and outer races are heated by electrical resistance or induction. The rolling and static elements of the bearing are monitored for speed, load, flow, and heating. The data are taken by high-speed cameras, by infrared thermography, by thermocouples fixed on the outer race, and by supplemental thermocouples attached to the inner race and connected to external circuits via a slipring. The data are scaled by nondimensional techniques to the size, flow, and speed of a real bearing.

The large-scale bearing enables the visualization of such complex heating and flow patterns as those that occur in forced-convection nucleate and film-boiling situations. Such patterns cannot be developed by analytical methods in cryogenic subcritical-pressure coolant flows of oxygen, hydrogen, and methane, for example.

This work was done by William R. Wagner of Rockwell International Corp. for **Marshall Space Flight Center**. *No further documentation is available.*

Inquiries concerning rights for the commercial use of this invention should be addressed to the Patent Counsel, Marshall Space Flight Center [see page 16]. Refer to MFS-29284.

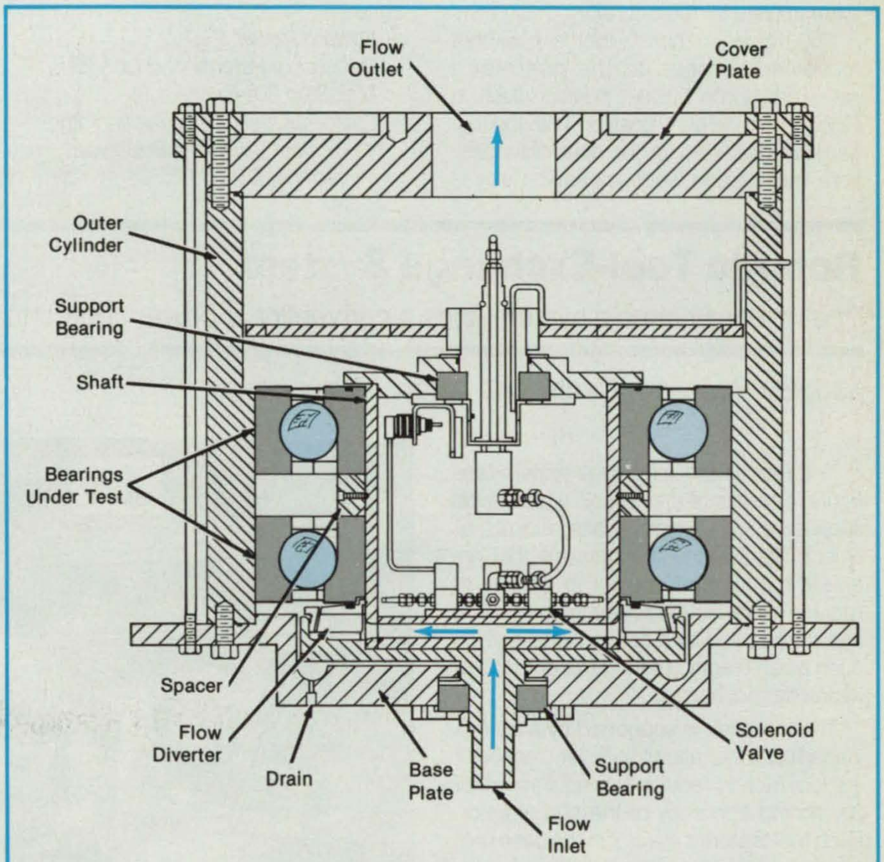

A **Model of a Ball Bearing,** six times larger than the real bearing, is rotated in a test machine. The transparency of the walls and the simulated lubricant reveal flow patterns and allow visible-light and infrared photographs to be made.

Handheld Controller for Robotic End Effector

This controller provides both position and force feedback.

NASA's Jet Propulsion Laboratory, Pasadena, California

A robot end-effector controller is equipped with position and force feedback. The controller accepts simple control actuation commands for claw control and provides easily understood feedback functions all through the same finger. Other fingers are thus free to execute other control functions. Moreover, because the manipulations through the finger do not require eye contact, the operator can pay more attention to other functions; hence, the controller can be integrated into a robot-arm master controller.

Primitive force/position feedback systems have used levers to transmit forces back to the operators. However, with these cumbersome systems, it is difficult to adjust the feedback ratios. Many teleoperator controls using joysticks provide feedback in either the force or the displacement mode only. At the moment of grasping, the mode could be switched from position to force; however, because the transition from claw movement to claw-grasp force is not instantaneous, the operator should have both feedbacks during the transition.

The controller (see figure) provides two degrees of freedom for the feedback such that the operator can perceive two distinct sensations in his control hand. To control the end-effector motion, the operator exerts force on the trigger with a finger or pushes outwardly against the trigger guard for reversed motion. Strain gauges measure this force and translate it into electrical signals that regulate the end-effector motor. Claw motions or clamping forces are thus proportional to the trigger force applied by the operator.

The trigger is "hard"; that is, it will not move in response to the operator's squeezing force but will position itself in response to the claw position, with the trigger fully protruded for the open-claw position. The position-feedback servomotor is located at the base of the handgrip and operates through a spindle-and-linkage mechanism to pivot the trigger back and forth.

As the end-effector claw exerts a clamping force, the force-feedback loop sends control signals to the force-feedback servomotor in the top of the grip. This causes the trigger to rotate about its longitudinal axis. Because the trigger surface is a concave cylinder the rotation is felt by the operator's finger as a tilting of the cylinder.

This work was done by Bruno M. Jau of Caltech for **NASA's Jet Propulsion Laboratory**. *For further information, Circle 149 on the TSP Request Card.*

In accordance with Public Law 96-517, the contractor has elected to retain title to this invention. Inquiries concerning rights for its commercial use should be addressed to

Edward Ansell
Director of Patents and Licensing
Mail Stop 301-6
California Institute of Technology
1207 East California Boulevard
Pasadena, CA 91125

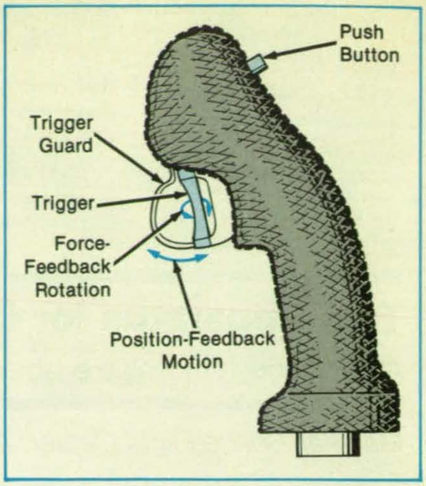

The Hand Grip houses the controller. The end-effector force and position are fed back to the operator's hand through the rotation of the trigger and the rocking of the trigger guard.

Refer to NPO-16732, volume and number of this NASA Tech Briefs *issue, and the page number.*

Robotic Tool-Exchange System

The relatively simple system uses a conventional power source to exchange tools.

Langley Research Center, Hampton, Virginia

The robotic tool-exchange system (see figure) consists of a tool rack, which holds such tools as screwdriver bits, sockets, or twist drills, and the mechanisms that enable a robotic end effector to pick up or replace a tool. Rotary power for the system can be supplied by a conventional source such as an electric motor or pneumatic or hydraulic mechanism.

The tool rack is supported by a spring-loaded base that allows sufficient motion of the tool rack to reduce the requirement of positioning accuracy of the end effector. Each tool is stored in a slot in the base until needed. At that time, the tool previously in use is removed from the end effector by a special pawl-and-bracket mechanism. The tool slides toward the bottom of an empty slot until the tool-retaining pawls are spread apart by inclined planes on the disengaging brackets. The end effector is withdrawn from the rack, leaving the previous tool in the rack. The end effector is then repositioned to insert the end of its shaft into the desired tool until the retaining pawls are seated on the tool. The upward motion of the end effector then removes the tool from the rack, and the tool interchange is complete.

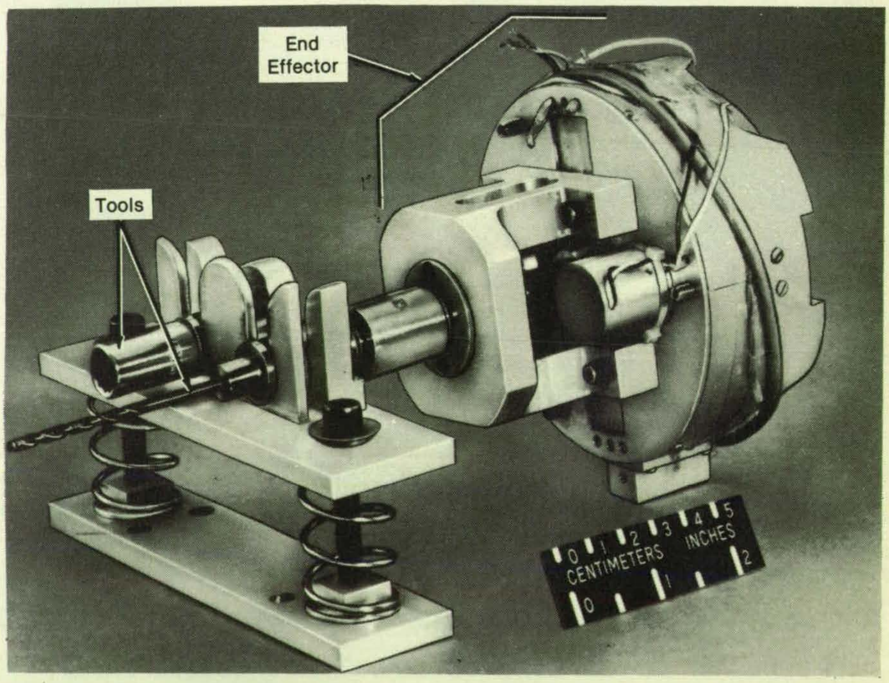

The **End-Effector Design** and spring-mounted tool-rack base make the tool-exchange system relatively simple and effective.

Although several automatic tool exchangers are already available, the spring mounting of the tool-rack base to provide some degree of freedom in positioning accuracy and the end-effector design for gripping the tools make this system relatively simple and effective. The system has been demonstrated at Langley Research Center for tool exchange in the replacement of spacecraft modules.

This work was done by Marion A. Wise and Barry S. Lazos of **Langley Research Center**. *No further documentation is available.*
LAR-13558

Books and Reports

These reports, studies, handbooks are available from NASA as Technical Support Packages (TSP's) when a Request Card number is cited; otherwise they are available from the National Technical Information Service.

Simulating Unpowered Helicopter Landings

Sensory cues are important in the simulation of emergencies.

A report presents the results of an experiment with visual, aural, and motion cues in simulations of helicopter landings without engine power. Flight simulations offer safety for training pilots and for trying out risky maneuvers. Existing helicopter simulators, however, do not offer a realistic environment, particularly in sensory cues for near-ground, low-speed flight. Accordingly, the experiment evaluated the importance of various cues in difficult autorotation (no-power) landings.

The automation experiment was conducted in the vertical-motion simulator at Ames Research Center with experienced pilots as the subjects. The performance of the simulator was varied, as were the content and details of the visual scene and the fidelity of the engine noise.

The experimenters found that high-fidelity motion cues generally improve pilot performance. Smaller motion cues poorly tailored to the control task may distract a pilot more than no motion cues at all. A motionless simulator would be adequate, given enough training time. All the subjects found that they could attain skill in a motionless simulator if they had sufficient visual cues.

Longitudinal linear acceleration assisted one pilot's judgment and timing. Lateral linear acceleration cues helped pilots in the cross-axis task of lateral and directional control. With the pilots' attention concentrated on speed and height during autorotation, lateral motion cues helped them control sideslip.

The addition to the simulated landing scenes of such easily recognized scaling objects as people and vehicles helped pilots use the available visual cues. This is particularly important in the abstract, textureless scene in the usual computer-generated image. Low-altitude height sensing—crucial to hovering landings—was difficult in all scenes generated by the image system used in the experiment.

Sound cues are essential for a pilot during autorotation. The addition of subtle sound cues increased pilots' acceptance of simulations, and good low-frequency sound reproduction was especially important.

This work was done by William A. Decker, Charles F. Adam, and Ronald M. Gerdes of **Ames Research Center.** *To obtain a copy of the report, "Pilot Use of Simulator Cues for Autorotation Landings," Circle 14 on the TSP Request Card.*

Inquiries concerning rights for the commercial use of this invention should be addressed to the Patent Counsel, Ames Research Center [see page 16]. Refer to ARC-11715.

Computing the Compliances of Gear Meshes

The sharing of loads among gear teeth can be improved.

A computer model simulates the compliance and the sharing of loads in a spur-gear mesh. This model adds the effect of rim deflections to previously-developed, state-of-the-art gear-tooth-deflection models. By the use of the solid-body analysis as a lower bound and the rim analysis as an upper bound for the mesh compliance, reasonable approximations can be obtained for the compliance in a spur-gear mesh.

Furthermore, the model demonstrates that a rim on the large output gear in a spur-gear mesh can improve the load-sharing characteristics of the mesh. The improvement in load sharing reduces the fraction of the load upon a tooth of the driving pinion as the tooth enters the mesh. The effects of this reduction in the initial load fraction are a potential reduction in dynamic loading on the tooth and an increase in the total compliance of the mesh, with consequent reduction of sensitivity to the errors in the distances between gears in parallel-path power transmissions.

This model can be applied to a gear mesh composed of two external gears or an external gear driving an internal gear. This feature makes the program a good tool for the analysis and design of planetary transmissions.

This work was done by D. G. Lewicki of **Lewis Research Center** *and M. Savage, R. J. Caldwell, and G. D. Wisor of the University of Akron. Further information may be found in NASA TM-88843 [N87-10892/NSP], "Gear Mesh Compliance Modeling."*

Copies may be purchased [prepayment required] from the National Technical Information Service, Springfield, Virginia 22161, Telephone No. (703) 487-4650. Rush orders may be placed for an extra fee by calling (800) 336-4700. LEW-14554

Fabrication Technology

Hardware, Techniques, and Processes

Rotary Reactor Makes Large Latex Particles

A machine reduces the gravitational effects that interfere with particle growth.

Marshall Space Flight Center, Alabama

A chemical reactor produces large latex particles — up to 100 μm in diameter. Previously such large particles could be produced only in the gravity-free environment of space. On Earth, buoyancy and sedimentation prevented the polymerization reaction from continuing after the particles grew larger than about 3 μm. Stirring to prevent separation did not help; it had to be done so rapidly that it caused violent collisions and consequent flocculation of the soft, sticky particles.

The new reactor includes a cylinder that rotates in a constant-temperature water bath (see figure). The slow rotation of the cylinder mixes the reactants to prevent separation, while the bath ensures a uniform reaction temperature. A stirrer in the cylinder provides additional mixing if needed. The rotation and stirring are gentle enough not to cause collision flocculation. The reactor chamber is completely filled with reactants; no air is present to mix with the contents and promote flocculation.

A piston that constitutes an end wall of the reactor moves to accommodate the changing volume of reactants. The moving piston also drives a linear variable-differential transformer (LVDT), the electrical output of which indicates the volume of the chamber and thus provides information on the stage of the polymerization reaction.

The prototype reactor holds 235 ml of fluid. Although the variation in the size of the latex particles produced in this reactor is somewhat greater than the 2-percent variation of particles made in space, the product should become more uniform as latex recipes are improved.

This work was done by Dale M. Kornfeld of **Marshall Space Flight Center**. *For further information, Circle 156 on the TSP Request Card.*
MFS-28214

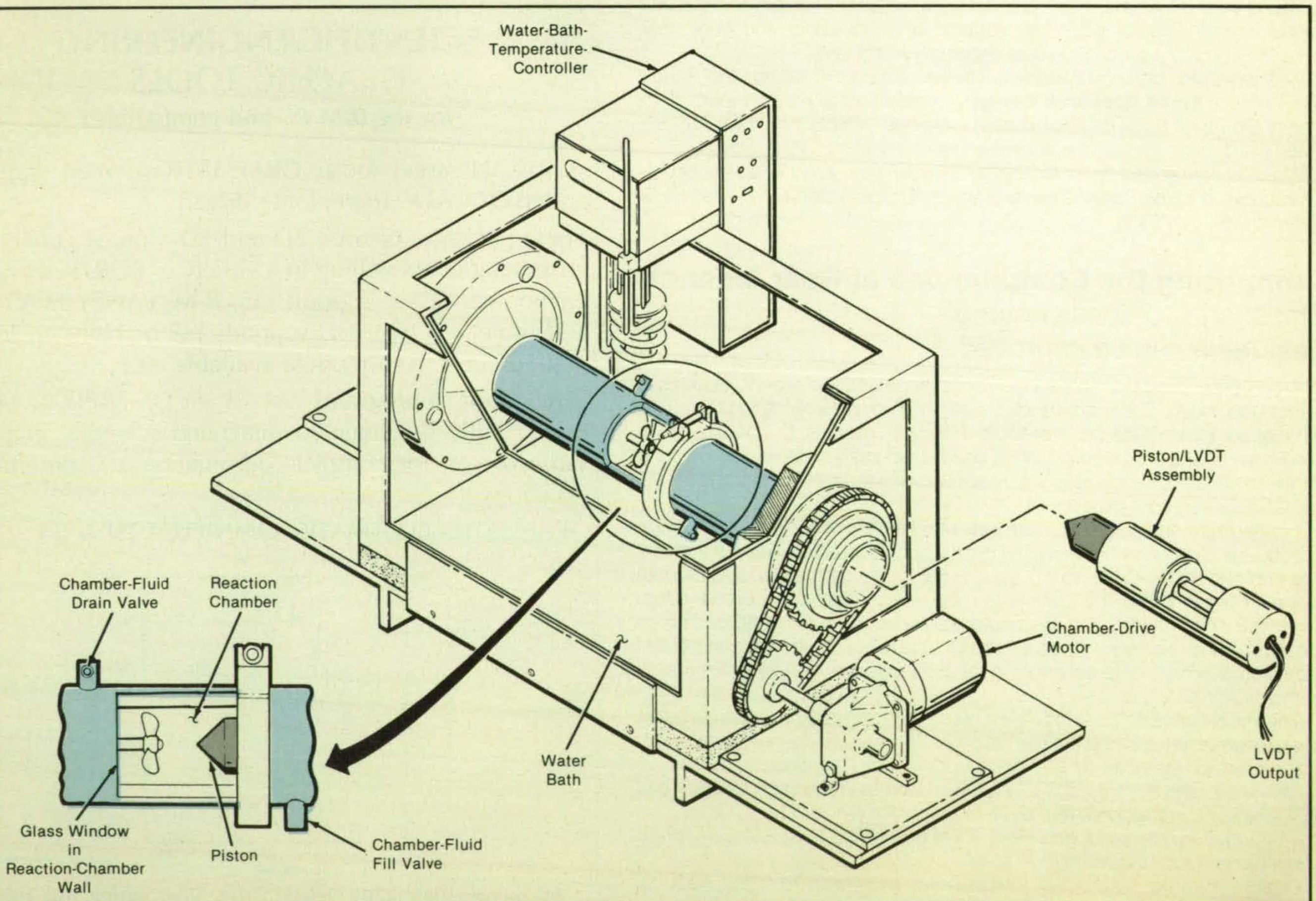

The **Reaction Chamber Rotates** while the polymerization of latex proceeds. A motor (not shown) at the far end of the machine turns the stirrer. The chamber is made of stainless steel with glass windows.

Holder for Shot Peening

A fixture delimits the peened area precisely while boosting productivity.

Marshall Space Flight Center, Alabama

A fixture holds parts for shot peening, acting as a mask so that only a limited, predetermined area is exposed to the shot. While it helps to control the dimensions of the shot-peened area, the fixture also enables workpieces to be loaded and unloaded quickly.

The fixture was developed for the fabrication of turbine blades. Previously, the area to be treated was delineated by a soft mask of tape and rubber or plastic. The new hard fixture not only offers greater dimensional stability and repeatability but also increases productivity. According to estimates, it will save about $100,000 in the production of 6,000 engines.

This work was done by Bill E. Coker of Rockwell International Corp. for **Marshall Space Flight Center**. *No further documentation is available. MFS-29242*

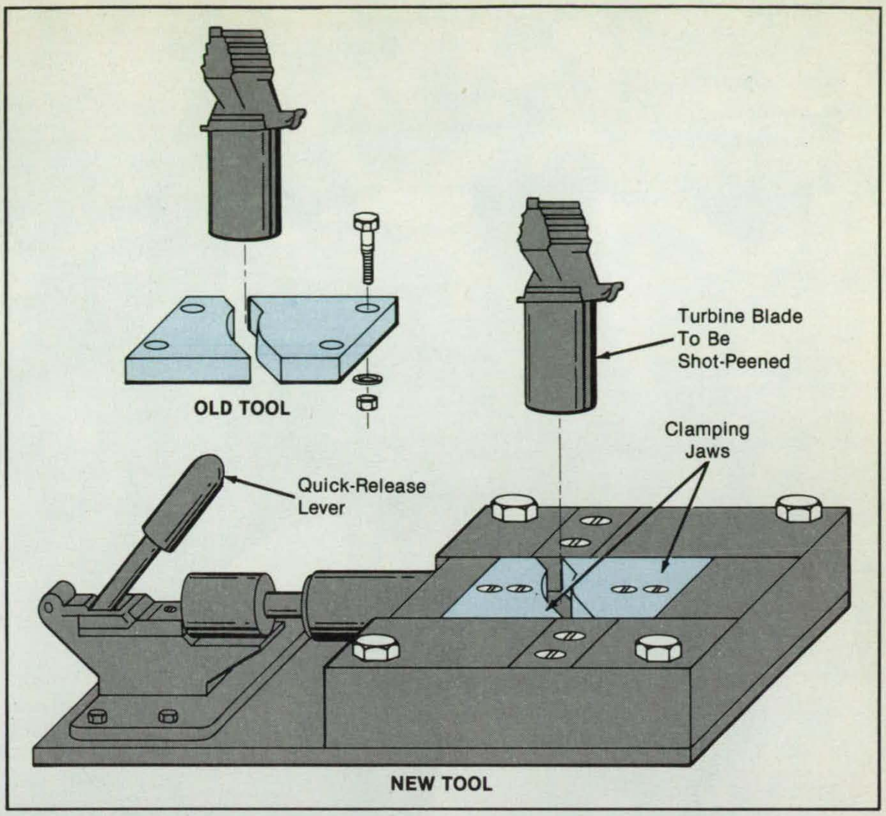

The **New Fixture Ensures Small Tolerances** essential for turbine blades. It can be opened and closed quickly so that a finished part can be removed and a new part inserted.

Heat-Shrinkable, Seamless Fabric Tube

Weaving produces a generally tapered shape; heat-shrinking gives a final shape.

Lyndon B. Johnson Space Center, Houston, Texas

A seamless fabric tube under consideration for use in pressure suits like those worn by astronauts may also be useful on Earth for protective garments. The tube is woven in a tapered shape from polyester yarn. It is then placed on a heated mandrel. The heat shrinks the fibers so that the sheath thus assumes the shape of the mandrel. The sheath is then coated with an impermeable material.

The fabric is a flexible supporting structure for the coating and, therefore, impedes the wearer's movements as little as possible. Since the fabric is continuous, leakage is reduced, and excess thickness at the seams is eliminated. The garment made from this fabric is expected to be durable and to require less hand labor than does a sewn suit.

The fabric is woven on a standard textile broadloom. The weaver removes warp yarns at predetermined locations to produce a taper. Yarns may be removed from either or both edges or from the center of the warp beam.

This work was done by Donat J. E. LaPointe, Laurence J. Vincent, and Lawrence T. Wright of Albany International Research Co. for **Johnson Space Center**. *For further information, Circle 109 on the TSP Request Card.*

This invention is owned by NASA, and a patent application has been filed. Inquiries concerning nonexclusive or exclusive license for its commercial development should be addressed to the Patent Counsel, Johnson Space Center [see page 16]. Refer to MSC-21082.

Assuring Precise LFC-Suction-Strip Porosities

A masking technique is used in bonding perforated titanium sheets to substructures.

Langley Research Center, Hampton, Virginia

A technique has been developed to obtain precise control of the widths of perforated titanium suction strips. This precision is required for successful laminar-flow control (LFC) in flight environments. The exact strip widths must be maintained to achieve design suction porosities throughout fabrication processes.

During bonding of the perforated skins to trapezoidal fluted composite substructures, the skins, with electron-beam-perforated holes [0.0025-in. (0.064-mm) diameter and 0.025-in. (0.64-mm) center distances, typical], are exposed to harsh etching solutions. Also, in the bonding of the composite pads with adhesive films to the skins and substructures, high temperatures and pressures occur during the autoclave curing cycles, possibly causing resin and adhesive to flow and wick into the perforated holes. Thus, the fabrication processes that are needed for strong bond lines can be detrimental to the porosities of the LFC panel suction strips because these proc-


DP-8

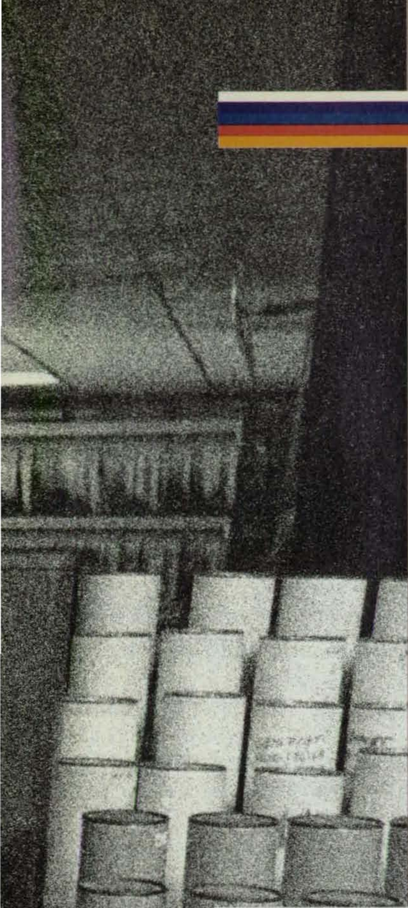

For nearly three decades, companies have drawn on Houston Instrument.

Now it's your turn.

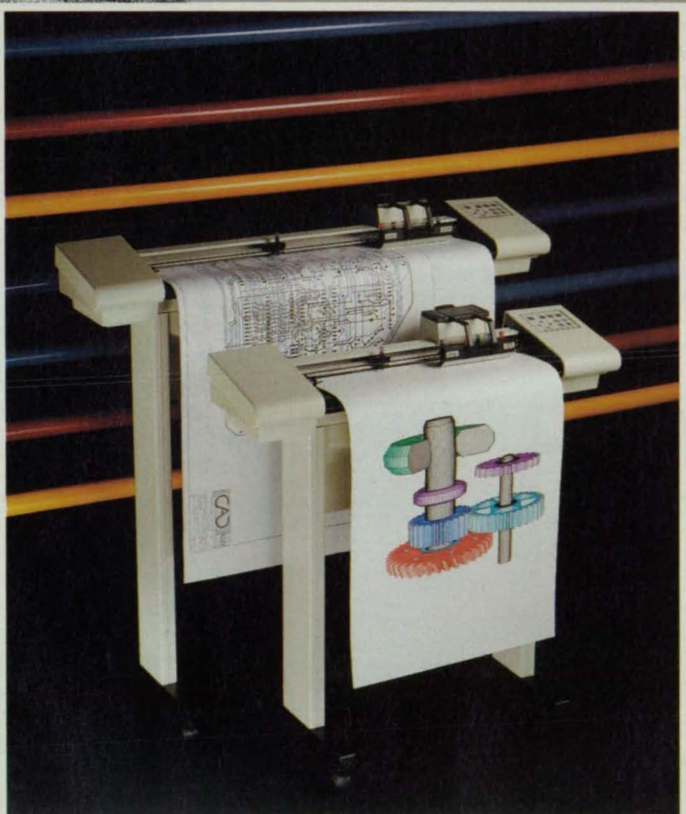

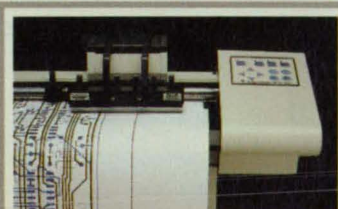

Houston Instrument, PRIORITY RESPONSE, and SCAN–CAD are trademarks of AMETEK, Inc.

Select a Houston Instrument™ plotter, and you're not only opting for the best price/performance on the market—you're choosing an industry leader with a proven track record. For nearly 30 years, companies have relied on HI for quality products, reliable service, *and* attractive prices.

Take HI's sleek new DMP–60 Series plotters—they're designed to impress even the most demanding CAD professional. Industry experts agree:

"Houston Instrument's DMP–61 delivers a remarkable combination of high speed, gorgeous plots, and very competitive price."

PC MAGAZINE *Editor's Choice Dec. 22, 1987*

HI's commitment to solid, innovative products is underlined by designed–in versatility. The SCAN–CAD™ option lets a DMP–60 Series plotter double as a scanner. The Multi–Pen accessory speeds colorful, complex drawings. And HI's one megabyte buffer board lets the DMP–60 Series plot several originals—without tying up your computer.

Proven performance, proven value—that's HI plotters. Flexible. Fast. Accurate. Software compatible. Reliable. And backed by HI's PRIORITY RESPONSE™ customer support programs which include overnight product–replacement service, leasing, and warranty coverage.

All this from an industry leader that companies have drawn on for nearly three decades—Houston Instrument.

Now it's your turn. Begin by calling 1-800-444-3425 or 512-835-0900 or writing Houston Instrument, 8500 Cameron Road, Austin, Texas 78753.

HOUSTON INSTRUMENT
A DIVISION OF AMETEK

Circle Reader Action No. 550

esses result in unpredictable margins and changes in hole sizes.

Two masking techniques were developed to maintain the design suction porosities throughout the panel-fabrication processes. Prior to the use of these techniques, the porosities of the test regions were mapped, and the suction flow as a function of pressure was measured and plotted for comparison with the results achieved after fabrication.

In the more successful of the two methods, the test area was masked with Mylar® polyethylene terephthalate tape over the suction strips 0.250 in. (6.4 mm) wide. The bonding lands were then taped, leaving 0.050-in. (1.3-mm) gaps to the taped suction regions. The gaps and the 0.250-in. (6.4-mm) taped suction regions were then coated with two heavy coats [0.005-in. (0.13-mm) each] of maskant. With the maskant semicured, the bonding-land tape was removed. The final masking operation was to tape the back, or airfoil, surface 100 percent. After these precise masking operations, the perforated titanium test sheet was processed, and composite pads were bonded between the suction strips of the test sheet by autoclave using an adhesive film.

Visual examination of the test area showed that very little etchant solution penetrated the 0.050-in. (1.3-mm) maskant gaps. The flowing and wicking of resin and adhesive were also isolated from the porous strips. These protective maskant margins prevented any visual changes in the critical porous suction strips 0.250 in. (6.4 mm) wide. [Suction strips on flight articles could vary from 0.10 to 0.60 in. (2.5 to 15.2 mm) by use of the same methods.] Subsequent suction-test results verified the visual inspections. The porosity of the test area after fabrication showed a very slight decrease, which was within a range that could be accounted for by normal tolerances and misalignments of equipment of the test console.

This work was done by Frank H. Gallimore of McDonnell Douglas Corp. for **Langley Research Center**. *For further information, Circle 54 on the TSP Request Card.*

Inquiries concerning rights for the commercial use of this invention should be addressed to the Patent Counsel, Langley Research Center *[see page 16]**. Refer to LAR-13638.*

Ink-Jet Printer Forms Solar-Cell Contacts

Contacts are formed in controllable patterns with metal-based inks.

NASA's Jet Propulsion Laboratory, Pasadena, California

A developmental ink-jet printing system forms upper metal contact patterns on silicon photovoltaic cells. The system uses metallo-organic ink, which decomposes when heated, leaving behind a metallic, electrically conductive residue in the printed area.

A cell to be printed is placed on an x-y positioning table beneath the printing head. The movement of the table and the pulses that command the printing head to squirt small drops of ink are coordinated through a digital data-processing system to form the specified contact pattern.

The system (see figure) is controlled by a personal computer that acts alone or in communication with a mainframe computer. The personal computer will be used to create and edit programs that will display contact patterns on a color cathode-ray tube to facilitate design. When a design is acceptable, the personal computer will feed programs to a microcomputer for almost instantaneous printing of the pattern.

The microcomputer contains 2K of electrically-programmable read-only memory, 4K of random-access memory, and both serial and parallel ports. Machine-code programs for general operation of the system and specific contact patterns are transmitted from the personal computer to the microcomputer through the serial port. The microcomputer translates the received programs into control signals for the printing-head and positioning-table control units.

The printing-head control unit includes a group of pulse drivers and switches to select 1 or more of 12 nozzles in the printing head. This unit also includes circuits that set the durations and amplitudes of the ink-jet-triggering pulses to the specified values. These pulses are sent to the printing-head driver on the printing-head/positioning-table assembly.

The positioning-table control unit includes the indexing- and driving-circuit boards for both the x and y axes. The indexing-circuit boards receive information on movements from the microcomputer in parallel fashion and respond by sending control signals to the driving-circuit boards, which are connected to the stepping motors of the x-y table. The information from the indexing boards is also sent to the position indicator, which gives the position along each axis in a 4-digit display.

The printing-head/positioning-table assembly contains the supply of ink and its pressure-control system, a controllable heater for the platform on the table, and the printing-head driver, which generates the large pulses necessary to actuate the piezoceramic drivers in the printing head. The system can print a pattern as large as 2 in. (5 cm) square. In experiments, the system has produced contact patterns that yield cell efficiencies (in the absence of antireflection coatings) of 8 to 9 percent.

This work was done by Paul Alexander, Jr., of Caltech and R. W. Vest, Don A. Binford, and Eric P. Tweedell of Purdue University for **NASA's Jet Propulsion Laboratory**. *For further information, Circle 45 on the TSP Request Card. NPO-17172*

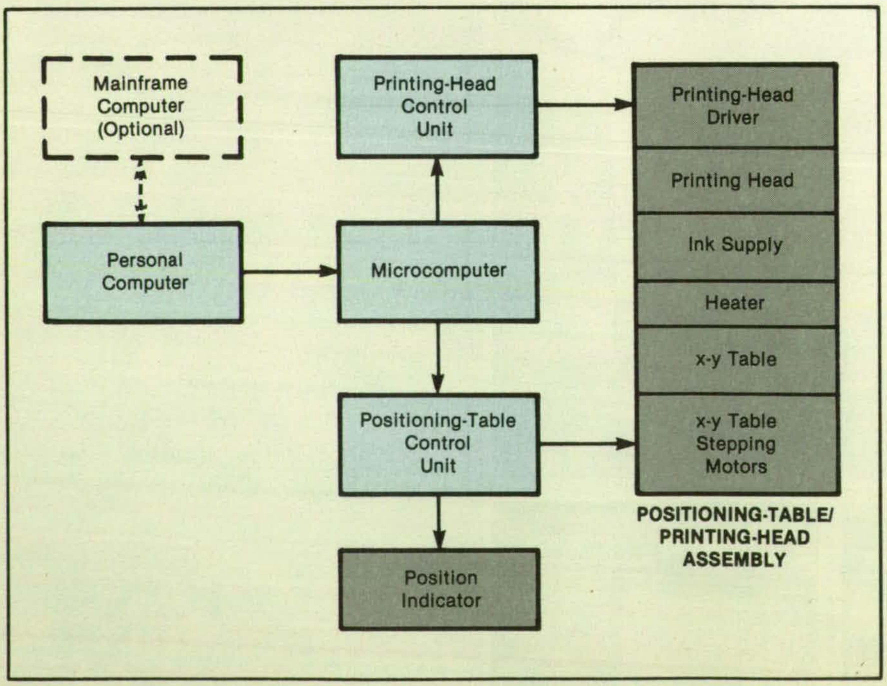

Digital Printing-Head-Control Circuits establish the contact pattern, which is then deposited in the form of metallo-organic ink.

Algorithm To Design Finite-Field Normal-Basis Multipliers

A way is found to exploit the Massey-Omura multiplication algorithm.

NASA's Jet Propulsion Laboratory, Pasadena, California

A generalized algorithm locates a normal basis in a Galois field $GF(2^m)$ and enables the development of another algorithm to construct a product function. Once the product function is defined, the design of a Massey-Omura multiplier is straightforward.

Finite-field arithmetic logic is essential for some error-correcting coders and some cryptographic devices. There is a need for good multiplication algorithms that can be realized easily. The Massey-Omura multiplication algorithm for finite fields is based on a normal-basis representation. The fundamental design of a Massey-Omura multiplier is based on a product function. Using the normal-basis representation, the design of a finite-field multiplier is simple and regular.

The Massey-Omura multiplier obtains the product of two elements in the finite field $GF(2^m)$. In the normal-basis representation an element in $GF(2^m)$ is squared by a simple cyclic shift of its binary digits. In normal-basis representations, multiplication requires the same logic function for any one bit of the product as it does for any other. The generation of adjacent product digits differs only in the inputs to the product function, which are cyclically shifted versions of one another. Hence, designing a Massey-Omura multiplier is exactly the same as designing a product function. A pipeline architecture suitable for very-large-scale integration has been developed for a Massey-Omura multiplier of $GF(2^m)$.

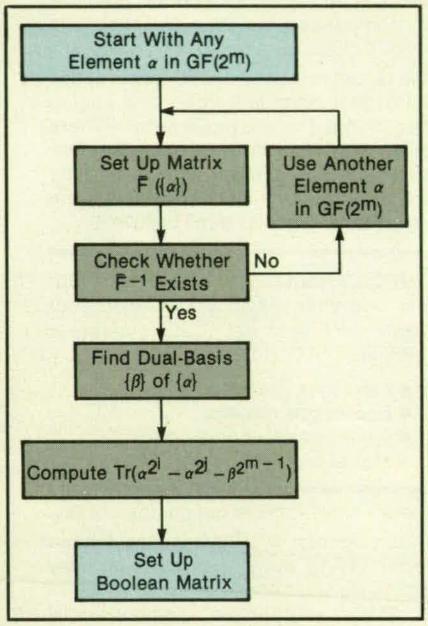

The **Boolean Matrix**, which defines the product function, is generated by an algorithm that starts with any element in the basis $\{\alpha\}$.

The design of a Massey-Omura multiplier is based on a normal basis

$$\{\alpha\} = \{\alpha, \alpha^2, \alpha^{2^2}, \ldots, \alpha^{2^{m-1}}\},$$

which is the set of roots of an irreducible polynomial

$$P(x) = x^m + c_1 x^{m-1} + \ldots + c_m$$

In general, it is difficult to verify the linear independence of the roots. A straightforward way to do this is to represent α^{2^i}, $i = 0, 1, \ldots, m-1$, by m-dimensional vectors in the canonical basis $\{\alpha\}$ and then to check whether the $m \times m$ matrix formed from these vectors is nonsingular. For large m, this method ordinarily requires a great number of computations.

The new algorithm makes it possible to locate a normal basis in any field $GF(2^m)$. A special $m \times m$ matrix $\bar{F}(\alpha)$ must be set up, and its nonsingularity must be verified. However, the number of required computations is reduced below what was previously thought necessary: Due to some special properties of this matrix, the setup procedure requires only m, rather than the usual m^2 entry computations; and the verification of the nonsingularity can be based on some quick-check rules.

The new method (see figure) for defining the product function of the Massey-Omura multiplier uses the concept of the basis $\{\beta\}$ that is dual to the basis $\{\alpha\}$. The coefficients of the product function are the trace values of some particular elements in $GF(2^m)$ that can be computed by the chosen normal basis and its dual basis. The algorithm leads to a new matrix called the "Boolean" matrix, which defines the product function. Hence, the design of a Massey-Omura multiplier can be based on any arbitrary normal basis in $GF(2^m)$, which need not be the roots of the generator polynomial.

This work was done by Charles C. Wang of Caltech for **NASA's Jet Propulsion Laboratory**. *For further information, Circle 114 on the TSP Request Card.*
NPO-17109

Algorithm for the Discrete-Optimal-Output-Feedback Problem

The change in cost function due to a change in feedback gain is calculated.

Langley Research Center, Hampton, Virginia

An algorithm for feedback control systems considers the stochastic, infinite-time, discrete-output-feedback problem for time-invariant linear systems. The optimal-output-feedback problem formulates a modern control-law-design problem in which only a selected number of plant-state variables are used, whereas prior methodology required that all plant-state variables be used in the feedback control law. This formulation enables the control designer to solve more-realistic control problems using little trial and error. The application of the algorithm to this approach indicates a fast rate of convergence and

TEAMWORK.

Combine the waveform capturing abilities of a Nicolet digital oscilloscope with the computing abilities of your IBM PC.
Connected via the RS-232 or the IEEE-488 (GPIB) interface, the power of modern signal analysis can be easily realized.

800/356-3090
or 608/273-5008

Nicolet Digital Oscilloscopes

The Scopes. Nicolet digital oscilloscopes offer ten times the accuracy and as much as one hundred times the resolution of analog oscilloscopes. A wide range of digitizer speeds provide solutions for virtually every measurement problem. Our latest plug-in module, the 4570, has 12-bit resolution at the unprecedented digitizing speed of 10 MHz. Accuracy does not have to be sacrificed for speed! Neither does sweep length. Waveforms composed of up to 16k data points are available regardless of the speed. Cursor readout of measurement values, "zoom" expansion to X256, continuously variable pretrigger data capture, and built-in disk drives all contribute to Nicolet's measurement expertise.

From low cost portables to high performance laboratory systems, Nicolet digital oscilloscopes were the first and are still the best.

Nicolet Software

The Software. Powerful, easy to use software packages are available for every Nicolet scope. Data transfers into the PC as well as mathematical data manipulation (FFT, integration, RMS, multiplication, etc.) can be accomplished without programming or computer expertise. Waveforms can be displayed on the PC screen, stored on the disk drive, and plotted on paper. The powerful new Waveform BASIC program can also operate as a waveform manipulation *language*. Using commands similar to standard BASIC, customized waveform calculations can be written quickly and easily.

Capture, analyze, store, and plot data with the convenience and ease of a Nicolet oscilloscope and Nicolet software.

Nicolet Test Instruments Division
P.O. Box 4288
5225-2 Verona Road
Madison, WI 53711-0288

NIC Nicolet
"Instruments of Discovery"

Circle Reader Action No. 350

considerable numerical reliability.

Under loose constraints, the algorithm is theoretically guaranteed to produce a sequence of control gains with monotonically decreasing costs and with cost gradients that converge to zero. Thus, the algorithm is theoretically guaranteed to obtain a critical point of the cost function corresponding to a stable gain. The critical point obtained need not be the global minimum of the cost function.

The algorithm is currently being applied to design an outer-loop control system for a typical small transport jet aircraft. The purpose of the outer-loop system is to feed guidance errors back to the inner-loop control system so that the aircraft tracks a three-dimensional flightpath. The numerical results for this 13th-order problem show a rate of convergence considerably faster than that of two other algorithms that were used for comparison.

This algorithm should be of considerable value in work relating to automatic control systems and for systems that are designed with digital techniques. It should have widespread application in terrestrial, aeronautical, and space systems.

This work was done by Nesim Halyo of Information and Control Systems, Inc., for **Langley Research Center**. *Further information may be found in NASA CR-3838 [N84-31217/NSP], "Investigation, Development, and Application of Optimal Output Feedback Theory: Volume I — A Convergent Algorithm for the Stochastic Infinite-Time Discrete Optimal Output Feedback Problem."*

Copies may be purchased [prepayment required] from the National Technical Information Service, Springfield, Virginia 22161, Telephone No. (703) 487-4650. Rush orders may be placed for an extra fee by calling (800) 336-4700.
LAR-13684

Recursive Algorithm for Linear Regression

The order of a model is determined more easily.

Lyndon B. Johnson Space Center, Houston, Texas

A linear-regression algorithm includes recursive equations for the coefficients of a model of increased order. Older algorithms were not recursive: when one increased the order of a linear-regression model, it was necessary not only to compute the linear-regression coefficient for the new variable but also to compute anew the coefficients of all the previous variables. By enabling the updating of existing coefficients, the new algorithm eliminates some duplicative calculations and thereby facilitates the search for the minimum order of the linear-regression model that fits a set of data satisfactorily.

The new algorithm is intended for use with a time sequence of samples of the quantity X, which varies randomly with time. In a linear-regression model of order m, the value Y of the $m+1$st sample of X is predicted from the preceding m samples by

$$Y = \varepsilon_m + \sum_{k=1}^{m} A_k^m X_k$$

where A_k^m is the mth-order regression coefficient for the kth sample, X_k is the kth sample of X, and ε_m is a residual term. There are several techniques for finding the regression coefficients that lead to "best" estimates of Y according to various criteria. The most common criterion and the one used here is that of the minimum mean squared error; that is, the regression coefficients are chosen to minimize the mean-square error between the predicted values Y and the measured values X_{m+1}.

An auxiliary mth-order model is introduced for the $m+1$st sample:

$$X_{m+1} = \nu_m + \sum_{k=1}^{m} B_k^m X_k$$

where the B_k^m are also chosen for a least-square fit. The auxiliary model is multiplied by an arbitrary fraction K_m and subtracted from the mth-order regression model. The value of Y is also formally expressed by the $m+1$st-order model equation

$$Y = \varepsilon_{m+1} + \sum_{k=1}^{m+1} A_k^{m+1} X_k$$

The value of K_m is then chosen so that the averages, over all ℓ, of $\varepsilon_{m+1}X_\ell$ and of $(\varepsilon_m - K_m\nu_m)X_\ell$ are both zero.

Then a direct term-by-term comparison of the $m+1$st-order model with the mth model modified by the auxiliary model leads directly to the recursion formulas

$$A_k^{m+1} = A_k^m - K_m B_k^m$$

for the first m coefficients and

$$A_{m+1}^{m+1} = K_m$$

for the $m+1$st coefficients.

The linear-regression concepts and the recursion formulas are applicable to stationary stochastic processes. The random time series that can be characterized by such techniques arise in the processing of speech and images and in the analysis of vibrations and spectra.

This work was done by S. V. Varanasi of Lockheed-EMSCO for **Johnson Space Center**. *For further information, Circle 16 on the TSP Request Card.*
MSC-21068

New on the Market

The Eastman Kodak Company's Solid State Relay Group has introduced two new **solid state relays**, 10A and 20A, which are easily PCB mounted for control circuitry. Both units switch loads up to 240 VAC and down to a 0.3 power factor. Potential applications include industrial equipment, business machines, and circuitry for processing controls.
Circle Reader Action Number 796.

MAGNUM, a 12-volt **handheld spotlight** from Collins Dynamics, Aurora, CO, is so powerful it could light the top of Chicago's Sear's Tower from ground level. With a 1,250,000 candlepower beam, the MAGNUM maintains full beam intensity for over one-half mile. MAGNUM's non-sealed quartz halogen bulb draws less than eight amps and lasts over 100 hours. The spotlight's nine foot, coiled cord plugs into a standard cigarette lighter or—for portable operation—into the Collins Ni-Cad Battery Pack.
Circle Reader Action Number 798.

The Parker Hannifin Corporation's Instrumentation Valve Division has created a new **bellows manifold system** requiring fewer connections than individually piped switching or mixing valves, thereby significantly reducing pump-down time and the number of entrapment zones. Titled MP4, the compact system employs standard Parker externally pressurized bellow valves. The addition of two cartridge ports allows for the installation of Parker's new o-ring poppet check valve, designed to increase system flexibility. This innovation permits the user to change the flow characteristics by simply reversing the poppet and spring in the cartridge.
Circle Reader Action Number 784.

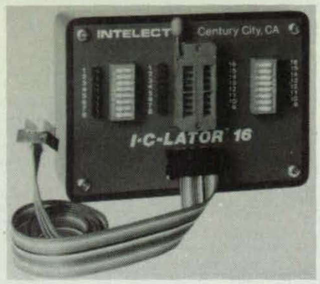

Probing troublesome ICs is made easier with INTELECT's I-C-LATOR 16 **testing instrument**, which enables users to quickly open loops, inject signals, and modify circuits. A virtual "extension cord" for signals and voltage paths, the I-C-LATOR 16 can be applied outside the original assembly without card extenders. The user simply replaces the IC with the I-C-LATOR 16's cable and then inserts the IC in the tester's ZIF socket. The I-C-LATOR 16 accomodates from 6 to 16 pins on analog or digital ICs, and can be used in conjunction with emulator probes, function generators, logic analyzers, or scopes.
Circle Reader Action Number 792.

AutoPE STRUCTURAL™, an AutoCAD® -based **application program** developed by Acuware Inc., Portland, OR, helps structural engineers design plans quickly and easily by automating most of their drafting tasks. The product offers rapid revision response time, effective CAD management and drafting standards, and a fast learning curve. Created for an IBM PC/XT/AT or compatible, the program draws on extensive material libraries of steel, concrete, timber, and masonry—all accessed through AutoLISP®, Macros, and C language programs. AutoPE STRUCTURAL comes with a durable AutoPE tablet template, a wall chart of drafting standards, eight floppy disks, and a 200 page training and reference guide.
Circle Reader Action Number 780.

The Oriel Corporation of Stratford, CT has announced a new line of **safety eyewear** for protection against direct laser hits. Available in both spectacle and goggle styles, the eyewear is made with glass filters that provide maximum visibility and user protection. The filters are recessed in the frames to guard against scratching. Eyebrow cushioning and adjustable temple and side shields ensure optimum user comfort.
Circle Reader Action Number 800.

Honeywell Inc. of Denver, CO has released the Omnilight 8M36, a compact **transient recorder** featuring three recording modes: waveform, X-Y, and data logging. The waveform function allows for both digital and analog recording, while the X-Y function permits recordings from real-time signals or high frequency data captured in memory. Data logging through the Omnilight provides a hard copy printout in alphanumeric sequence. The portable recorder can be equipped with an RS-232C, remote or GP-1B and remote input/output, enabling stored data to be transferred to other computers for analysis. Conversely, external data can be input for recording.
Circle Reader Action Number 790.

Programmers can add state-of-the-art graphics to their FORTRAN and BASIC programs with GEOGRAF, a new **graphics package** marketed by GEOCOMP Corp., Concord, MA. GEOGRAF's library of subroutines and functions can be applied to create virtually any graph or figure on graphics cards, dot matrix printers, plotters, and laser printers. Using simple commands, the programmer can scale the plot, draw and label axes, plot and connect data points, and add text of various sizes and angles. A detailed user's manuel describes each routine and gives examples of typical plots. GEOGRAF runs on an IBM PC or compatible with 128K minimum memory.
Circle Reader Action Number 776.

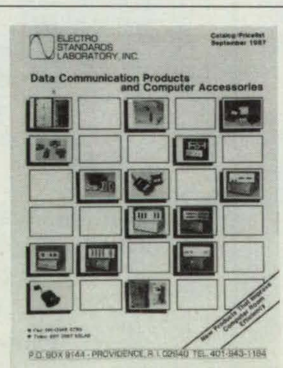

A new **catalog** from Electro Standards Laboratory Inc., Providence, RI, illustrates the company's line of data communication products and computer accessories. Available free of charge, the catalog features breakout boxes, cable adaptors, line drivers, modem eliminators, PC cables, and printer switches, among other items.
Circle Reader Action Number 782.

Lixi Inc, Downers Grove, IL, has developed an **x-ray workstation** for inspection of surface mount devices (SMDs) and PC boards. The Lixi® Microfocus Workstation magnifies even the smallest product defect over 100 times, instantly displays the defect on a monitor, and produces a photo in under 20 seconds. The vertically mounted and enclosed x-ray unit allows for hands-free operation; the SMD or PC board is simply slid into position for inspection. Lixi's workstation can be moved anywhere in the plant—even to the production line—for on-the-spot inspection.
Circle Reader Action Number 778.

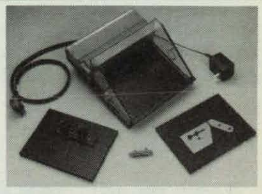

The Model 2010 **Test Fixture** from Electro Scientific Industries, Portland, OR, is designed for safety and flexibility in manual flash testing of components. A key feature of the Model 2010 is a safety cover that protects the operator during high-voltage DWV testing. When opened, the cover activates a multiple interlock system that interrupts power to the testing module and discharges the component being tested. The Model 2010 also offers two interchangeable test module options for fast switching between radial/axial leaded and chip components.
Circle Reader Action Number 794.

An eight page **technical paper** describing superconducting thin-film deposition processes and equipment is available free of charge from CVC Products Inc., Rochester, NY. The paper summarizes superconductivity research performed by CVC Products in conjunction with the Rochester Department of Electrical Engineering, and discusses the benefits of the CVC/Rochester thin-film process of sputtering from a loose powder oxide target. Other successful deposition processes, including sintered targets and high pressure reactive evaporation, are also detailed.
Circle Reader Action Number 788.

Inco Alloys International, Huntington, WV, has developed a new **nickel-iron alloy**, designated INCOLOY alloy 908, for sheathing superconducting magnet coils. The new alloy is derived from Inco Alloy International's series of controlled expansion superalloys developed for gas turbine and aerospace engineering. It is presently being used to provide protective sheathing for the internally cooled superconducting cable created by the Massachusetts Institute of Technology.
Circle Reader Action Number 786.

Subject Index

Advertiser's Index

***RAC** stands for **Reader Action Card.** For further information on these advertisers, please circle the RAC number on the Reader Action Card elsewhere in this issue. This index has been compiled as a service to our readers and advertisers. Every precaution is taken to ensure its accuracy, but the publisher assumes no liability for errors or omissions.

A product of NASA technology, PIMS offers a way to free the estimated one million insulin-dependent diabetics in the U.S. from their daily injections of the pancreatic hormone.

During the 1970's NASA's Goddard Space Flight Center undertook a major research effort aimed at transfering space technology to the medical field. From this research has emerged a revolutionary technique for treatment of insulin-dependent diabetics: the Programmable Implantable Medication System (PIMS), a computerized insulin pump surgically implanted in the diabetic's abdomen. The pump infuses insulin at a pre-programmed rate, allowing for more precise control of blood sugar levels while at the same time freeing the diabetic from the burden of daily insulin injections.

"With the implant I enjoy a more normal lifestyle," said F. Jackson Piotrow, a 56-year-old PIMS recipient. "I don't have to worry anymore about scheduling my activities around injections. The convenience factor is tremendous."

PIMS was created by the Applied Physics Laboratory of Johns Hopkins University, in cooperation with the Goddard Center and MiniMed Technologies, a California-based manufacturer of medical equipment. The implant consists of a refillable drug reservoir, a pumping mechanism, a catheter leading from the pump to the diabetic's intestines, a microcomputer and a lithium battery—all encased in a titanium shell 3.2 inches in diameter and three-quarters of an inch thick.

"The pump's tiny dimensions are the product of years of work in sizing things down for satellites," said Donald Friedman, head of Goddard's Technology Utilization Office and PIMS Project Manager. "The microminiaturization techniques NASA developed for its small astronomy satellites were transferred directly to the PIMS program."

NASA technology also helped create the system's pumping mechanism, which is based on a design for the biological laboratory of the Mars Viking space probe. The device delivers insulin into the abdominal cavity in short bursts or "pulses" designed to conserve battery power. This pulsatile delivery "sets PIMS apart from all previous attempts at implantable pumps," according to Dr. Christopher Saudek, Director of PIMS testing at the Johns Hopkins Diabetes Center. "Earlier pumps used roller mechanisms that were much more energy-intensive," he explained. "As a result, they only lasted a few days or months. Pulsatile delivery has reduced the energy requirements to the point where we now anticipate a five year battery life for our implants."

Both patient and physician can adjust the insulin delivery rate via digital telemetry—a technology originally used by NASA to control spacecraft attitude. By holding a transmitting antenna over the implant and dialing one of ten preprogrammed codes, the diabetic can change the infusion rate or ask for a "bolus", a supplemental dose of insulin administered before meals or when blood sugar levels are elevated. Another code puts the physician in touch with the implanted microcomputer. Using a desktop computer and modem, the physician can access information from the pump's stored memory, reprogram insulin delivery, and create printouts and floppy disk records. In doctor/computer communication, another space spinoff—called pulse coded modulation—plays a safeguarding role: the implant will only accept properly coded instructions and will not respond to false signals generated by other sources.

A Second Generation

Since clinical trials began in November, 1986, there have been 18 successful PIMS implants. Later this year testing will begin on an advanced version of PIMS called the MiniMed® Programmable Implantable Infusion System, developed by MiniMed Technologies. The new device features a wider range of delivery settings than PIMS and more frequent pulses for a given dose of insulin. These changes are designed to further stabilize the diabetic's blood sugar levels, according to Dr. Saudek. "Between each pulse of insulin, there is a rise in blood sugar," he explained. "More frequent pulsing means less fluctuation in blood sugar levels and therefore better overall control."

"Our research with PIMS has shown that better blood glucose control can pay off in terms of more normal metabolism, and may even delay progression of long-term complications of diabetes like kidney disease and blindness," added Peter Lord, Director of Implantable Pump Technology for MiniMed.

For Mr. Piotrow, the payoff has already been substantial. "The pump has virtually eliminated the excessive highs and lows I used to suffer when taking injections," he said. "My blood sugar is more stable and I feel healthier. I can work harder and play harder. It's a wonderful feeling." □

Grumman's best-designed aircraft are tested by Gould's best-designed recorders.

Flight testing is the most critical method by which Grumman Aircraft Systems evaluates tactical aircraft designs for both its planes and those from other aerospace companies. So, when Grumman puts these jets through series of strenuous test points, a recording system they rely on is from Gould.

Gould's 3000 Series programmable recorders permit Grumman flight test engineers to make real-time analysis of critical flight parameters with split-second timing. This allows decisions to be made that increase the productivity and safety of each test flight.

That's because Grumman's ATS (Automated Telemetry System) controls each Gould 3000 recorder with an entire series of planned test points for a specific flight. This way, while the plane and its pilot are in the air, everything is automatic. It allows the test engineers to get answers quickly, reducing both hazardous and costly flight time.

"The programmability of the Gould 3000 recorder provides greater productivity in a number of ways," says Tom Kastner, Grumman corporate manager of automated telemetry. "First, it allows faster, easier test setup with computer control of all parameter settings. "Second, it allows us to tie more resources together on-line. And, third, we can make fast changes to meet modifications in the flight plan. We're now able to make accurate value judgments and technical decisions to continue with our established flight plan or to modify it," concludes Kastner.

With the Gould 3000 recorder, Grumman has been able to expand its flight testing capabilities, speed development and delivery of aircraft, and reduce test costs. When Grumman relies on Gould to help them make a better airplane, it's not just a flight of fancy.

To get more information on this application or on the Gould 3000 Series recorders, call **1-800-GOULD-10**, or write Gould Inc., Test and Measurement, 3631 Perkins Avenue, Cleveland, OH 44114.

Gould: making its mark in Test and Measurement Instrumentation.

GOULD
Electronics

Circle Reader Action No. 486

BREAKTHROUGH: QUICK COOL ALLOYS SO THEY CAN TAKE THE HEAT.

Build a plane that can fly from the U.S. to the Orient between lunch and tea? It can be done. But to build it, new lightweight materials are needed that can survive the heat of hypersonic speeds.

Our solution: A metallurgical recipe using molten titanium alloy and a special process in which the hot liquid metal is solidified into powder by extremely rapid cooling. After the powder is processed into a solid and worked into sheets, designers have a practical material for helping get hypersonic flight off the ground.

We're creating breakthroughs that make a difference in the way things work and the way people live.

We're McDonnell Douglas.

For more information, write:
Orient Express, McDonnell Douglas,
Box 14526, St. Louis, MO 63178.

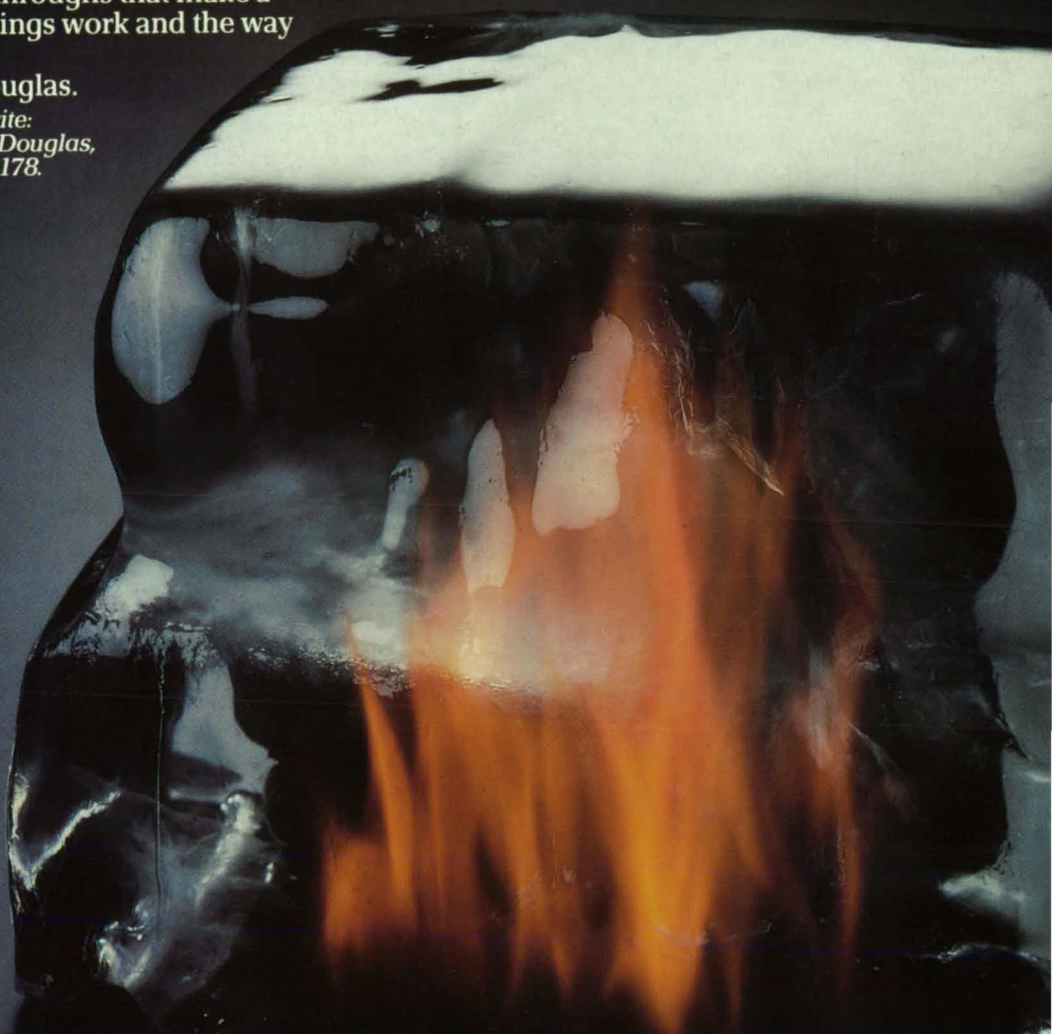

MCDONNELL DOUGLAS

SPACECRAFT & MISSILES MILITARY & COMMERCIAL AIRCRAFT HEALTHCARE SYSTEMS INFORMATION SYSTEMS HELICOPTERS FINANCING